Increasing heat waves require human-biometeorological analyses on the planning-related potential to mitigate human heat stress within urban districts

Thesis submitted in partial fulfilment of the requirement of the degree of *Dr. rer. nat.*
of the Faculty of Environment and Natural Resources,
Albert-Ludwigs-University, Freiburg i. Brsg., Germany

by

Hyunjung Lee

Freiburg im Breisgau

2015

Dean: Prof. Dr. Tim Freytag

1st reviewer: Prof. Dr. Helmut Mayer

2nd reviewer: Prof. Dr. Wilhelm Kuttler

Day of thesis defence: 16 June 2015

Acknowledgements

First of all, I am greatly indebted to Prof. Dr. Helmut Mayer, who saw the valuable insights of my scientific work as well as has been a scientific mentor. His warm kindness and brilliant intelligence have made me successful in the long journey of my thesis. Without his enduring encouragement and support, my work would not have taken place. I would like to give my special thanks to my second reviewer, Prof. Dr. Wilhelm Kuttler, who has expressed kind concern for my research. Sincere thanks are given to Prof. Dr. Michael Bruse for providing new versions of the ENVI-met model and advising me on questions about human-biometeorological simulations using the ENVI-met model.

During my research, many people have offered their advice and support. I would like to thank PD Dr. Dirk Schindler, who gave his time and let me participate in his experience about my research theme. I am thankful to Dr. Jutta Holst, who advised me with her valuable expertise in urban human-biometeorology as well as provided experimental data for my study. I would also like to thank Prof. Dr. Gerd Jendritzky for giving me his advice on the analysis of human thermal comfort.

Thanks also to all the members of the Chair of Meteorology and Climatology, Albert-Ludwigs-University of Freiburg, particularly Andrea Hug, Manuel Mohr, Dirk Redepenning and Jochen Schönborn, who have contributed to a comfortable working atmosphere.

Most of all, I thank my parents, Huwon Lee and Hwajung Yun, for their great tolerance, belief and support. Without their love and devotion, I would not be here. I would like to send my true love to my brother and sister-in-law, Sangsoo Lee and Jonghee Park, as well as my lovely niece Yunseo Lee for inspiring me to my work in Germany.

Preface

As a cumulative dissertation, this thesis summarises the contents of the following publications:

I Shevchenko, O., Lee, H., Snizhko, S., Mayer, H., 2014: Long-term analysis of heat waves in Ukraine. International Journal of Climatology 34, 1642-1650, DOI: 10.1002/joc.3792.

II Lee, H., Holst, J., Mayer, H., 2013: Modification of human-biometeorologically significant radiant flux densities by shading as local method to mitigate heat stress in summer within urban street canyons. Advances in Meteorology 2013, article ID 312572, 13 pages, DOI: 10.1155/2013/312572.

III Lee, H., Mayer, H., Schindler, D., 2014: Importance of 3-D radiant flux densities for outdoor human thermal comfort on clear-sky summer days in Freiburg, Southwest Germany. Meteorologische Zeitschrift 23, 315-330, DOI: 10.1127/0941-2948/2014/0536.

IV Lee, H., Mayer, H., Chen, L., 2015: Contribution of trees and grasslands to the mitigation of human heat stress in a residential district of Freiburg, Southwest Germany. Landscape and Urban Planning, DOI: 10.1016/j.landurbplan.2015.12.004.

Contents

List of symbols and abbreviations

a: short-wave albedo

a_1: regression coefficient

a_2: regression coefficient

A: horizontal area

ASHRAE: American Society of Heating, Refrigerating and Air-Conditioning Engineers

BVOCs: biogenic volatile organic compounds

CAT: Canyon Air Temperature

CO_2: carbon dioxide

CTTC: Cluster Thermal Time Constant

d: index of agreement

D: diffuse sky radiation

H: height of buildings

HW: heat wave

HWs: heat waves

H/W: aspect ratio

ITS: Index of Thermal Stress

$K\downarrow$: downward short-wave radiant flux density from the upper half space

$K\downarrow_{max}$: daily 1-h peak value of $K\downarrow$

$K\downarrow \cdot a$: reflected short-wave radiant flux density

$K\downarrow_{abs}$: downward short-wave radiant flux density from the upper half space absorbed by the human-biometeorological reference person

$K\downarrow_{abs,max}$: daily 1-h peak value of $K\downarrow_{abs}$

$K\uparrow$: upward short-wave radiant flux density from the lower half space (equivalent to: short-wave radiant flux density reflected from the lower half space)

$K\uparrow_{abs}$: upward short-wave radiant flux density from the lower half space absorbed by the human-biometeorological reference person

K_i: short-wave radiant flux densities from different directions i (i = downward, upward, E, S, W, N) within the three-dimensional urban environment

$K_{i,abs}$: short-wave radiant flux densities from different directions i within the three-dimensional urban environment absorbed by the human-biometeorological reference person

$K_{hor,abs}$: total of the horizontal short-wave radiant flux densities from the cardinal points E, S, W and N absorbed by the human-biometeorological reference person

$K_{vert,abs}$: total of the two vertical short-wave radiant flux densities (downward and upward) absorbed by the human-biometeorological reference person

K^*_{abs}: total of the 3-D (two vertical and four horizontal) short-wave radiant flux densities absorbed by the human-biometeorological reference person

L: length of a street canyon

$L\downarrow$: downward long-wave radiant flux density from the upper half space

$L\downarrow_{abs}$: downward long-wave radiant flux density from the upper half space absorbed by the human-biometeorological reference person

$L\uparrow$: upward long-wave radiant flux density from the lower half space

$L\uparrow_{abs}$: upward long-wave radiant flux density from the lower half space absorbed by the human-biometeorological reference person

$L\rightarrow$, $L\leftarrow$: long-wave radiant flux densities from vertical walls in opposite directions

L_i: long-wave radiant flux densities from different directions i (i = downward, upward, E, S, W, N) within the three-dimensional urban environment

$L_{i,abs}$: long-wave radiant flux densities from different directions i within the three-dimensional urban environment absorbed by the human-biometeorological reference person

$L_{hor,abs}$: total of the horizontal long-wave radiant flux densities from the cardinal points E, S, W and N absorbed by the human-biometeorological reference person

$L_{vert,abs}$: total of the two vertical long-wave radiant flux densities (downward and upward) absorbed by the human-biometeorological reference person

L^*_{abs}: total of the 3-D (two vertical and four horizontal) long-wave radiant flux densities absorbed by the human-biometeorological reference person

M: metabolic rate

NO_2: nitrogen dioxide

O_3: ozone

PET: physiologically equivalent temperature

PM_{10}: particulate matter characterised by an aerodynamic diameter less than 10µm

R^2: coefficient of determination

RH: relative humidity

RMSE: root mean square error

RMSEs: systematic root mean square error

RMSEu: unsystematic root mean square error

Q_H: sensible heat flux

$Q_{\lambda E}$: latent heat flux

Q_{Re}: heat flux due to respiration

Q_{Sw}: heat flux due to sweat evaporation

Q^*: net radiation

S: direct solar radiation

SVF: sky view factor

$SVF_{0\text{-}360}$: sky view factor related to the whole upper half space

$SVF_{90\text{-}270}$: sky view factor related to the southern part of the upper half space

T_a: near-surface air temperature

$T_{a,max}$: daily maximum of T_a

$T_{a,min}$: daily minimum of T_a

T_g: globe temperature

T_{mrt}: mean radiant temperature

T_s: surface temperature

UHI: Urban Heat Island

UTCI: Universal Thermal Climate Index

VP: water vapour pressure

W: width of a street canyon

W_i: angular factors of the standing human-biometeorological reference person for K_i and L_i, respectively, (i = downward, upward, cardinal points E, S, W, N)

v: wind speed

α_k: absorption coefficient of the human-biometeorological reference person for the 3-D short-wave radiant flux densities K_i

α_l: absorption coefficient of the human-biometeorological reference person for the 3-D long-wave radiant flux densities L_i

Δ: difference

σ: Stefan-Boltzmann-constant ($5.67 \cdot 10^{-8}$ W/(m^2 K^4))

Abstract

This cumulative thesis concerns the planning-related potential to mitigate local human heat stress within urban spaces of Central European cities. Facing regional climate change, particularly the embedded heat waves, this represents a current issue of urban human-biometeorology.

Four publications addressing specific objectives within this issue are the basis of the thesis:

I. Shevchenko, O., Lee, H., Snizhko, S., Mayer, H., 2014: Long-term analysis of heat waves in Ukraine. International Journal of Climatology 34, 1642-1650, DOI: 10.1002/joc.3792.

II. Lee, H., Holst, J., Mayer, H., 2013: Modification of human-biometeorologically significant radiant flux densities by shading as local method to mitigate heat stress in summer within urban street canyons. Advances in Meteorology 2013, article ID 312572, 13 pages, DOI: 10.1155/2013/312572.

III. Lee, H., Mayer, H., Schindler, D., 2014: Importance of 3-D radiant flux densities for outdoor human thermal comfort on clear-sky summer days in Freiburg, Southwest Germany. Meteorologische Zeitschrift 23, 315-330, DOI: 10.1127/0941-2948/2014/0536.

IV. Lee, H., Mayer, H., Chen, L., 2015: Contribution of trees and grasslands to the mitigation of human heat stress in a residential district of Freiburg, Southwest Germany. Landscape and Urban Planning, DOI: 10.1016/j.landurbplan.2015.12.004.

Using the example of the Ukraine in the territory of 2012, paper I is dealing with the heat wave (HW) issue. This country in Eastern Europe has been selected due to two major reasons: (i) it shows different regional climate conditions caused by its relatively large area and (ii) retrospective statistical investigations on HW characteristics have not been conducted up to now. According to an IPCC recommendation, a period of more than five consecutive days with daily peak values of the near-surface air temperature $T_{a,max} \geq 5$ K above the mean daily $T_{a,max}$ for the normal climate period 1961 to 1990 was identified as a HW. The investigation period covers the years 1951 to 2011 at least. For statistical HW analyses, quality-controlled daily $T_{a,max}$ values were available for selected 13 stations of the Ukrainian Hydrometeorological Centre, which are distributed over the whole territory.

The investigation reveals a regional differentiation of HW characteristics caused by the different regional climate conditions in territory of Ukraine. The most heat waves (HWs) occurred in the eastern and southern Ukraine. However, the results of the statistical analyses also point to nationwide tendencies. For almost all stations, the number of HWs was the highest in the period 2001 to 2010. The maximum length of HWs varied between 7 days at the southern coastal region and 24 days in the eastern Ukraine. The extremely severe HW in Western Russia in August 2010 also influenced the Ukraine. Related to the whole investigation period, the station-specific HWs in August 2010 showed their longest duration at almost all analysed stations.

The results contained in paper I are in line with the patterns of HW characteristics in Central Europe, which follow from similar retrospective analyses. Their results as well as findings

from simulations on the development of the regional climate situation in Central Europe in the future point to an HW intensification. This represents the atmospheric background condition for the papers II to IV. Based on different methodical approaches, they aim at the quantification of the local mitigation potential for heat stress perceived by humans in different urban spaces on hot summer days. It is assessed by the physiological equivalent temperature PET. All experimental investigations and numerical simulations including statistical analyses are related to various sites in Freiburg, a mid-size city in Southwest Germany.

Paper II deals with experimental human-biometeorological investigations conducted on two comparable clear-sky summer days at a shaded and a sunny site, respectively, in a street canyon in the southern part of Freiburg. Their aim is to analyse the importance of buildings and trees as two planning-related measures to mitigate local human heat stress by shading the direct solar radiation. The magnitude of shading is quantified by the sky view factor $SVF_{90\text{-}270}$ for the southern part of the upper half space derived from fish-eye-photos. Due to the shaded direct solar radiation, all short- and long-wave radiant flux densities from the three-dimensional environment of the human-biometeorological reference person are reduced at the respective sites. The radiant flux densities are investigated from a (i) meteorological and (ii) human-biometeorological point of view. The assessment concept for the perception of heat by humans considers the projection surface of the standing human-biometeorological reference person for the radiant flux densities from the 3-D environment by angular factors. The whole radiation heat absorbed by the reference person is quantified by the mean radiant temperature T_{mrt}.

The results show that the differences of the totals of the absorbed short-wave radiant flux densities from the six dominating spatial directions (K^*_{abs}) between the sunny and the shaded sites are higher than those of the totals of the absorbed long-wave radiant flux densities from these six spatial directions (L^*_{abs}). For both shading measures, the reduction of T_a amounts to 6 % averaged over the period 12 to 15 CET. It is relatively low and does not vary dependent on the specific shading measure. In contrast, the lowering of mean T_{mrt}, which is 51 % in the case of shading by tree canopies and 47 % in the case of shading by a building, turns out to be distinctly higher than that of T_a. With respect to trees, the transmission of short-wave radiant flux densities by their canopies counteracting a stronger T_{mrt} reduction has to be considered. The lowering of mean PET is higher in the case of tree canopies (41 %) than in the case of a building (31 %). This may be primarily caused by the additional implications of different $SVF_{90\text{-}270}$ values at the investigation sites for the near-surface airflow. The shading by a building reduces $SVF_{90\text{-}270}$ from 65 % to 20 %, while the shading by tree canopies leads to a lowering of $SVF_{90\text{-}270}$ from 70 % to 6 %.

Although based only on two case studies, the investigation described in paper II explicitly analyses the modified radiant flux densities due to shading measures. The achieved findings are extended and become more reliable by the results of the statistical study in paper III. The magnitude of the horizon restriction by street, building and green design, which is relevant to the radiant flux densities, is determined by $SVF_{90\text{-}270}$. An increased shading of the direct solar radiation is reflected by a lowering of $SVF_{90\text{-}270}$. The data analyses of this investigations are based on values of all relevant radiant flux densities as well as T_a, T_{mrt} and PET, which were

determined by 1-day measuring campaigns at 87 different sites in Freiburg. They were conducted on clear-sky summer days in the period 2007 to 2010. In order to get a higher representativity of the results, the values of all absorbed radiant flux densities as well as T_a, T_{mrt} and PET were averaged over the period 10-16 CET. It can be regarded as typical of the highest daily heat stress on humans in Central European cities. The results of the study quantify the importance of $SVF_{90\text{-}270}$ for the different short- and long-wave radiant flux densities from the three-dimensional environment absorbed by the standing human-biometeorological reference person. In addition, the varying influence of the different absorbed short- and long-wave radiant flux densities on T_a as a variable for meteorological heat as well as T_{mrt} and PET as variables for human thermal comfort is revealed.

The detailed results presented in paper III indicate that the correlations between the absorbed short-wave radiant flux densities ($K_{i,abs}$) und $SVF_{90\text{-}270}$ are closer than those between $K_{i,abs}$ and $SVF_{0\text{-}360}$, where $SVF_{0\text{-}360}$ is related to the total upper half space shown by fish-eye photos. This finding can be transferred to each city located in the northern hemisphere. Among T_a, T_{mrt} and PET, T_{mrt} shows the closest correlation with $SVF_{90\text{-}270}$ (coefficient of determination $R^2 = 0.77$). Therefore, T_{mrt} is closer correlated with $K_{i,abs}$ ($R^2 \geq 0.90$) than with $L_{i,abs}$ ($R^2 \leq 0.76$). The increase of shading of the direct solar radiation causes a decrease of the relative K^*_{abs} values and an increase of the relative L^*_{abs} values. The reference base is the total of K^*_{abs} and L^*_{abs}. With respect to the conditions at all experimental sites in Freiburg, the respective linear regressions show that the fraction of relative K^*_{abs} to T_{mrt} does not exceed 40 %, while the fraction of relative L^*_{abs} to T_{mrt} is not lower than 60 %. As a consequence, the magnitude of T_{mrt} is primarily determined by L^*_{abs}. However, the fluctuations of T_{mrt} are mainly governed by K^*_{abs}.

The analyses reveal that correlations between T_a and $K_{i,abs}$ do not exist for the averaging period 10-16 CET. Compared with this, T_a is correlated with $L_{i,abs}$, particularly from the four horizontal directions E, S, W and N, and consequently with L^*_{abs} ($R^2 = 0.66$). PET shows a closer correlation with L^*_{abs} ($R^2 = 0.72$) than that with K^*_{abs} ($R^2 = 0.45$). T_{mrt} can be estimated in a reliable way by a multiple regression ($R^2 = 0.98$), where K^*_{abs} and the absorbed long-wave radiant flux density from the lower half space ($L\uparrow_{abs}$) are the independent variables. Replacing K^*_{abs} by the easier available absorbed short-wave radiant flux density from the upper half space ($K\downarrow_{abs}$) leads to a slightly lower $R^2 = 0.94$. By analogy, a multiple regression with T_{mrt} and T_a as independent variables also enables a reliable estimation of PET ($R^2 = 0.95$). T_{mrt} can be replaced by $K\downarrow_{abs}$ without any change of R^2.

With reference to the dependence of the absorbed radiant flux densities on their directions, the human-biometeorological effects of a varying surface albedo of building walls were investigated. Using the ENVI-met model, version 3.1, numerical simulations were performed for a simple E-W street canyon on a clear-sky summer day. The results show that the surface temperature T_s of a S-facing building wall is reduced by up to 25 % when its surface albedo increases from 0.1 to 0.9. At the S-facing sidewalk, however, T_{mrt} and PET are higher by up to 31 % and 18 %, respectively. A higher wall albedo reduces T_s, which in turn leads to a lower long-wave emission, but this is offset by the increased reflection of solar radiation.

The papers II and III are related to problem-specific, human-biometeorological experiments. Therefore, their results on the planning-related potential to mitigate local human heat stress have a spot character for a meteorological background situation, which is of increased significance due to regional climate change in Central Europe. The subsequent question on how this potential will be modified by the change from a spot to a spatial analysis is addressed in paper IV. It is focused on the mitigation potential of green coverage changes i.e., of trees and grasslands. The methodical approach consists of numerical simulations by use of the grid-based micrometeorological model ENVI-met, version 4.0 BETA, including the sub-module BioMet, version 1.0, to calculate PET.

The simulation domain covers an area of 2.25 ha and is located within a residential district in the northern downtown of Freiburg. The horizontal and vertical grid width in the simulation domain is 1 m. The study area has been selected because results of experimental human-biometeorological investigations conducted at five sites within this area on a hot summer day (27 July 2009) were available. They enabled the validation of the performance of the used ENVI-met version. Taking account of the validation of the performance of previous ENVI-met versions, this validation also refers to PET for the first time. Quantitative validation measures of the model performance show that the version 4.0 BETA of the ENVI-met model is capable of simulating heat in terms of T_a and human thermal comfort in terms of T_{mrt} and PET in a reliable manner.

The problem-specific numerical simulations in the selected domain were performed on the heat wave day of 4 August 2003. Related to the regional climate change, it is assumed that it represents the future meteorological summer conditions in Central Europe starting in the mid-21st century. As this day was at the beginning of the severe heat wave 2003 in Central and Western Europe, urban greening did not suffer from water stress. To analyse the mitigation potential of urban greening for local human heat stress, a kind of inverted method was applied to green coverage changes. The starting point was the current land use in the simulation domain showing buildings, asphalt areas, trees and other green areas (case A). In the following step, all trees were removed from the simulation domain (case B). Subsequently, the remaining green areas, which mostly consist of grassland, were replaced by asphalt areas (case C). This means that the simulation domain only consisted of buildings and asphalt areas.

T_a, T_{mrt} and PET are the target variables of the numerical simulations. Referring to paper III, the simulation results are averaged over the period 10-16 CET. In addition, the nocturnal period 22 to 5 CET is considered in the data analyses. The daytime T_a, T_{mrt} and PET results are presented as grid-related values for the whole simulation domain. In tables, the simulation results for both periods are additionally compiled as mean values for (i) the whole simulation domain, (ii) an embedded ESE-WNW street canyon, (iii) an embedded NNE-SSW street canyon, (iv) the SSW-facing sidewalk of the ESE-WNW street canyon and (v) the NNE-facing sidewalk of the same street canyon.

The simulation results show in the daytime that the shading effect by tree canopies leads to a higher reduction of T_{mrt} (by 6.6 K in the whole simulation domain) than the decrease of asphalt areas by the addition of grassland (by 2.4 K). This refers to a decrease of the fraction of

asphalt areas from 69.5 % to 41.3 % in the whole simulation domain. At night T_{mrt} is slightly increased (by 0.4 K) due to the tree canopies, while the partial change from asphalt to grassland areas reduces T_{mrt} by 1.5 K. As PET is mainly governed by T_{mrt} on Central European heat wave days, the PET simulation results reflect the tendencies of T_{mrt}. Thus, daytime PET is lowered by 3.0 K averaged over the whole simulation domain by the shading effect, whereas the grassland effect reduces PET by 1.0 K. At night, mean PET does not show any response to canopy effects. The decrease of asphalt areas by adding of grassland, however, causes a mean PET reduction by 1.1 K.

In contrast to T_{mrt} and PET, the decrease of asphalt by an increase of grassland areas leads to a higher T_a reduction (in the daytime: by 1.1 K, at night: by 0.7 K) than the tree canopy effect (in the daytime: by 0.6 K, at night: by 0.2 K). Altogether, the discussion of the thermal consequences due to green coverage changes should consider that the base level of T_a, T_{mrt} and PET is distinctly higher in the daytime than at night.

With respect to the different selected areas within the whole simulation domain, daytime thermal stress for humans is the highest at the SSW-facing sidewalk within the ESE-WNW street canyon. Trees with large canopies are the most effective measure to mitigate the regionally predetermined human heat stress at this local site. The extent of the areas shaded by trees depends on (i) their canopy characteristics (e.g. dimensions) and (ii) the current sun position. Related to the geographical location of Freiburg (47° 59' N, 7° 51' E), the solar altitude at the simulation day of 4 August 2003 varied between 46° at 10 CET (azimuth: 121°) and 38° at 16 CET (azimuth: 252°). Its peak value during this period was 59°. Among the analysed selected areas, the shading effects by tree canopies on T_{mrt} and PET are the highest in the NNE-SSW street canyon because there are the most mature trees in the case A.

Zusammenfassung

Diese kumulative Dissertation beschäftigt sich mit dem planungsbezogenen Potenzial, den lokalen Hitzestress für Menschen in mitteleuropäischen Stadträumen zu reduzieren. Vor dem Hintergrund des regionalen Klimawandels, besonders der eingebetteten Hitzewellen, ist diese Untersuchung auf eine aktuelle Fragestellung in der urbanen Human-Biometeorologie ausgerichtet.

Vier Publikationen mit speziellen Zielsetzungen innerhalb dieser allgemeinen Problematik bilden die Grundlage für diese Dissertation:

I. Shevchenko, O., Lee, H., Snizhko, S., Mayer, H., 2014: Long-term analysis of heat waves in Ukraine. International Journal of Climatology 34, 1642-1650, DOI: 10.1002/joc.3792.

II. Lee, H., Holst, J., Mayer, H., 2013: Modification of human-biometeorologically significant radiant flux densities by shading as local method to mitigate heat stress in summer within urban street canyons. Advances in Meteorology 2013, article ID 312572, 13 pages, DOI: 10.1155/2013/312572.

III. Lee, H., Mayer, H., Schindler, D., 2014: Importance of 3-D radiant flux densities for outdoor human thermal comfort on clear-sky summer days in Freiburg, Southwest Germany. Meteorologische Zeitschrift 23, 315-330, DOI: 10.1127/0941-2948/2014/0536.

IV. Lee, H., Mayer, H., Chen, L., 2015: Contribution of trees and grasslands to the mitigation of human heat stress in a residential district of Freiburg, Southwest Germany. Landscape and Urban Planning, DOI: 10.1016/j.landurbplan.2015.12.004.

Die Publikation I setzt sich mit der Hitzewellenproblematik am Beispiel der Ukraine im Landeszuschnitt von 2012 auseinander. Dieses Land in Osteuropa war aus zwei wesentlichen Gründen ausgewählt worden: (i) aufgrund seiner relativ großen Fläche weist es unterschiedliche regionale Klimabedingungen auf und (ii) bis jetzt fehlen retrospektive statistische Untersuchungen zur Charakteristik von Hitzewellen. Unter Bezug auf eine IPCC Empfehlung wurde eine Periode von mehr als fünf aufeinanderfolgenden Tagen als Hitzwelle bezeichnet, an denen das Tagesmaximum der bodennahen Lufttemperatur ($T_{a,max}$) um mindestens 5 K über dem mittleren $T_{a,max}$ für den jeweiligen Tag in der Klimanormalperiode 1961 bis 1990 liegt. Der Analysezeitraum umfasst mindestens die Jahre 1951 bis 2011. Für ihn standen qualitätskontrollierte, tägliche $T_{a,max}$ Werte von 13 Stationen des Hydrometeorologischen Zentrums der Ukraine zur Verfügung, die über das ganze Land verteilt sind.

Die Ergebnisse zeigen einerseits eine regionale Differenzierung, die unter Berücksichtigung der Größe des Landes und seiner unterschiedlichen regionalen Klimabedingungen verständlich ist, und andererseits landesweit übergreifende Tendenzen. So traten die meisten Hitzewellen im Osten und Süden der Ukraine auf. An fast allen Stationen war die Anzahl der Hitzwellen im Zeitraum 2001 bis 2010 am größten. Die maximale Länge von Hitzewellen schwankte zwischen 7 Tagen im südlichen Küstenbereich und 24 Tagen im Osten der Ukraine. Die äußerst extreme Hitzewelle im August 2010 im westlichen Russland hatte auch Aus-

wirkungen auf die Ukraine, da in diesem Zeitraum an fast allen untersuchten Stationen auch die längste Dauer der stationsspezifischen Hitzewellen im Untersuchungszeitraum auftrat.

Die Ergebnisse in der Publikation I stimmen mit den Charakteristika von Hitzewellen in Mitteleuropa überein, die sich aus vergleichbaren retrospektiven Untersuchungen ergeben. Ihre Resultate sowie Ergebnisse über die Entwicklung des zukünftigen regionalen Klimas in Mitteleuropa, die u.a. auf eine Intensivierung von Hitzewellen hinweisen, bilden die atmosphärische Hintergrundbedingung für die Publikationen II bis IV. Basierend auf verschiedenen methodischen Ansätzen zielen sie auf die Quantifizierung des lokalen Reduzierungspotenzials für thermischen Stress ab, dem Menschen in verschiedenen urbanen Bereichen an heißen Sommertagen ausgesetzt sind. Er wird über die physiologisch äquivalente Temperatur PET bewertet. Alle experimentellen Untersuchungen und numerischen Simulationen sowie die damit in Zusammenhang stehenden statistischen Analysen beziehen sich auf unterschiedliche Standorte in Freiburg, eine mittelgroße Stadt in Südwestdeutschland.

Die Publikation II beschäftigt sich mit experimentellen human-biometeorologischen Untersuchungen, die während zweier vergleichbarer Sommertage an jeweils einem abgeschatteten und einem besonnten Standort in einer Straßenschlucht im südlichen Freiburg durchgeführt wurden. Ihr Ziel ist die Analyse der Bedeutung von Gebäuden und Bäumen als zwei planungsbezogene Möglichkeiten, die direkte Sonnenstrahlung abzuschatten, um damit den lokalen Hitzestress für Menschen zu erniedrigen. Das Ausmaß der Abschattung wird über den Sky View Factor $SVF_{90\text{-}270}$ für den südlichen Teil des oberen Halbraums auf der Grundlage von Fish-eye Fotos quantifiziert. Als Folge der abgeschatteten direkten Sonnenstrahlung werden alle kurz- und langwelligen Strahlungsflussdichten aus der dreidimensionalen Umgebung der human-biometeorologischen Referenzperson an den entsprechenden Untersuchungsstandorten reduziert. Sie werden unter zwei verschiedenen Aspekten betrachtet: (i) im meteorologischen Sinn und (ii) unter human-biometeorologischem Aspekt. Das Bewertungskonzept für die Wahrnehmung von Wärme durch Menschen berücksichtigt über Winkelfaktoren die Projektionsfläche der stehenden human-biometeorologischen Referenzperson für die kurz- und langwelligen Strahlungsflussdichten aus der 3-D Umgebung. Die dadurch von der Referenzperson absorbierte Strahlungswärme wird über die mittlere Strahlungstemperatur T_{mrt} quantifiziert.

Die Ergebnisse zeigen, dass die Differenzen der Summen der absorbierten kurzwelligen Strahlungsflussdichten aus den sechs dominierenden Raumrichtungen (K^*_{abs}) zwischen den besonnten und den abgeschatteten Standorten größer als diejenigen für die absorbierten langwelligen Strahlungsflussdichten aus diesen sechs Raumrichtungen (L^*_{abs}) sind. Für beide Abschattungsvarianten beträgt die Erniedrigung von T_a, gemittelt über den Zeitraum 12 bis 15 Uhr MEZ, 6 %, d.h. sie ist relativ klein und variiert nicht in Abhängigkeit von der Art der Abschattung. Demgegenüber ist die mittlere Reduzierung von T_{mrt} mit 51 % für die Abschattung durch Baumkronen und 47 % infolge der Abschattung durch ein Gebäude deutlich größer. Bei Bäumen ist die Strahlungstransmission durch Baumkronen zu berücksichtigen, die einer stärkeren Reduzierung von T_{mrt} entgegenwirkt. Für die Erniedrigung von PET ergeben sich deutlichere Unterschiede zwischen den beiden Abschattungsvarianten. Sie ist im Mittel über 12 bis 15 Uhr MEZ bei der Abschattung durch Baumkronen (41 %) größer als bei der

Abschattung durch ein Gebäude (31 %). Ausschlaggebend dafür dürften hauptsächlich die Konsequenzen der unterschiedlichen $SVF_{90\text{-}270}$ Werte an den Untersuchungsstandorten für die bodennahe Strömung sein. Bei der Abschattung durch ein Gebäude wird $SVF_{90\text{-}270}$ von 65 % auf 20 % reduziert, während sich $SVF_{90\text{-}270}$ bei der Abschattung durch Baumkronen von 70 % auf 6 % erniedrigt.

In der Publikation III werden die Ergebnisse aus der Publikation II, die sich auf zwei experimentelle Fallstudien zu den durch Abschattungen modifizierten Strahlungsflussdichten beziehen, auf eine vertiefte und breitere Basis gestellt. Über $SFV_{90\text{-}270}$ wird das Ausmaß der Horizonteinengung durch Straßen- und Bebauungsdesign sowie Ausstattung an Grün für die Strahlung erfasst. Die zunehmende Abschattung der direkten Sonnenstrahlung spiegelt sich in einer Abnahme von $SVF_{90\text{-}270}$ wider. Die statistischen Datenanalysen beruhen auf experimentell bestimmten Werten aller relevanten Strahlungsflussdichten sowie von T_a, T_{mrt} und PET. Sie wurden in 87 eintägigen Messkampagnen an verschiedenen Standorten in Freiburg ermittelt, die an Strahlungstagen im Sommer im Zeitraum 2007 bis 2010 erfolgten. Um eine höhere Repräsentativität der Resultate zu erzielen, wurden die Werte aller absorbierten Strahlungsflussdichten sowie von T_a, T_{mrt} und PET über die Periode 10 bis 16 Uhr MEZ gemittelt. Sie kann als typisch für den Zeitraum mit der größten täglichen Wärmebelastung von Menschen in mitteleuropäischen Städten aufgefasst werden. Die Ergebnisse dieser Untersuchung quantifizieren die Bedeutung von $SFV_{90\text{-}270}$ für die kurz- und langwelligen Strahlungsflussdichten aus der dreidimensionalen Umgebung, die von der stehenden humanbiometeorologischen Referenzperson absorbiert werden. Weiterhin wird der variierende Einfluss der verschiedenen absorbierten kurz- und langwelligen Strahlungsflussdichten auf T_a als Variable für Hitze im meteorologischen Sinn sowie T_{mrt} und PET als Variable für den thermischen Komfort von Menschen untersucht.

Die detaillierten Ergebnisse in der Publikation III weisen darauf hin, dass die Korrelationen zwischen den absorbierten kurzwelligen Strahlungsflussdichten ($K_{i,abs}$) und $SVF_{90\text{-}270}$ enger als jene zwischen $K_{i,abs}$ und $SVF_{0\text{-}360}$ sind. Dabei ist $SVF_{0\text{-}360}$ auf den gesamten oberen Halbraum bezogen, der in einem Fish-eye Foto gezeigt wird. Diese Erkenntnis lässt sich auf jede Stadt auf der Nordhalbkugel übertragen. Unter T_a, T_{mrt} und PET weist T_{mrt} die engste Korrelation mit $SVF_{90\text{-}270}$ auf (Bestimmtheitsmaß $R^2 = 0.77$). Deshalb ist T_{mrt} auch enger mit $K_{i,abs}$ ($R^2 \geq 0.90$) als mit $L_{i,abs}$ ($R^2 \leq 0.76$) korreliert. Die Zunahme der Abschattung der direkten Sonnenstrahlung verursacht eine Abnahme des relativen K^*_{abs} und eine Zunahme des relativen L^*_{abs}, wobei jeweils die Summe aus K^*_{abs} und L^*_{abs} als Bezugsbasis dient. Für die Bedingungen an allen experimentellen Untersuchungsstandorten in Freiburg zeigen die entsprechenden linearen Regressionen, dass der Anteil des relativen K^*_{abs} an T_{mrt} 40 % nicht überschreitet, während der Anteil des relativen L^*_{abs} an T_{mrt} nicht unter 60 % fällt. Daraus lässt sich ableiten, dass die Größenordnung von T_{mrt} hauptsächlich durch L^*_{abs} bestimmt wird. Die Schwankungen von T_{mrt} werden hingegen primär über K^*_{abs} gesteuert.

Aus den Korrelationsanalysen folgt, dass für den Mittelungszeitraum 10 bis 16 Uhr MEZ keine Korrelation zwischen T_a und $K_{i,abs}$ besteht. Jedoch ist T_a mit $L_{i,abs}$, besonders aus den vier horizontalen Richtungen E, S, W und N, und als Folge davon mit L^*_{abs} ($R^2 = 0.66$) korreliert. PET weist eine stärkere Korrelation mit L^*_{abs} ($R^2 = 0.72$) als mit K^*_{abs} ($R^2 = 0.45$) auf. T_{mrt}

lässt sich belastbar über eine multiple Regression mit K^*_{abs} und der absorbierten langwelligen Strahlung aus dem unteren Halbraum ($L\uparrow_{abs}$) als unabhängige Variable schätzen (R^2 = 0.98). Wird darin K^*_{abs} durch die leichter verfügbare absorbierte kurzwellige Strahlung aus dem oberen Halbraum ($K\downarrow_{abs}$) ersetzt, reduziert sich R^2 auf 0.94. In Analogie dazu kann PET über eine multiple Regression geschätzt werden, in der T_{mrt} und T_a die unabhängigen Variablen bilden. T_{mrt} lässt sich durch $K\downarrow_{abs}$ ersetzen, ohne dass sich R^2 (0.95) verändert.

Die Bedeutung der richtungsspezifischen Abhängigkeit der absorbierten Strahlungsflussdichten insbesondere für T_{mrt} und PET veranlasste numerische Simulationen zur planungsbezogenen Fragestellung über die human-biometeorologischen Auswirkungen einer variablen Albedo von Hausfassaden. Die Simulationen wurden mit dem Modell ENVI-met, Version 3.1, für eine simple Straßenschlucht in E-W Richtung an einem Strahlungstag im Sommer durchgeführt. Die Ergebnisse zeigen, dass die Oberflächentemperatur T_s einer nach Süden orientierten Hausfassade um bis zu 25 % reduziert wird, wenn ihre Albedo von 0.1 auf 0.9 ansteigt. Auf dem davor liegenden, ebenfalls nach Süden orientierten Bürgersteig erhöhen sich T_{mrt} und PET um bis zu 31 % bzw. 18 %. Eine Zunahme der Albedo erniedrigt also T_s, was zu einer reduzierten langwelligen Ausstrahlung dieser Fläche führt. Dieser Effekt wird jedoch durch ihre erhöhte kurzwellige Reflexstrahlung mehr als kompensiert, was insgesamt zu einer höheren Wärmebelastung für Menschen führt.

Die Publikationen II und III beziehen sich auf problemspezifische, human-biometeorologische Experimente. Deshalb weisen ihre Resultate zum planungsbezogenen Potenzial, den lokalen Hitzestress für Menschen zu reduzieren, einen Punktcharakter für eine meteorologische Hintergrundsituation auf, die unter Berücksichtigung des regionalen Klimawandels in Mitteleuropa von hervorgehobener Bedeutung ist. Die sich daran anschließende Frage, wie sich dieses Potenzial beim Übergang von der Punkt- auf eine Flächenbetrachtung verändert, wurde in der Publikation IV untersucht. Dabei steht das Mitigationspotenzial von urbanem Grün, d.h. von Bäumen und Grasland, im Mittelpunkt. Der methodische Ansatz sieht numerische Simulationen mit dem gitternetzbasierten, mikrometeorologischen Modell ENVI-met, Version 4.0 BETA, einschließlich des Submoduls BioMet, Version 1.0, zur Berechnung von PET vor.

Das Simulationsgebiet von 2.25 ha liegt in einem Wohnviertel im nördlichen Zentrum von Freiburg. Die horizontale und vertikale Gitternetzweite beträgt im Simulationsgebiet 1 m. Das Untersuchungsgebiet war deswegen ausgewählt worden, weil für fünf darin liegende Standorte Resultate aus experimentellen human-biometeorologischen Untersuchungen an einem heißen Sommertag (27. Juli 2009) vorhanden waren, die für die Validierung von ENVI-met Simulationsergebnissen verwendet werden konnten. Unter Bezug auf Validierungen von früheren ENVI-met Versionen berücksichtigt diese Validierung der Simulationsergebnisse erstmals PET. Aus quantitativen Validierungsmaßen für die Modellperformance folgt, dass die Version 4.0 BETA des ENVI-met Modells in der Lage ist, Hitze, repräsentiert durch T_a, und thermischen Komfort, quantifiziert über T_{mrt} und PET, belastbar zu simulieren.

Die problemspezifischen numerischen Simulationen im gewählten Untersuchungsgebiet wurden für den Hitzwellentag 4. August 2003 durchgeführt. Bezogen auf den regionalen Klimawandel wird angenommen, dass er die zukünftigen meteorologischen Bedingungen im mitteleuropäischen Sommer ab der Mitte des 21. Jahrhunderts repräsentiert. Da dieser Tag

am Beginn der extremen Hitzewelle in Mittel- und Westeuropa 2003 lag, bestand für das urbane Grün noch kein Wasserstress. Um das Mitigationspotenzial von urbanem Grün in Bezug auf den lokalen Hitzestress für Menschen zu analysieren, wurde eine Art von inverser Methode angewandt, die an Änderungen der grünen Oberflächenbedeckung orientiert war. Den Ausgangspunkt bildete die derzeitige Ausstattung des Simulationsgebiets mit Gebäuden, Asphaltflächen, Bäumen und Grünflächen (Fall A). In der nächsten Stufe wurden alle Bäume aus dem Simulationsgebiet entfernt (Fall B). Anschließend wurden die übrig gebliebenen Grünflächen, bei denen es sich hauptsächlich um Grasland handelt, durch Asphaltflächen ersetzt, so dass das Simulationsgebiet nur aus Gebäude- und Asphaltflächen bestand (Fall C).

Zielgrößen der numerischen Simulationen sind T_a, T_{mrt} und PET. Zur Erhöhung der Repräsentativität werden die Simulationsergebnisse - in Anlehnung an die Publikation III - über den Zeitraum 10-16 Uhr MEZ gemittelt. Zusätzlich wird der nächtliche Zeitraum von 22 bis 05 Uhr MEZ betrachtet. Die Ergebnisse für die Zielgrößen werden für den Tageszeitraum in Form von gitterzellenbezogenen Werten für das gesamte Simulationsgebiet dargestellt. Zusätzlich werden die Simulationsergebnisse für die Tages- und Nachtperiode tabellarisch als Mittelwerte für (i) das gesamte Simulationsgebiet, (ii) eine darin liegende ESE-WNW Straßenschlucht, (iii) eine darin liegende NNE-SSW Straßenschlucht, (iv) den nach SSW orientierten Bürgersteig in der ESE-WNW Straßenschlucht und (v) den NNE orientierten Bürgersteig in der gleichen Straßenschlucht zusammengefasst.

Die Simulationsergebnisse zeigen, dass tagsüber der Abschattungseffekt durch Baumkronen zu einer stärkeren Reduzierung von T_{mrt} (um 6.6 K im gesamten Simulationsgebiet) führt als die Verkleinerung der Asphaltflächen durch die Aufnahme von Graslandflächen (um 2.4 K). Das ist auf die Abnahme des Anteils der Asphaltflächen von 69.5 % auf 41.3 % im gesamten Simulationsgebiet bezogen. Nachts wird T_{mrt} durch Baumkronen geringfügig erhöht (um 0.4 K), während die partielle Umwandlung von Asphalt- in Graslandflächen zu einer Reduzierung von T_{mrt} (um 1.5 K) führt. Da PET an mitteleuropäischen Hitzwellentagen weitgehend durch T_{mrt} gesteuert wird, weisen die Simulationsresultate für PET die durch T_{mrt} vorgegebene Tendenz auf. So wird PET tagsüber durch den Abschattungseffekt um 3.0 K im Mittel über das gesamte Simulationsgebiet reduziert. Der alleinige Graslandeffekt verkleinert PET jedoch nur um 1.0 K. In der Nacht zeigt der PET Mittelwert für das gesamte Untersuchungsgebiet keine Reaktion auf Baumkroneneffekte, während die Einschränkung der Asphaltflächen durch die Aufnahme von Graslandflächen eine mittlere PET Abnahme um 1.1 K verursacht.

Im Gegensatz zu T_{mrt} und PET führt die Verkleinerung der Asphaltflächen durch die Aufnahme von Grünflächen zu einer stärkeren Reduzierung von T_a im gesamten Simulationsgebiet (tagsüber um 1.1 K, nachts um 0.7 K) als der Abschattungseffekt durch Baumkronen (tagsüber um 0.6 K, nachts um 0.2 K). Bei der Diskussion der thermischen Konsequenzen infolge von Veränderungen in der Grünaustattung muss allerdings berücksichtigt werden, dass tagsüber das Ausgangsniveau von T_a, T_{mrt} und PET deutlich höher als in der Nacht liegt.

Bezogen auf die untersuchten Teilflächen sind tagsüber die thermischen Belastungen für Menschen auf dem nach SSW orientierten Bürgersteig innerhalb der ESE-WNW Straßenschlucht am größten. Hier bilden großkronige Bäume die effektivste Methode, den großräu-

mig vorgegebenen Hitzestress lokal zu reduzieren. Das Ausmaß der durch Bäume abgeschatteten Flächen hängt von (i) Charakteristika ihrer Kronen (z.B. Dimensionen) und (ii) der aktuellen Sonnenposition ab. Unter Berücksichtigung der geographischen Breite von Freiburg (47° 59' N, 7° 51' E) variierte die Sonnenhöhe am Simulationstag 4. August 2003 zwischen 46° um 10 Uhr MEZ (Azimut: 121°) und 38° um 16 Uhr MEZ (Azimut: 252°). Das Maximum der Sonnenhöhe in diesem Zeitraum betrug 59°. Unter den analysierten Teilflächen sind tagsüber die Abschattungseffekte auf T_{mrt} und PET in der NNE-SSW Straßenschlucht am größten, weil dort im Fall A relativ viele großkronige Bäume stehen.

1. Introduction

Cities are embedded into atmospheric background conditions on a regional scale (Holst and Mayer, 2010, 2011; Kleerekoper et al., 2012). They are influenced in turn by the large-scale weather situation, regional topography, current land use and emission of air pollutants. The topography can be very simple or relatively complex as in the case of Freiburg. This city is located at the eastern part of the NNE-SSW oriented southern Upper Rhine plain in Southwest Germany (Fig. 1) and bordered by two low mountain ranges: (i) the Black Forest in the east and (ii) the Vosges mountains in the west.

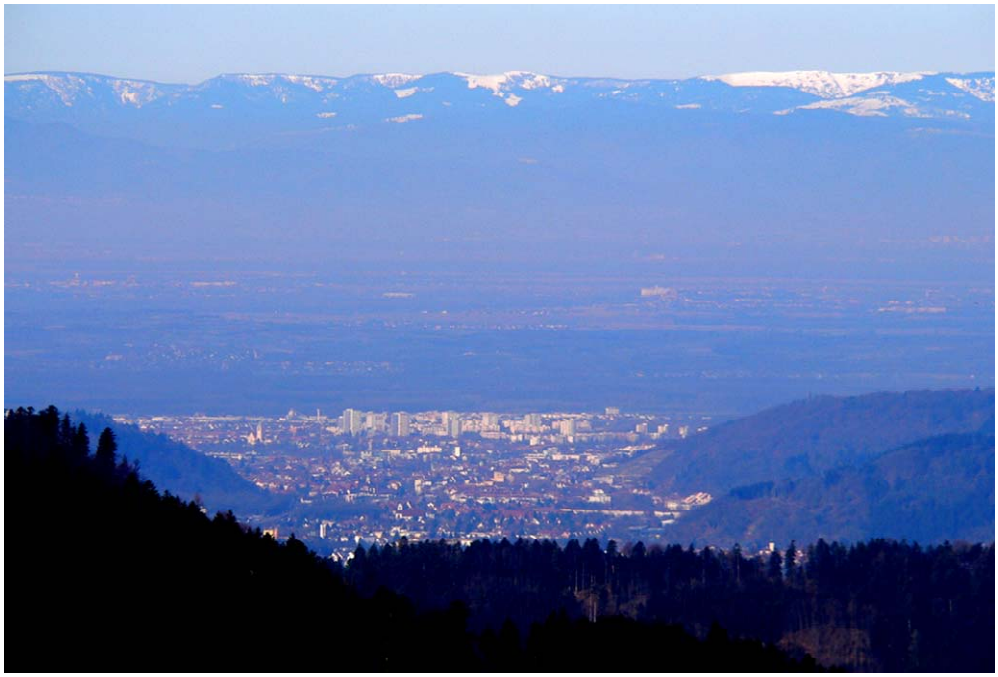

Fig. 1: View from the western Black Forest over the city of Freiburg (Southwest Germany) and the Southern Upper Rhine plain to the Vosges mountains (picture taken on 19 March 2009)

The atmospheric background conditions can be divided into different components (Mayer, 1993). Two of them, the thermal and the air pollution component, become particularly important for urban planning (Mayer, 2006).

Due to varying land use, morphology and energetic processes, cities themselves modify the atmospheric background conditions by a ±Δ, which is not constant. It is a function, which depends on weather, time, urban land use and urban emission of air pollutants. ±Δ is related to

- meteorological variables such as near-surface air temperature T_a, vapour pressure VP or mean radiant temperature T_{mrt},
- air pollutants such as NO_2, O_3 or PM_{10},
- atmospheric flux densities such as the turbulent heat flux density or the turbulent CO_2 flux density.

If a city is considered as a whole in contrast to the rural surroundings, the formation of a specific urban climate results from ±Δ (Arnfield, 2003; Wienert and Kuttler, 2005; Menberg et al., 2013; Müller et al., 2014a; Mills, 2014; Parlow et al., 2014). Related to an intra-urban differentiation, which is of importance for urban planning, the spatial patterns of ±Δ lead to different urban microclimates or local climate zones within cities (Souch and Grimmond, 2006; Kuttler, 2010a, 2010b; Kotthaus and Grimmond, 2012; Stewart and Oke, 2012; Stewart et al., 2014). They represent human-biometeorological conditions for citizens, which can be characterised as an impairment of their efficiency, well-being and health outdoors as well as indoors (Mayer, 1999; Nikolopoulou et al., 2001; Laschewski and Jendritzky, 2002; Holst and Mayer, 2010; Erell et al., 2011; Scherer et al., 2013).

The number of people living in urban agglomerations is still increasing (UN, 2014). Therefore, urban climate develops worldwide more and more to a planning factor of continuously rising importance (Mills et al., 2010; Ren et al., 2011; Ng, 2012). However, a prerequisite is that results on urban climate meet the demands of urban planning (Grimmond et al., 2010a). This includes the direct reference to well-being and health of citizens. Therefore, processes and resulting phenomena of urban climate have to be evaluated in a human-biometeorologically significant way (Mayer, 1993; Holst and Mayer, 2010; McGregor, 2011; Krüger et al., 2013). For instance, the perception of heat by citizens does not depend only on the near-surface air temperature, but on all meteorological variables, which influence the human energy balance. In addition, citizens are breathing air, which does not consist of only one air pollutant, but of a mixture of different species.

The interdisciplinary field of human-biometeorology has developed assessment methods for both the thermal and the air pollution component of urban climate (Mayer and Höppe, 1987; Höppe, 1993, 1999; Mayer et al., 2004; Mayer and Kalberlah, 2009; Jendritzky et al., 2012). They were successfully tested for different urban environments (e.g. Ali-Toudert and Mayer, 2006; Mayer et al., 2008a, 2008b; Holst and Mayer, 2011; Mahmoud, 2011; Blazejczyk et al., 2012; Chen and Ng, 2012; Andreou, 2013; Erell et al., 2014; Lee et al., 2013, 2014; Lee and Mayer, 2013, 2015). Therefore, these methods can be used in investigations on urban meteorology related to sustainable urban planning. This application represents an essential part of urban human-biometeorology.

In recent years, urban planning is faced with enormous challenges, particularly in Central European cities (Kuttler, 2011a, 2011b; Goldberg et al., 2013; Dütemeyer et al., 2013a, 2013b; Masson et al., 2014; Müller et al., 2014b). From the point of view of urban human-biometeorology, they are mainly caused by

- regional climate change,
- inner urban development,
- the increase of the risk group 'elderly people' due to demographic change.

While the inner urban development is primarily influencing the local atmospheric environment, the increase of the elderly people results in an enhanced importance of local atmospheric situations within a city, which are dangerous to human health. Regional climate change can be characterised by a long-term trend of meteorological variables such as of T_a

and embedded extreme weather, which can cause flooding, heat stress and drought (Lehner et al., 2006; Christidis et al., 2012, 2015; Hansen et al., 2012; Nikolowski et al., 2013). These extreme weather situations are meteorological phenomena on a regional scale. They change the atmospheric background conditions of cities in a negative way.

During severe heat, the usual human-biometeorological impairments are enhanced to local human heat stress by the combination of extreme weather on the regional scale and the inner urban development on the local scale (Katavoutas et al., 2009; Pantavou et al., 2011; Schuster et al., 2014). Thus, not only the efficiency and well-being of citizens become more impaired, but also their morbidity and mortality rates are increased (Rey et al., 2007; Vanos et al., 2010; Vaneckova et al., 2011; Klein Rosenthal et al., 2014). In principle, three options exist to mitigate the local impacts of severe regional heat on citizens:

a) heat warning systems of national weather services (Koppe and Jendritzky, 2005; Pascal et al., 2006; Sheridan, 2007),

b) adjustment of the individual behaviour towards severe heat, e.g. by prevention of physical stress or heat-adapted clothing (Höppe, 1999),

c) application of heat-related planning measures.

The options a) and b) have a short-term character aiming at a rapid adaptation of individuals to severe heat. In contrast, the long-term preventive option c) has the objective to enable local thermal comfort for citizens even under severe regional heat. For that purpose, urban planning in Central European cities has to develop, apply and validate measures, which contribute to a local reduction of severe heat (Lee and Mayer, 2013; Goldberg et al., 2013; Müller et al., 2014b; Carter et al., 2015). As these measures should be focused on citizens, they have to be based on findings in urban human-biometeorology (Mayer, 1993; Höppe, 1999; Thorsson et al., 2011; Chen and Ng, 2012; Jendritzky et al., 2012; Kántor et al., 2012a, 2012b; Dütemeyer et al., 2013a, 2013b).

On the basis of four papers, which are listed in the previous chapter "preface", the current thesis mainly deals with the human-biometeorological basis of heat-related planning measures. They address essential aspects of

- severe heat on the regional scale,
- methods to assess the heat perception by citizens in a thermo-physiologically significant way using the approach of indices derived from the human heat budget,
- importance of meteorological variables for human-biometeorological variables during severe heat, which should be primarily modified by planning measures for a locally effective heat mitigation in the daytime,
- potential of green coverage changes as a local planning measure to mitigate the impacts of severe heat on citizens in different urban spaces.

2. Working hypotheses and objectives

Taking account of the current state of scientific knowledge in urban human-biometeorology, this thesis has the following working hypotheses:

a) Severe heat lasting more than only one day is referred to as a heat wave (HW). It is caused by the large-scale weather situation. Therefore, a HW can be regarded as a meteorological hazard on the regional scale.

b) To describe the characteristics of heat waves (HWs), an index-related concept proves to be appropriate. As daily T_a values are easily available worldwide, most of these indices are based on daily extreme T_a values, particularly $T_{a,max}$.

c) Results of retrospective $T_{a,max}$ analyses show for Central Europe that the frequency and intensity of HWs have already increased in the past. Results of regional climate simulations performed for Central Europe project an intensification of HWs in the future.

d) Although the Ukraine is the second largest country in Europe, spatio-temporal HW characteristics in the past were not analysed up to now.

e) HWs negatively impact human health, particularly in cities, where the environmental situation is additionally impaired by the inner urban development and accumulated population.

f) In Central European cities, urban land use, urban morphology and citizens are not adapted to an intensified severe heat. Therefore, urban planning faces the enormous challenge to counteract this meteorological hazard on the local urban scale in a way that is related to the thermal perception of citizens.

g) Counteracting measures of urban planning require a suited human-biometeorological basis. This includes an assessment concept for human thermal stress and information on the potential of urban morphology and green to maintain local human thermal comfort even under regionally severe heat.

h) From the point of view of urban human-biometeorology, the urban mitigation potential during severe summer heat and its physical basis, respectively, can be basically analysed by different investigation methods such as experiments, statistical analyses and numerical simulations.

These working hypotheses lead to the general objectives of this thesis:

a) discussion on HW indices;

b) statistical investigation on the retrospective tendency of spatio-temporal HW characteristics in the Ukraine, basis: long-term $T_{a,max}$ values of selected stations;

c) review on the method to assess the thermal urban environment in a human-biometeorologically significant way;

d) processed-based investigation of the human-biometeorological effect of two shading measures within an urban district on clear-sky summer days, basis: comparative human-

biometeorological experiments in terms of spot measurements in Freiburg (Southwest Germany);

e) identification of meteorological processes and resulting variables, which have the most pronounced influence on outdoor human thermal comfort within different urban districts on clear-sky summer days, basis: collective of suitable data obtained by numerous human-biometeorological experiments in terms of spot measurements in different urban districts in Freiburg;

f) quantification of the impact of changed albedo values of vertical building walls within an E-W street canyon on human thermal comfort in the extreme case of a Central European HW day, basis: numerical simulations by use of the ENVI-met model;

g) statistical estimation of human heat stress by multiple regressions for human-biometeorological variables; basis: collective of suitable human-biometeorological data from numerous spot measurements in different urban districts in Freiburg on clear-sky summer days and numerical simulations by use of the ENVI-met model conducted for a residential district in Freiburg on a HW day;

h) quantification of the potential of green coverage changes to mitigate human heat stress in different spaces within a residential district in Freiburg on a heat wave day, basis: numerical simulations by use of the ENVI-met model.

These general objectives are addressed in detail in the papers I to IV of this thesis.

3. Characteristics of heat waves

3.1 Importance of heat waves

Heat waves (HWs) in Europe typically occur on synoptic scales and are often associated with the development of large stationary or quasi-stationary high pressure systems in the extratropics (Koffi and Koffi, 2008). HWs are important phenomena of the European climate and have major negative impacts on the natural environment and society (Lhotka and Kyselý, 2014). For instance, HWs may impair well-being, efficiency, morbidity and mortality of humans (Kovats and Ebi, 2006; Basu, 2009; Gosling et al., 2009; Scherer et al., 2013; Guirguis et al., 2014; Steeneveld et al., 2014).

In general, a HW represents an atmospheric situation, which is excessively hotter than normal for several consecutive days or longer (Gosling et al., 2007, 2009; Lau and Nath, 2012; Perkins and Alexander, 2013). Based on this description, HWs can be both summertime and annual events. They can be related to the daily $T_{a,max}$ as well as the daily $T_{a,min}$, because high $T_{a,min}$ values can further exacerbate HW conditions (Trigo et al., 2005; Nicholls et al., 2008).

In the light of increasing intensity, duration and frequency of HWs in Europe during the last decades (Schär et al., 2004; Rebetez et al., 2009; Koffi and Koffi, 2008; Ballester et al., 2010; Kyselý, 2010), analysing HWs has developed to a crucial task. Particularly after the most severe HWs, which occurred in June and August 2003 in Western and Central Europe (Fink et al., 2004; Luterbacher et al., 2004; Rebetez et al., 2006) and resulted in more than 70,000 additional deaths in European countries (Kyselý and Kříž, 2008; Robine et al., 2008), there is growing interest in analysing characteristics of HWs.

3.2 Identifying heat waves

A review on HW investigations reveals that many indices to characterise HWs (Hajat et al., 2006; Gosling et al., 2009; Huang et al., 2010; Erlat and Türkeş, 2013) tend to be constructed with a certain impact group or sector in mind (e.g., human health, management, transport, electricity, and power). Due to their complexity, they may not be transportable across more than one region or group. Furthermore, the methodology and required variables may not allow for the investigation of changes of index values over long periods. Therefore, it is understandable that a plethora of metrics or indices exists (Meehl and Tebaldi, 2004; Tan et al., 2007; Gerschunov et al., 2009; Gosling et al., 2009; Monteiro et al., 2013) all attempting to provide quantitative information on periods of extreme or excess heat (Li and Bou-Zeid, 2013; Perkins and Alexander, 2013).

According to Robinson (2001), a basic definition of a HW implies that it is an extended period of unusually heat stress caused by specific weather conditions, which leads to temporary modifications in lifestyle and may impair human health (Kovats and Ebi, 2006; Gosling et al., 2009). This means that HWs represent meteorological phenomena, but they cannot be assessed without reference to human impacts. For this purpose, thermo-physiological assessment indices, which are derived from the human heat budget, should be used for an impact-related HW definition (McGregor, 2011). Appropriate thresholds must be established for

them, considering both daytime and night situation and being related to the climatic variability common to the investigation area.

However, it is difficult to approximate the meteorological variables, which are necessary for the calculation of a thermo-physiological assessment index, from climatological fields. Therefore, using T_a may provide an alternative to bridge the gap between the availability of climatological data and more specific HW indices in terms of human health (Robinson, 2001; Fischer and Schär, 2010; Perkins and Alexander, 2013). Since the complexity of sector-based HW indices eliminates their ability to be calculated on climatological scales, great emphasis is placed on T_a based diagnostics. As T_a is measured very frequently around the world, daily $T_{a,min}$ and $T_{a,max}$ extremes turn out to be particularly useful. Sometimes, the additional influence of the humidity is considered in empirical thermal indices such as the apparent temperature (Steadman, 1984) or heat index (Robinson, 2001). But as they are not accounting for thermal physiology, they have to be regarded as not being current state-of-the-art in human-biometeorology (Höppe, 1999).

A simple approach to identify HWs uses the exceedance of a fixed absolute threshold of daily $T_{a,max}$. Kalkstein and Davis (1989) introduce a 'threshold temperature' as a T_a value, beyond which mortality increases above the baseline level. For instance, this threshold temperature amounts to 33 °C in New York City and mortality increases dramatically at a T_a value above this level. The Royal Netherlands Meteorological Institute focuses on the case of $T_{a,max} \geq 25$ °C or higher for at least five days, whereby at least three days with $T_{a,max} \geq 30$ °C must be included (Huynen et al., 2001; Gershunov et al., 2009; Gosling et al., 2009). The United Sates National Weather Service suggests early warning related to HWs when the daytime heat index (Robinson, 2001) reaches 40.6 °C and $T_{a,min}$ = 26.7 °C lasts for at least 48 h (Gershunov et al., 2009; Gosling et al., 2009). In Portugal, the heat index is also used to identify HWs, which is a period of at least two consecutive days when the heat index is above 41 °C (Monteiro, 2013).

Based on the characterisation of a "heat day" by the Chinese Meteorological Administration as a day with $T_{a,max} > 35$ °C, Tan et al. (2007) and Huang et al. (2010) defined HWs as a period with at least three consecutive heat days. Erlat and Türkeş (2013) focus on $T_{a,max} \geq 30$ °C for finding changes and trends in the extremes of HWs in Turkey. In investigations related to the Czech Republic (Huth et al., 2000; Kyselý, 2002, 2010), a HW is defined as a continuous period when (i) daily $T_{a,max}$ is higher than a threshold value T1 in at least three days, (ii) mean $T_{a,max}$ over the whole period is higher than T1, and (iii) daily $T_{a,max}$ does not drop below a threshold value T2. In accordance with a climatological practice commonly applied in the Czech Republic, which refers to the days with $T_{a,max}$ reaching or exceeding 30.0 °C and 25.0 °C as tropical and summer days, respectively, the threshold values were set to T1 = 30.0 °C and T2 = 25.0 °C (Huth et al., 2000). For analysing hot episodes in Germany during the 20th and 21st century, Tinz et al. (2008) used a definition referring to Kyselý (2002): a hot episode is a period of at least five consecutive days with mean $T_{a,max} \geq 30$ °C. Within such a period, daily $T_{a,max}$ should not be below 25 °C.

In the case of a region characterised by a large areal extent, a fixed threshold of $T_{a,max}$ is insufficient to quantify HWs because a large territory often covers different climate conditions

(Gong et al., 2004; Shevchenko et al., 2014). In order to compensate this defect, the National Weather Service of the United Kingdom uses regionally various $T_{a,max}$ and $T_{a,min}$ thresholds during two consecutive days and the intermediate night (Gershunov et al., 2009; Gosling et al., 2009). In a similar way, Météo-France identifies HWs by the exceedance of mean $T_{a,max}$ and $T_{a,min}$ thresholds over three consecutive days, which vary geographically (Fouillet et al., 2008; Antics et al., 2013; Pascal et al., 2013).

Another way to detect HWs is based on the concept of suited reference periods such as the normal climate period 1961-1990. The method is related to the exceedance of mean daily $T_{a,max}$ values in the reference period by daily $T_{a,max}$ values. The threshold values can be determined by various fixed percentiles. For example, a HW is identified as a period of at least six consecutive days with exceeding the 90^{th} percentile of $T_{a,max}$ during the reference period 1961-1990 (Beniston et al., 2007). Gosling et al. (2007) focus on periods lasting three or more consecutive days when the daily $T_{a,max}$ was at least equal to the 95^{th} percentile of $T_{a,max}$ over the reference period. In addition, another percentiles of $T_{a,max}$ are considered to identify HWs (Gong et al., 2004; Meehl and Tebaldi, 2004; Pascal et al., 2006; Casati et al., 2013).

Altogether, a standardised definition of a HW does not exist up to now. Therefore, an analysis of HWs should include a suitable HW definition, which considers the spatial and temporal HW variability as well as the meteorological data necessary for the HW identification.

3.3 Regional patterns of heat waves

Reviews have shown that extreme hot weather events are associated with varied factors including HW magnitude, timing in season, population experience on HW events and public health responses (Kovats and Hajat, 2008; Lau and Nath, 2012). Although the previous investigations have used different definitions and analysis methods, the results account for the differences in various temporal and spatial HW aspects (Pascal et al., 2006; Gosling et al., 2007, 2009; Antics et al., 2013; Casati et al., 2013).

The negative HW impact is relative to a local climate zone, as the same meteorological conditions can lead to a HW at one place but not at another. Therefore, it is necessary to prepare HWs prevention methods, which consider regional characteristics of climate and meteorological events. In addition, they should be based on a suitable HW definition and HW analysis in terms of the country with spatially different climate zones.

Many investigations have already been performed in Western and Central European countries where severe HWs occurred during the summer 2003 (Beniston, 2004; Heudorf and Meyer, 2005; Díaz et al., 2006; Pascal et al., 2006, 2013; Rebetez et al., 2006, 2009; Fouillet et al., 2008; Kovats and Hajat, 2008; Kyselý and Kříž, 2008; Robine et al., 2008; Gosling et al., 2009; García-Herrera et al., 2010; Kyselý, 2010; Antics et al., 2013; Monteiro et al., 2013). Regional HW differences have been already found in previous studies dealing with long-term statistical HW analyses for parts of Europe (Kyselý, 2002, 2010; Meehl and Tebaldi, 2004; Pascal et al., 2006, 2013; Beniston et al., 2007; Koffi and Koffi, 2008; Tinz et al., 2008; Barriopedro et al., 2011; Radinović and Ćurić, 2012).

However, there are only a few studies on HWs in Eastern Europe, although a particularly extreme HW occurred in Eastern Europe as well as Western Russia in July and August 2010 (Barriopedro et al., 2011; Grumm, 2011; Rahmstorf and Coumou, 2011; Coumou and Rahmstorf, 2012; Otto et al., 2012; Konstantinov et al., 2014). Especially in the case of the large territory of the Ukraine in Eastern Europe, where HWs including their health impacts on humans also represent a serious problem, spatio-temporal HW characteristics in the past were not statistically analysed up to now.

3.4 Retrospective analyses of heat waves in the Ukraine

Given this background related to regional differences of HW occurrences and trends in Eastern Europe, paper I of this thesis (Shevchenko et al., 2014) concerns HWs in the Ukraine as the second largest country (603.700 km^2 including the Crimea peninsula) in Europe. Ukraine is located very close to Russia and not far from Central Europe. According to a recommendation of the Intergovernmental Panel on Climate Change (IPCC), a period of more than five consecutive days with daily $T_{a,max} \geq 5$ K than the respective mean daily $T_{a,max}$ for the 1961-1990 reference period was defined as a HW (IPCC, 2007; Radinovíc and Ćurić, 2012). This HW definition is not based on absolute daily $T_{a,max}$ thresholds. Therefore, it can be applied in Ukraine with its different climate zones (Shevchenko et al., 2014).

In the light of available long-term $T_{a,max}$ time series in the summer months June, July and August as well as the locations of the meteorological stations within the network of the Ukrainian Hydrometeorological Centre, measured daily $T_{a,max}$ values from 13 selected stations (Table 1) were used to analyse HW characteristics in the Ukraine for the first time. Complete and reliable $T_{a,max}$ time series were available for all selected stations in the period 1951-2011. For some stations, the $T_{a,max}$ time series has already started some years earlier.

The results of the temporal variability of HWs related to decades during the investigation period show that most of the HW episodes occurred in the last decade 2001-2010. Related to their spatial distribution, the eastern and southern part of Ukraine were exposed to 13 HWs in Izmail and 12 HWs in Simferopol, both in the southern part, as well as 11 HWs in Kharkiv and Lugansk, both in the eastern and southeastern part, respectively. The lowest HW events were determined for all stations in the two decades 1961-1980.

The results in the Table 1 point to regional differences of HW episodes, which can be clearly identified by the total number of HWs as well as the longest and mean duration of HWs. The longest HW duration varies between 7 d in Henichesk (Southern seashore) and 24 d in Lugansk (southeastern Ukraine). This is closely connected with the extremely long and the strong HW in July and August 2010 in Western Russia (Konstantinov et al., 2014), which borders on the Ukraine.

The cumulative $T_{a,max}$ excess (Kyselý, 2002, 2010) was also applied to characterise the HW intensity. The cumulative $T_{a,max}$ excess during different HWs was calculated as the sum of differences between daily $T_{a,max}$ and the mean daily $T_{a,max}$ in the standard period 1961-1990 increased by 5 K. The results of this analysis show that HWs with the longest duration mostly represent the strongest HWs. For instance, the 24 d HW in 2010 in Lugansk bordering west-

ern Russia was the strongest HW quantified by a cumulative $T_{a,max}$ excess of 128 K in the investigation period.

Table 1: Total number of HWs as well as the longest HW and mean duration of HWs for the selected 13 stations in Ukraine (according to Shevchenko et al., 2014)

station	**region**	**total number of HWs**	**longest HW duration** (d)	**date of the longest HW duration**	**mean HW duration** (d)
Chernivtsi	southwest	18	14	9-22 August 1946	7.3
Henichesk	south	4	7	13-19 June 1924	7.0
			7	30 July to 5 August 1998	
			7	24-30 July 2001	
			7	24-30 August 2007	
Izmail	south	23	13	5-17 July 2002	7.3
			18	31 July to 17 August 2010	
Kerch	south (Crimea)	8	19	31 July to 18 August 2010	8.3
Kharkiv	east	43	20	30 July to 18 August 2010	7.2
Kyiv	north	32	18	31 July to 17 August 2010	8.9
Lubny	central	28	18	31 July to 17 August 2010	8.2
Lugansk	southeast	41	24	26 July to 18 August 2010	8.0
Lviv	west	20	10	25 July to 3 August 1994	6.9
			10	3-12 June 1998	
Odessa	south	16	12	13-24 August 2008	8.4
			12	5-16 August 2010	
Simferopol	south (Crimea)	19	20	30 July to 18 August 2010	8.1
Uzhhorod	west	29	19	22 July to 9 August 1994	7.4
Vinnytsya	central	24	15	19 July to 2 August 1936	8.0
			15	10-24 August 1946	

The results of the analyses described in paper I (Shevchenko et al., 2014) of this thesis reveal regional differences of HW characteristics. Thus, HWs in the past mainly occurred in the southern and eastern parts of Ukraine, i.e. they can be regarded as vulnerable regions with respect to HWs. Based on the results of paper I, it can be assumed that the geographic location of Ukraine will contribute to a distinct probability of HW occurrences in the future.

3.5 Human-biometeorological approaches for impact-related heat wave analyses

Long-term HW studies in the past were almost always based on daily T_a extremes measured at one meteorological station within a city or at an adjacent airport. Therefore, these investigations reveal regional differences of HW characteristics like in paper I of this thesis, which are governed by atmospheric influences on the synoptic scale. They can be considered as

atmospheric background situation. Related to the HW impacts on humans, which are mostly living within cities (UN, 2014), the knowledge on intra-urban patterns of HW characteristics is equally important. This particularly concerns cities located in a vulnerable region, where measures to reduce human HW impacts at a local scale have a high significance. Respective investigations have not been conducted up to now - mainly due to the fact that the necessary data basis in a suited spatial resolution is not available.

T_a represents one of the meteorological variables, which are available on a long-term basis worldwide. Therefore, it is hardly surprising that daily $T_{a,max}$ extremes are often used to identify HWs. In this context, studies on the relationship between T_a and the mortality as an extremely negative HW impact, which were conducted in the past few years in various locations (Tan et al., 2007; Kovats and Hajat, 2008; Basu, 2009), have to be understood. However, as mortality is related to humans, human-biometeorological methods and principles should be increasingly used in HW analyses (Laschewski and Jendritzky, 2002; Koppe and Jendritzky, 2005; Jendritzky and Koppe, 2008; Oleson et al., 2013; Thach et al., 2015). They should be aimed at the magnitude of the mortality increase by HWs and the effectiveness of human-related measures against HWs. Therefore, the human impact of HWs can not be sufficiently investigated, if HWs are identified by only T_a. Against this background, the discussion in paper by Shevchenko et al. (2014) highlights that thermal indices derived from the human heat budget should be applied to identify human-related HWs and to analyse the change of their characteristics in the past and in the future.

4. Human-biometeorological assessment of the thermal urban environment

4.1 Human-biometeorological fundamentals

According to the state-of-the-art in human-biometeorology, the thermo-physiologically significant assessment of the thermal environment should be performed by assessment indices, which were derived from the human heat budget in the last 30 years (Höppe, 1984, 1993; Havenith, 2001; McGregor, 2011; Nagano and Horikoshi, 2011; Jendritzky et al., 2012; Staiger et al., 2012; Pantavou and Lykoudis, 2014). The physiologically equivalent temperature PET (Mayer and Höppe, 1987) based on the human heat budget in terms of the model MEMI (Höppe, 1984, 1993) represents one of these indices. PET provides a measure for the perception of heat by a collective of humans, which is represented by a standardised human-biometeorological reference person of standing position (Mayer and Höppe, 1987; Höppe, 1999). To calculate PET, the following meteorological variables are primarily necessary:

- air temperature T_a,
- water vapour pressure VP,
- wind speed v,
- mean radiant temperature T_{mrt}.

Physical characteristics of humans are often set constant, if the level of human thermal comfort at different sites should be compared. In order to be representative for humans, PET is related to the human-biometeorologically significant height of 1.1 m a.g.l., which matches the average height of a standing person's centre of gravity in Europe (Höppe, 1993).

The method to determine PET within an urban environment is schematically explained in Fig. 2. The regional weather conditions in terms of T_a, VP, v and radiant flux densities are modified by urban morphology and green, which leads to the formation of local climate zones (Stewart and Oke, 2012) within a city. They are characterised by specific patterns of T_a, VP, v as well as short- and long-wave radiant flux densities from the three-dimensional environment. The radiant heat absorbed by the human-biometeorological reference person is quantified by T_{mrt} (Thorsson et al., 2007, 2014; Kántor and Unger, 2011; Lindberg and Grimmond, 2011a, 2011b; Tan et al., 2013; Chen et al., 2014; Kántor et al., 2014a, 2014b; Krüger et al., 2014; Lindberg et al., 2014; Walikewitz et al., 2015). Based on local T_a, VP, v and T_{mrt} values related to 1.1 m a.g.l. and taking into account physical features of the reference person, the energy fluxes of the human heat budget and subsequently PET can be calculated.

Due to its unit "°C", PET results are more comprehensible to urban planners, who are not so familiar with the current terminology of urban human-biometeorology. For practical applications of PET, the assignment of ranges of PET values to a graded human thermal sensation scale is helpful. This can be achieved by statistical analyses of results from suitable questionnaires and parallel determinations of PET (Lin, 2009; Holst and Mayer, 2010; Lin et al., 2010, 2013; Makaremi et al., 2012; Ng and Cheng, 2012; Pantavou et al., 2013; Pearlmutter et al., 2014; Tung et al., 2014; Zeng and Dong, 2015). This method takes the acclimatisation and adaptation of humans into account. Therefore, the threshold values for different PET ranges are varying dependent on regional climate conditions. Using the example of Freiburg,

a classification scheme of PET (Table 2) was developed for different warm levels of human thermal sensation according to the ASHRAE thermal sensation scale (Holst and Mayer, 2010).

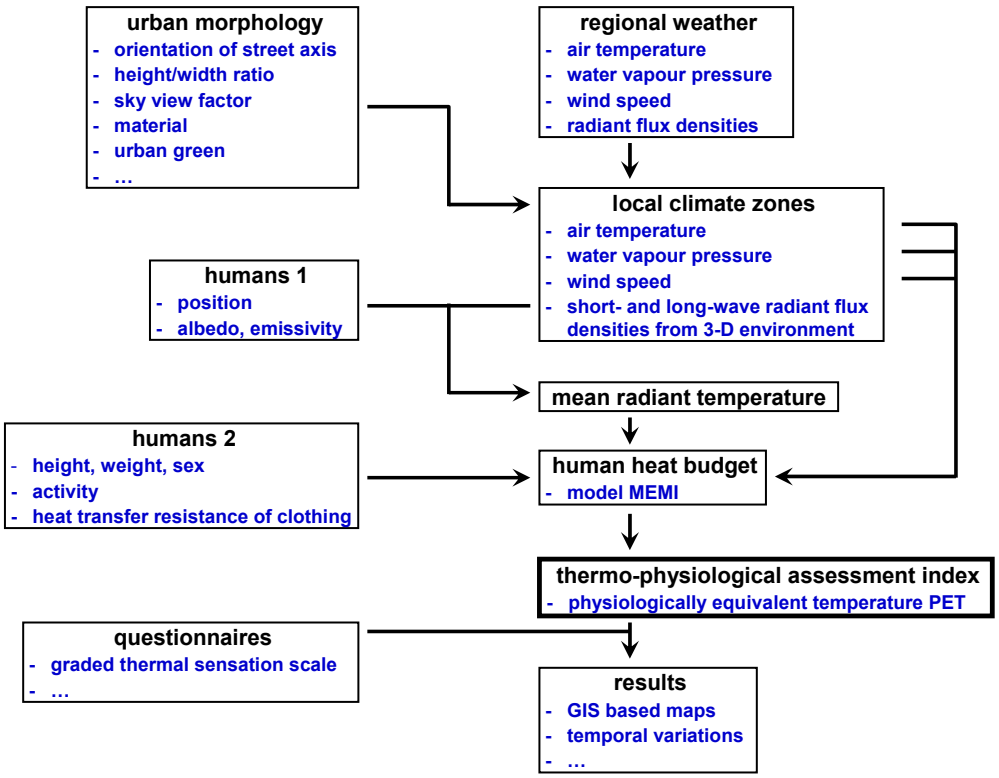

Fig. 2: Flowchart for the determination of the physiologically equivalent temperature PET as a thermo-physiological index to assess the perception of heat within the urban environment by humans (according to Mayer et al., 2008b)

Table 2: Ranges of PET values for different warm levels of human thermal sensation according to the ASHRAE thermal sensation scale determined for summer conditions in Freiburg (according to Holst and Mayer, 2010)

ASHRAE thermal sensation scale		PET range (°C)
name	scale	
slightly warm	+1	30 - 34
warm	+2	35 - 40
hot	+3	> 40

In the meanwhile, PET is applied worldwide and also successfully used for the analysis of human thermal comfort within different urban settings (Oliveira and Andrade, 2007; Andrade and Alcoforado, 2008; Lin, 2009; Holst and Mayer, 2010, 2011; Hwang et al., 2011; Mahmoud, 2011; Yang et al., 2011; Chen and Ng, 2012; Cohen et al., 2012; Kántor et al., 2012a; Makaremi et al., 2012; Andreou, 2013; Charalampopoulos et al., 2013; Égerházi et al., 2013;

Johansson et al., 2014; Konstantinov et al., 2014; Müller et al., 2014b; Pearlmutter et al., 2014; Giannaros et al., 2015; Oertel et al., 2015; Thach et al., 2015; van Hove et al., 2015; Zeng and Dong, 2015). The current experience with PET is based on its comprehensive applications. They also make comparisons between PET results of different investigations possible. Due to these reasons, PET is also used in the papers II-IV of this thesis.

For the calculation of PET, local T_a, VP, v and T_{mrt} values related to 1.1 m a.g.l. are necessary. They can be measured by suitable experimental investigations or simulated by appropriate numerical models. Usually, the experiments only provide spot-related results. However, they can be included in the validation process, which is necessary for each model in order to estimate the reliability of the simulation results.

In contrast to some investigations aiming at strategies to mitigate UHI (Unger, 2006; Bohnenstengel et al., 2011; Ketterer and Matzarakis, 2014b), Fig. 2 clearly points to the fact that the heat effect on humans cannot be described in a thermo-physiologically way only by T_a, urban heat island (UHI) intensity or statistical values based on T_a thresholds such as the number of summer and heat days or tropical nights. Thereby, it has also to be considered that the heat impact on citizens in outdoor urban spaces is most pronounced in the daytime. UHI, however, is primarily a nocturnal phenomenon, which is most apparent when cloudiness and wind speed are relatively low (Tan et al., 2010; Brandsma and Wolters, 2012).

A few years ago, another thermo-physiological assessment index - the Universal Thermal Climate Index UTCI - was developed by an international group of scientists within the scope of the COST action 730 (Jendritzky et al., 2012). Currently, UTCI is tested and already applied under different climate conditions (Blazejczyk et al., 2012, 2014; Bröde et al., 2012; Pantavou et al., 2013; Goldberg et al., 2013; Park et al., 2014; Watanabe et al., 2014).

4.2 Experimental method to determine PET

Experimental investigations to determine PET within different urban districts require special human-biometeorological measurements (Ali-Toudert and Mayer, 2007 b). It is nearly impossible to transfer meteorological data measured routinely at weather or climate stations to human-biometeorological sites within specific urban settings in the necessary accuracy. This particularly refers to the wind speed v.

During the experimental investigations on the influence of urban morphology and green on human thermal comfort, which were conducted from 2007 to 2010 within different urban districts of Freiburg (Mayer et al., 2008b; Holst and Mayer, 2010, 2011; Lee et al., 2013, 2014), two types of human-biometeorological measuring systems were used: a stationary and a mobile system. Both enabled the measurement of the meteorological variables necessary to calculate PET.

The stationary human-biometeorological measuring system (Fig. 3) is described in detail by Mayer et al. (2008b). Using a humicap, T_a and relative humidity RH are measured. VP is calculated from the T_a and RH values. The three-dimensional wind speed v is observed by a sonic anemometer. For the accurate calculation of T_{mrt}, the six-directional technique (Thors-

son et al., 2007; Host and Mayer, 2010, 2011; Kántor and Unger, 2011; Park and Tuller, 2011a; Kántor et al., 2014a, 2014b) suggested by Höppe (1992) is applied. For this purpose all short-wave radiant flux densities (K_i) and long-wave radiant flux densities (L_i) from the three-dimensional environment, which reach the human-biometeorological reference person, are measured by use of six pairs of radiant sensors. Each pair consists of one pyranometer and one pyrgeometer. They are mounted at three cantilevers oriented to the E, S and W direction and thus measure K_i and L_i from the six directions i (i = E, S, W, N, downward, upward).

Fig. 3: Stationary human-biometeorological measuring system used in Freiburg

Based on these data, T_{mrt} (in °C) can be calculated according to Höppe (1992):

$$T_{mrt} = \sqrt[4]{\frac{K^*_{abs} + L^*_{abs}}{\alpha_l \cdot \sigma}} - 273.15 \qquad (1)$$

where

K^*_{abs}: total of the short-wave radiant flux densities from the 3-D environment absorbed by the human-biometeorological reference person (in W/m^2),

L^*_{abs}: total of the long-wave radiant flux densities from the 3-D environment absorbed by the human-biometeorological reference person (in W/m^2),

α_l: long-wave absorption coefficient of the human-biometeorological reference person,

σ: Stefan-Boltzmann-constant ($5.67 \cdot 10^{-8}$ $W/(m^2 K^4)$).

K^*_{abs} and L^*_{abs}, respectively, are computed from measured K_i and L_i (both in W/m^2) by:

$$K^*_{abs} = \alpha_k \cdot \sum_{i=1}^{6} W_i \cdot K_i \quad (2)$$

$$L^*_{abs} = \alpha_l \cdot \sum_{i=1}^{6} W_i \cdot L_i \quad (3)$$

where α_k is the absorption coefficient of the human-biometeorological reference person for the short-wave radiant flux densities K_i. Frequently, the following values are used: $\alpha_l = 0.97$, $\alpha_k = 0.70$ (Mayer, 1993; Höppe, 1992), but due to their dependence on type and colour of clothing, it is possible to change both values. The angular factors W_i (Höppe, 1992; Park and Tuller, 2011b) of the standing human-biometeorological reference person, which is approximated by a rotationally symmetric shape, are set to 0.06 for the radiant flux densities from the upper and lower half space as well as 0.22 for the radiant flux densities from the cardinal points E, S, W and N (Höppe, 1992, 1993, 1999).

In terms of a traverse method, the mobile human-biometeorological measuring system (Fig. 4) can be used parallel to the stationary system (Fig. 3) in order to measure the meteorological variables necessary to calculate PET at sites of different orientations. During the experimental investigations in Freiburg from 2007 to 2010 (Mayer et al., 2008b; Holst and Mayer, 2010, 2011; Lee et al., 2013, 2014), approximately 5 sites turned out to be reasonable for one traverse, which should take up a time of 45 minutes at most.

Fig. 4: Mobile human-biometeorological measuring system used in Freiburg

The mobile human-biometeorological measuring system is also described in detail by Mayer et al. (2008b). In contrast to the stationary system, VP is determined by the psychrometer

technique and the wind speed is measured by a hot-wire anemometer. K_i and L_i are recorded by a combination of a pyranometer and a pyrgeometer, which can be turned horizontally and vertically. By this means, T_{mrt} can be determined according to the six-directional approach.

The use of a globe thermometer (Fig. 5), which directly measures the globe temperature T_g, also enables the calculation of T_{mrt} (Thorsson et al., 2007; Kántor and Unger, 2011; Johansson et al., 2014; Kántor et al., 2014b), provided that T_a and v values related to the human-biometeorological reference height are additionally available.

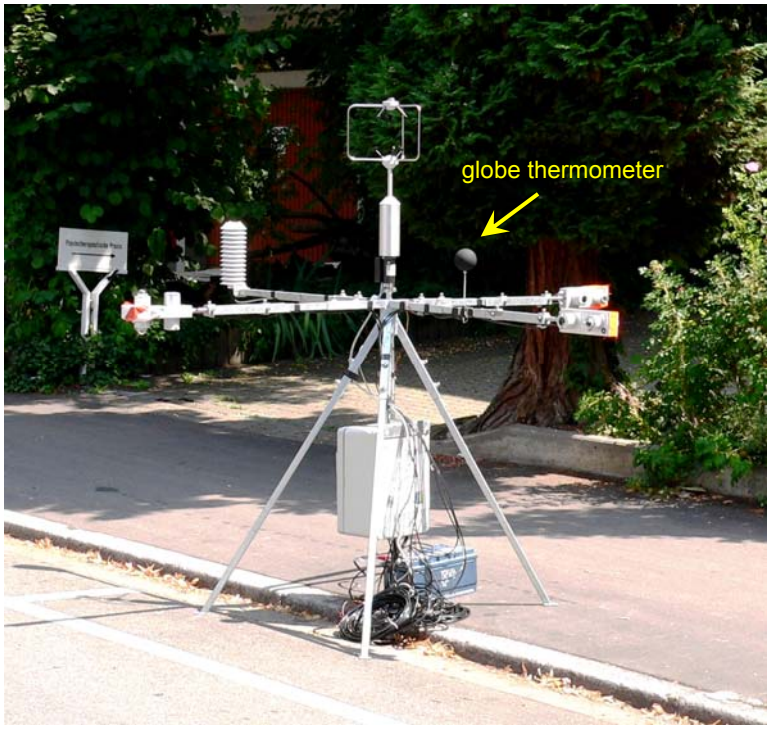

Fig. 5: Globe thermometer mounted at the stationary human-biometeorological measuring system during comparative measurements in Freiburg

This relatively easy and cheap method has two fundamental disadvantages, which are of importance for the discussion of urban planning measures to mitigate local heat impacts on citizens:

- It cannot be differentiated between the effects caused by the (i) short- and (ii) long-wave radiant flux densities.
- The spatial directions of the radiant flux densities cannot be taken into account.

Additional methodical shortcomings using the globe technique outdoors are listed by Kántor et al. (2014b).

For the interpretation of results on human thermal comfort obtained by experimental approaches, the weather conditions during the human-biometeorological measurements and the measuring sites should be described as accurate as possible. Related to the sites, this includes:

- site pictures taken from different directions,
- characterisation and quantification of the green and sealed coverage around the measuring site,
- aspect ratio H/W of street canyons (H: height of buildings, W: street width),
- orientation of street canyons to the sun,
- $SVF_{90\text{-}270}$ at the measuring site (sky view factor related to the southern part of the upper half space).

The sky view factor SVF is defined as the ratio of the radiation received (or emitted) by a planar surface to the radiation emitted (or received) by the entire hemispheric environment (Watson and Johnson, 1987). Within urban settings, SVF is influenced by the urban geometry (Svensson, 2004; Holst and Mayer, 2011; He et al., 2014). It can be regarded as a measure of the degree of sky visibility (Kastendeuch, 2013), which governs the radiation budget and accordingly the heat budget (Zhu et al., 2013).

There is a wide range of methods to determine SVF (Lindberg and Grimmond, 2010; Zhu et al., 2013; An et al., 2014; Gál and Unger, 2014), which can be grouped according to Chen et al. (2012) in

- analytical methods,
- photographic methods,
- GPS methods,
- software methods.

Photographic methods are often applied in experimental investigations on human thermal comfort (Ali-Toudert and Mayer, 2007b; Holst and Mayer, 2010, 2011; Lee et al., 2013, 2014). They use a fish-eye lens to take on-site photos that project the hemispheric environment onto a circular plane. The photos are then processed (converting colour to grey image, altering brightness and contrast, etc.) to define the skyline. The relation between obstructed and unobstructed parts of the sky, which represents SVF, is calculated by appropriate transformations (Lindberg and Grimmond, 2010).

4.3 Numerical simulation of PET

Based on experiments, the current thermal comfort situation for citizens at specific spots within different urban settings can be assessed by PET. Compared with this, a numerical simulation of PET has two advantages:

- Both the current and the future thermal comfort situation due to a combination of modified atmospheric conditions and urban planning measures can be assessed.
- Dependent on the selected model, the PET results are not restricted to single spots but related to the whole simulation area. Thus, interactions of the meteorological variables caused by urban morphology and green can be taken into account in an adequate way.

In order to obtain reliable simulation results, two requirements should be met at least:

- The meteorological variables to calculate PET in the human-biometeorological reference height (1.1 m a.g.l.) have to be simulated as accurate as possible.
- The simulation results for the current land use and weather situation should be validated in a suitable way.

In addition, each user of a simulation model should be familiar with its physical basis before simulation runs are started.

Currently, two freely available models are often applied for the simulation of PET: the RayMan model and the ENVI-met model. The physical basis of the RayMan model is explained in detail by Matzarakis et al. (2010). It is spot-related and needs T_a, VP and v data as meteorological input variables. As they are not directly simulated, they must be provided from elsewhere. The availability of v values proves to be particularly difficult because the approach applied by Fröhlich and Matzarakis (2013), Nastos and Matzarakis (2013) as well as Ketterer and Matzarakis (2014b) to extrapolate v from taller measuring heights to the human-biometeorological reference height is completely inappropriate in complex urban settings.

In the RayMan model, T_{mrt} is determined on the basis of approaches to simulate different short- and long-wave radiant flux densities, which are contained in guidelines edited by the Association of German Engineers (VDI). In addition, the determination of T_{mrt} requires values of the surface temperature T_s. For its calculation, the RayMan model uses an approach, which includes T_a, v, net radiation, ground heat flux and the Bowen ratio. Except for T_a, these data are usually not available for a current situation within complex urban settings. Therefore, they are often approximated by table values. This procedure, however, leads to an enhanced inaccuracy of the T_{mrt} simulation. For the calculation of PET, a respective routine according to Höppe (1984, 1993, 1999) is implemented in RayMan.

Although the physical basis of RayMan is not really suited for its application in complex urban settings (Matzarakis et al., 2010), this model is frequently applied worldwide (e.g. Gulyás et al., 2006; Lin et al., 2010; Hwang et al., 2011; Mahmoud, 2011; Andreou, 2013; Cohen et al., 2013; Nastos and Matzarakis, 2013; Ndetto and Matzarakis, 2013; Ketterer and Matzarakis, 2014b; Makaremi et al., 2014; van Hove et al., 2015). Indeed, the use of the RayMan model enables a quick evaluation of the thermal situation by PET, but the results do not attain the required accuracy and scientific reliability, respectively. The continuous application of this model for the analysis of human thermal comfort in urban districts suggests the assumption that not all RayMan users have made themselves familiar with its physical basis before running this model. Otherwise the knowledge of the physical restrictions of RayMan would have led to a distinctly lower application of this model, particularly in complex urban settings.

Compared to the spot-related RayMan model, ENVI-met is a grid based model (Bruse and Fleer, 1998; Bruse, 1999; Huttner, 2012). It incorporates micro-meteorological interactions caused by urban morphology and green within the simulation area. ENVI-met represents a three-dimensional Computational Fluid Dynamics (CFD) model that simulates surface-plant-air interactions in urban environments. The physical basis of ENVI-met is well explained in the literature (Bruse and Fleer, 1998; Ali-Toudert and Mayer, 2006, 2007a; Huttner, 2012;

Goldberg et al., 2013; Yang et al., 2013; Middel et al., 2014; Müller et al., 2014b; Skelhorn et al., 2014). The maximum simulation domain of ENVI-met covers 250 · 250 cells in horizontal and 30 cells in vertical direction. Buildings, vegetation and surfaces in the investigation area are designed on the 3-D grid with a typical resolution between 0.5 m and 5 m. The ENVI-met core uses a full 3-D prognostic meteorological model to calculate air flow, air and surface temperature, humidity and turbulence. It is coupled with a 1-D model that extends up to 2500 m a.g.l. to simulate processes in the boundary layer. ENVI-met simulations result in atmospheric outputs for each grid cell in the 3-D raster as well as surface and soil variables within the simulated environment. For the visualisation of simulation results, ENVI-met provides the software LEONARDO.

Due to its physical features, ENVI-met meets the following requirements:

- The grid size of the model area has to be small enough to resolve buildings.
- The model should implement the energy balance of surfaces of all types.
- The simulation of the physical and physiological properties of plants has to be included.
- The calculation of the atmospheric processes should be prognostic and transient.

As of 2010, ENVI-met has more than 1700 registered users from all over the world (Huttner, 2012). It is successfully used for simulations of the micro-meteorological conditions within urban districts including the impact of building and street design on human thermal comfort under different heat situations (Ali-Toudert and Mayer, 2006, 2007a; Emmanuel et al., 2007; Fahmy and Sharples, 2009; Chow et al., 2011; Yang et al., 2011; Chow and Brazel, 2012; Ng et al., 2012; Chen and Ng, 2013; Égerházi et al., 2013; Goldberg et al., 2013; Srivanit and Hokao, 2013; Yahia and Johansson, 2013, 2014; Yang et al., 2013; Ketterer and Matzarakis, 2014a; Middel et al., 2014; Perini and Magliocco, 2014; Skelhorn et al., 2014; Wang and Akbari, 2014). Therefore, the application of the ENVI-met model for the simulations described in paper IV of this thesis makes sense.

In contrast to the RayMan model, whose physical basis, particularly for the simulation of T_{mrt}, has not been updated since 2005, the ENVI-met model has been continuously improved. For instance, this becomes apparent by a comparison between its version 3.0 used by Ali-Toudert and Mayer (2006, 2007a) and its version 4.0 BETA (applied in paper IV of this thesis), which has the following essential advancements (Huttner, 2012; Yang et al., 2013):

- The topography of the investigation area including the micro-meteorological consequences has been taken into account. Therefore, the limitation of the ENVI-met application to horizontally homogeneous conditions is abolished.
- The calculation of the temperature of building façades has been advanced. The determination of the energy balance of building walls has been improved.
- A new 3-D vegetation model has been implemented.
- A forcing function related to T_a and RH has been developed and integrated in ENVI-met. This implies that 1-h mean values of T_a and RH measured at a meteorological station ad-

jacent to the simulation domain are included in order to provide more realistic simulation results.

- For the improved simulation of PET, the sub-module BioMet, version 1.0, has been developed, which is based on partly modified approaches for the fluxes of the human heat budget as compared to the routine according to Höppe (1984, 1993, 1999).

While the RayMan model cannot simulate T_a, VP and v, their simulation is included in the ENVI-met model. The calculation of T_{mrt} by use of RayMan and ENVI-met is based on partly different approaches for the underlying radiant flux densities. Their physical reliability is higher in the ENVI-met model (Lee et al., 2015).

In the past, some attempts have been taken to assess the performance of the ENVI-met model by comparing simulation results with data from on-site measurements (Emmanuel et al., 2007; Chow et al., 2011, 2012; Yang et al., 2011; Ng et al., 2012; Chen and Ng, 2013; Goldberg et al., 2013; Srivanit and Hokao, 2013; Yang et al., 2013; Chen et al., 2014; Middel et al., 2014; Müller et al., 2014b; Skelhorn et al., 2014). However, with the exception of Chen and Ng (2013), Yang et al. (2013) and Chen et al. (2014), this validation has been mostly focused on T_a and based on simulations using previous versions of ENVI-met. Altogether, these studies show that the thermal environment can be simulated by ENVI-met with an acceptable accuracy. Physical weaknesses of previous versions of ENVI-met reported in Goldberg et al. (2013) are eliminated in its current version 4.0 BETA to a great extent.

In paper IV of this thesis, a comparative validation of T_{mrt} and PET simulation results obtained by the ENVI-met model, version 4.0 BETA, and the RayMan model, version Pro 2.0, is reported. It is based on data of experimental investigations conducted on a clear-sky summer day at five measuring sites in Freiburg. The validation indicates that the used version of ENVI-met seems to be better suited than the applied version of RayMan to simulate T_{mrt} and PET in complex urban settings during summer heat. The relatively heterogeneous urban micro-environment at the five measuring sites and the spot-related character of the RayMan model may be the major reasons for the low reliability of the RayMan simulation results. Previous investigations (Thorsson et al., 2007; Kántor and Unger, 2011; Chen et al., 2014) have already pointed to the problems of RayMan to simulate particularly T_{mrt} in a sufficient accuracy. In addition, the ENVI-met sub-module BioMet, version 1.0, contains an update of the software to calculate PET, which is currently not implemented in the RayMan model.

The freely available model SOLWEIG (Lindberg et al., 2008, 2014) also simulates spatial (2-D) variations of 3-D radiation flux densities including T_{mrt} and shadow patterns in complex urban environments. As from version 2, the modelling procedure of SOLWEIG considers vegetation in the form of trees and bushes. The model has shown to enable an accurate estimation of the radiation flux densities for a number of different urban settings and weather conditions as well as in different regional situations (Lindberg et al., 2008, 2014; Lindberg and Grimmond, 2011a, 2011b; Thorsson et al., 2011, 2014; Onomura et al., 2015).

5. Efficient measures for mitigating human heat stress in local urban environments

5.1 Double strategy to mitigate human heat stress in summer

As climate change is a major driving force for threatening human health and quality of life, urban planning is focused on the improvement of the human thermal conditions within urban spaces (Gómez et al., 2013; Villadiego and Velay-Dabat, 2014). Reducing the negative human impacts of climate change and increasing the resilience of adaptation related to heat require suitable urban design strategies. The main objective of these strategies is to optimise the spatial distribution of urban land uses for reducing heat stress as a long-term prevention measure. In order to develop and apply the strategies, urban planning should understand the modification of the urban thermal environment by the regional climate change (Rannow et al., 2010; Carter et al., 2015). Knowing the change of the urban heat allows an insight into strategies for mitigation of human heat stress.

In Central Europe, severe heat occurs only in summer, when the day is longer than the night. Considering this different length, urban planning needs a double strategy to provide efficient measures aiming at the maintenance of human thermal comfort under severe regional heat (Lee and Mayer, 2013; Lee et al., 2013). Due to the longer daylight hours in summer, the planning measures should be primarily focused on the mitigation of daytime heat. On the other hand, approaches related only to nocturnal meteorological phenomena such as thermally induced down-slope or mountain air flow are often classified as secondary.

The general objective of planning measures in the daytime is to lower the heat input into all urban spaces. It should be achieved in compliance with targets of environmental protection. For instance, this implies the reduction of energy consumption as well as anthropogenic heat release by the avoidance of artificial air conditioning systems. In the night, the strategies focus on natural ventilation and procedures, which make an additional cooling possible to maintain thermally comfort zones for citizens. Although both strategies should be applied to lower urban heat, measures in the daytime take priority. The reduced heat input into urban spaces in the daytime contributes to a lowered heat situation at night and leads to the mitigation of the urban heat island phenomenon.

Focused on the reduction of the local urban heat in the daytime, studies concerning sustainable passive cooling have been conducted in terms of human thermal comfort and energy saving (Grimmond, 2007; Shashua-Bar et al., 2010a, 2010b). Results of previous investigations on outdoor thermal comfort carried out in inland cities on clear-sky summer days reveal that the radiant exchange is the dominant meteorological factor affecting human thermal comfort in the daytime. The spatio-temporal variation of the radiant flux densities within the urban environment is primarily determined by the shadow patterns generated by vegetation, buildings and topography as well as by surface materials (Lindberg and Grimmond, 2011a, 2011b; Lau et al., 2014; Rayner et al., 2014). Therefore, strategies to reduce the heat input into urban spaces should include quantitative analyses of the radiant exchange (Lee et al., 2013).

5.2 Shading devices as a measure to reduce daytime heat

The radiant exchange in terms of T_{mrt} plays a significant role in the human energy balance (Höppe, 1993, 1999; Park und Tuller, 2011a; Shashua-Bar et al., 2011; Lee et al., 2013, 2014). In order to prepare measures for the mitigation of local heat impacts on citizens, the influences of the varying radiant exchange within urban settings on human thermal comfort should be understood.

T_{mrt} can be interpreted as a measure for the heat of the short- and long-wave radiant flux densities from the three-dimensional environment absorbed by the human-biometeorological reference person (Mayer et al., 2008b; Holst and Mayer, 2011). The values for the coefficient of determination R^2 of linear regressions between 1-h mean values of PET, T_{mrt} and T_a (Table 3) reveal that T_{mrt} represents the most crucial variable for the daytime values of thermal indices such as PET on clear-sky summer days (Lee et al., 2013). The varying R^2 values also point to the different characteristic time scales of T_a, T_{mrt} and PET.

Table 3: Coefficient of determination R^2 of linear regression functions f between 1-h mean values of different human-biometeorological variables, basis: 1-h mean values in the period 10-16 CET from experimental investigations on typical Central European summer days in various urban districts of Freiburg from 2007 to 2010, 200 pairs of values (according to Lee et al., 2013)

	PET =				**T_{mrt} =**
	f (T_{mrt})	f (T_a)	f (VP)	f (v)	f (T_a)
R^2	0.89	0.59	0.02	0.03	0.31

The reduction of the direct solar radiation by shading measures proved to be the most effective measure to mitigate the thermo-physiologically significant heat in urban spaces (Ali-Toudert and Mayer, 2007a; Lin et al., 2010; Holst and Mayer, 2011; Shashua-Bar et al., 2011, 2012; Lindberg and Grimmond, 2011a, 2011b; Oliveira et al., 2011; Gross, 2012). Local shading of the direct solar radiation within the urban canopy layer, which leads to a T_{mrt} lowering, can be achieved by (Lee et al., 2013)

- optimised design of buildings, open spaces and streets,
- man-made devices such as awnings or sunshades,
- street trees.

A number of studies have already concerned local shading effects of the building morphology in terms of different urban meteorological objectives (Ali-Toudert and Mayer, 2006, 2007a; Holst and Mayer, 2011; Yahia and Johansson, 2013; Gómez et al., 2013; Ketterer and Matzarakis, 2014a; Lau et al., 2014; Yahia and Johansson, 2014; Taleghani et al., 2015). The shading effect by street trees was also analysed in previous studies (Bowler et al., 2010; Lin et al., 2010; Shashua-Bar et al., 2010a, 2010b, 2011, 2012; Chow et al., 2011; Holst and Mayer, 2011; Lindberg and Grimmond, 2011b; Oliveira et al., 2011; Chow and Brazel, 2012; Gross, 2012; Ng et al., 2012; Chen and Ng, 2013; Srivanit and Hokao, 2013; Müller et al.,

2014b; Wolch et al., 2014). However, they mostly represent specific case studies and, therefore, show a lack of systematic structure.

From a human-biometeorological point of view, which includes aesthetic and psychological aspects, shading by street trees has the highest significance despite conflicting goals (see also chapter 8) such as reducing the near-surface air flow (Gromke and Ruck, 2007; Gromke et al., 2008) or the emission of biogenic volatile organic compounds (BVOCs) as a precursor for the ozone formation (Kuttler, 2011b; Wagner and Kuttler, 2014).

In contrast, only a limited number of investigations have been conducted up to now on the shading effect by artificial devices. Besides the positively evaluated shading of the direct solar radiation, these overhead shading devices include problems such as the decrease of the convective heat loss (Shashua-Bar et al., 2009; Égerházi et al., 2013).

Numerous studies were conducted on the different shading effects, but most of them are focused on

- the influence of the shading by a single method,
- the consequences only for T_a.

There are scarcely investigations on the

- quantitative distinction of the effects between various shading methods,
- shading consequences for the components of the local radiation and heat budget,
- shading consequences on variables characterising human thermal comfort.

5.3 Impacts of a building and tree canopies as shading methods on human-biometeorologically significant radiant flux densities

The existing shortcomings about the human-biometeorological fundamentals of shading effects were the initial point for paper II (Lee et al., 2013) of this thesis. It particularly aims at the quantification of human-biometeorologically significant radiant flux densities modified by two effective methods to shade the direct solar radiation:

- shading by a building,
- shading by tree canopies.

The study described in paper II is based on two measuring campaigns, which are explained in detail by Lee et al. (2013). They were conducted in the Vauban district located in the southern part of Freiburg (Southwest Germany) on 15 July 2007 and 24 July 2008. The first measurement campaign had the specific goal to analyse the shading effects caused by a building. The second one was focused on the human-biometeorological consequences of shading by tree canopies. As the weather conditions on both clear-sky summer days were quite similar, the requirements for the human-biometeorologically oriented comparison between both shading methods were sufficiently met. The experimental investigations were carried out at the sidewalk within the same ESE-WNW street canyon but at different sites, which were about 300 m off each other. The stationary and mobile human-biometeorological

measuring systems (Fig. 3 and Fig. 4), which are described in chapter 4.2, were used in both measuring campaigns to determine all necessary meteorological variables, particularly K_i and L_i from the three-dimensional environment. In each campaign, the human-biometeorological measurements were taken parallel at a sunny and a shaded sidewalk for quantifying the shading effects.

In terms of the characteristics of the measurement sites, their $SVF_{90\text{-}270}$ values indicate the background conditions for the shading. In the case of shading by the building, $SVF_{90\text{-}270}$ was 65 % at the sunny site and 20 % at the shaded site. With respect to shading by tree canopies, $SVF_{90\text{-}270}$ was 70 % at the sunny site and 6 % at the shaded site (Lee et al., 2013).

Related to the sunny and shaded sites in the period 12-15 CET (Table 4 to Table 7), when shading was effective during both measuring campaigns, the results can be summarised as follows:

- For both cases, the mean short-wave radiant flux densities from different directions i (i = downward, upward, E, S, W, N) within the three-dimensional urban environment absorbed by the human-biometeorological reference person ($K_{i,abs}$) show a distinct anisotropy (Table 4 and Table 5), which is predetermined by the pattern of the K_i values according to equation (2). It was already indicated in the experimental investigations by Ali-Toudert and Mayer (2007b), Thorsson et al. (2007) and Mayer et al. (2008b).
- At the sunny site of both measuring campaigns, the absorbed short-wave radiant flux density from the southern direction ($K_{S,abs}$) is the highest among $K_{i,abs}$, while the absorbed upward short-wave radiant flux density from the lower half space ($K\uparrow_{abs}$) is the lowest. The absorbed downward short-wave radiant flux density from the upper half space ($K\downarrow_{abs}$) also reaches comparatively high values.

Table 4: Mean $K_{i,abs}$ values and mean K^*_{abs} over the period 12-15 CET at the sunny site as well as mean absolute and relative $K_{i,abs}$ and K^*_{abs} differences between the shaded (by the building) and the sunny site within a ESE-WNW street canyon in Freiburg, 15 July 2007

site	$K\downarrow_{abs}$	$K\uparrow_{abs}$	$K_{E,abs}$	$K_{S,abs}$	$K_{W,abs}$	$K_{N,abs}$	K^*_{abs}
sunny site	35 W/m²	4 W/m²	21 W/m²	67 W/m²	43 W/m²	16 W/m²	186 W/m²
shaded - sunny	-33 W/m² 94 %	-3 W/m² 75 %	-12 W/m² 57 %	-58 W/m² 87 %	-35 W/m² 81 %	-14 W/m² 88 %	-155 W/m² 83 %

Table 5: Mean $K_{i,abs}$ values and mean K^*_{abs} over the period 12-15 CET at the sunny site as well as mean absolute and relative $K_{i,abs}$ and K^*_{abs} differences between the shaded (by tree canopies) and the sunny site within a ESE-WNW street canyon in Freiburg, 24 July 2008

site	$K\downarrow_{abs}$	$K\uparrow_{abs}$	$K_{E,abs}$	$K_{S,abs}$	$K_{W,abs}$	$K_{N,abs}$	K^*_{abs}
sunny	37 W/m²	6 W/m²	41 W/m²	81 W/m²	23 W/m²	23 W/m²	211 W/m²
shaded - sunny	-34 W/m² 92 %	-5 W/m² 83 %	-33 W/m² 80 %	-77 W/m² 95 %	-18 W/m² 78 %	-12 W/m² 52 %	-179 W/m² 85 %

- The mean long-wave radiant flux densities from different directions i (i = downward, upward, E, S, W, N) within the three-dimensional urban environment absorbed by the human-biometeorological reference person ($L_{i,abs}$) show different patterns as compared to $K_{i,abs}$. The horizontal $L_{i,abs}$ values reach a similar magnitude (between 100 W/m^2 and 111 W/m^2) at the sunny site of both measuring campaigns (Table 6 and Table 7), while the horizontal $K_{i,abs}$ values are distinctly lower and cover a wider range.
- At the sunny site of both measuring campaigns, the absorbed downward long-wave radiant flux density from the upper half space ($L\downarrow_{abs}$) is lower than the absorbed upward long-wave radiant flux density from the lower half space ($L\uparrow_{abs}$). Taking account of $K_{i,abs}$ values, $K\downarrow_{abs}$ is higher than $L\downarrow_{abs}$, but $K\uparrow_{abs}$ is clearly lower than $L\uparrow_{abs}$.

Table 6: Mean $L_{i,abs}$ values and mean L^*_{abs} over the period 12-15 CET at the sunny site as well as mean absolute and relative $L_{i,abs}$ and L^*_{abs} differences between the shaded (by the building) and the sunny site within a ESE-WNW street canyon in Freiburg, 15 July 2007

site	$L\downarrow_{abs}$	$L\uparrow_{abs}$	$L_{E,abs}$	$L_{S,abs}$	$L_{W,abs}$	$L_{N,abs}$	L^*_{abs}
sunny	25 W/m^2	35 W/m^2	111 W/m^2	110 W/m^2	109 W/m^2	109 W/m^2	499 W/m^2
shaded - sunny	-1 W/m^2 4 %	-7 W/m^2 20 %	-10 W/m^2 9 %	-7 W/m^2 6 %	-8 W/m^2 7 %	-7 W/m^2 6 %	-40 W/m^2 8 %

Table 7: Mean $L_{i,abs}$ values and mean L^*_{abs} over the period 12-15 CET at the sunny site as well as mean absolute and relative $L_{i,abs}$ and L^*_{abs} differences between the shaded (by tree canopies) and the sunny site within a ESE-WNW street canyon in Freiburg, 24 July 2008

site	$L\downarrow_{abs}$	$L\uparrow_{abs}$	$L_{E,abs}$	$L_{S,abs}$	$L_{W,abs}$	$L_{N,abs}$	L^*_{abs}
sunny	23 W/m^2	33 W/m^2	107 W/m^2	100 W/m^2	101 W/m^2	108 W/m^2	472 W/m^2
shaded - sunny	3 W/m^2 13 %	-6 W/m^2 18 %	-9 W/m^2 8 %	-2 W/m^2 2 %	-4 W/m^2 4 %	-5 W/m^2 5 %	-23 W/m^2 5 %

- For each measuring campaign, the shading effect is described by the absolute differences of $K_{i,abs}$ and $L_{i,abs}$ between the shaded and the sunny site as well as their relative values related to the conditions at the sunny sites. Independent of the shading device, the shading extent is more marked for $K_{i,abs}$ than for $L_{i,abs}$.
- $K_{S,abs}$ shows the highest absolute shading extent for both shading devices. For shading by the building, its value is -58 W/m^2, but it is -77 W/m^2 for shading by tree canopies due to the higher reduction of $SFV_{90\text{-}270}$. For both measuring campaigns, the relative shading extent is the highest for $K_{S,abs}$ and $K\downarrow_{abs}$. Varying site-specific urban design causes different values of the relative shading extent between both shading devices.
- The absolute shading extent in terms of $L_{i,abs}$ does not exceed 10 W/m^2. For both shading devices, $L\uparrow_{abs}$ shows the highest relative shading extent (20 % in the case of shading by the building and 18 % in the case of shading by tree canopies).

- At the sunny site of both measuring campaigns, K^*_{abs} is lower than L^*_{abs}. K^*_{abs}/L^*_{abs} amounts to 37 % for the measuring campaign on 15 July 2007 and 45 % for the measureing campaign on 24 July 2008. The absolute K^*_{abs} value in the campaign 2007 is lower by 25 W/m^2 than that in the campaign 2008, while the absolute L^*_{abs} value in the campaign 2007 is higher by 27 W/m^2 than that in the campaign 2008. These differences are caused by the site-specific urban design. At the sunny sites, the totals of K^*_{abs} and L^*_{abs} are quite similar in the campaigns 2007 (685 W/m^2) and 2008 (683 W/m^2).
- The shading by tree canopies leads to a slightly higher K^*_{abs} reduction (by 85 %) than the shading by the building (83 %). Related to L^*_{abs}, the reduction is slightly lower for the shading by tree canopies (5 %) than that for the shading by the building (8 %).
- Considering the different magnitudes of the absolute K^*_{abs} and L^*_{abs} values, the shading leads to a total of K^*_{abs} and L^*_{abs}, which is higher by 9 W/m^2 for the shading by the building (490 W/m^2) than for the shading by tree canopies (481 W/m^2). This difference is mainly caused by the $L_{i,abs}$ values.

As expected by the decisive physical processes, the results of the two measurement campaigns demonstrate that the human-biometeorological shading effect indicated by the difference Δ between the shaded and the sunny site is mainly reflected in T_{mrt} and PET but hardly in T_a (Table 8). Peak ΔT_a reached only -1.7 K for both shading devices, i.e. the T_a reduction did not exceed 2 K. This threshold value can increase at sites in subtropical and tropical climate zones by up to 3 K (Shashua-Bar and Hoffman, 2004; Shashua-Bar et al., 2010a; Vailshery et al., 2013).

Table 8: Maximal absolute and relative reduction Δ of T_a, T_{mrt} and PET by two shading methods related to the mean values of T_a, T_{mrt} and PET over 12-15 CET, basis: human-biometeorological measuring campaigns in an ESE-WNW street canyon in Freiburg during typical Central European summer weather (according to Lee et al., 2013)

shading method	**ΔT_a**	**ΔT_{mrt}**	**ΔPET**
shading by a building (15 July 2007)	-1.7 K 6 %	-29.0 K 47 %	-13.1 K 31 %
shading by tree canopies (24 July 2008)	-1.7 K 6 %	-32.8 K 51 %	-15.7 K 41 %

The peak ΔT_{mrt} and ΔPET values reveal the potential to mitigate human heat stress by the specific shading device at the local measuring sites. Compared to the Δ value for the shading by the building, the shading by tree canopies causes a slightly higher peak value of ΔT_{mrt} (Table 8) due to the lower total of K^*_{abs} and L^*_{abs}. According to the daytime importance of T_{mrt} for PET on clear-sky summer days (Table 3), the higher peak value of ΔT_{mrt} also causes a higher peak value of ΔPET for shading by tree canopies.

Despite the different peak values of ΔPET for both shading devices, they correspond to a mitigation of the human thermal sensation from "hot" to "slightly warm" according to the

ASHRAE scale (Table 2). Related to mean values of T_a, T_{mrt} and PET over 12-15 CET as the period when shading was effective during both measuring campaigns, the maximal relative reduction is equal for ΔT_a (6 %). However, it is slightly higher for ΔT_{mrt} (51 %) and ΔPET (41 %) in the case of shading by tree canopies compared to ΔT_{mrt} (47 %) and ΔPET (31 %) for shading by the building.

6. Importance of three-dimensional radiant flux densities for human thermal comfort on clear-sky summer days

6.1 Investigation design

Based on two measuring campaigns at selected sites in Freiburg, paper II (Lee et al., 2013) of this thesis mainly concerns the human-biometeorological impacts of two specific shading devices to mitigate daytime heat on clear-sky summer days. In contrast to this relatively limited data collective, paper III (Lee et al., 2014) of this thesis considers all 1-day experiments on human thermal comfort, which were conducted at 95 different sites in Freiburg from 2007 to 2010. As they were focused on the local mitigation of human heat stress during regionally predetermined heat, the experiments were carried out only on clear-sky summer days. They were part of the joint research project KLIMES (Mayer et al., 2008b) and the bilateral German-Israeli project 'The contribution of vegetation to urban heat island mitigation in the global climate change era' (Holst and Mayer, 2011; Lee et al., 2014). As with the investigations described in paper II, both the stationary human-biometeorological measuring system (Fig. 3) and the mobile human-biometeorological measuring system (Fig. 4) were used in the measuring campaigns. After an extensive data quality control, 87 sites with 1-day measurements remained as basis for problem-specific statistical data analyses. This comprehensive experimental data basis is unprecedented worldwide up to now.

The main objectives of paper III are:

- to quantify the importance of SVF as an urban design-dependent variable for the short- and long-wave radiant flux densities from different directions of the three-dimensional (3-D) environment,
- to analyse the varying impact of the 3-D short- and long-wave radiant flux densities on T_{mrt},
- to investigate whether T_a and PET are also influenced by the 3-D radiant flux densities in a similar way.

The results presented in detail in paper III (Lee et al., 2014) and summarised in the following subchapters should have a human-biometeorological relevance for the daytime heat in urban open spaces. Therefore, the radiant flux densities absorbed by the human-biometeorological reference person were considered. As shown in paper II of this thesis, they substantially differ from the radiant flux densities in terms of meteorology due to the standing position of the reference person, which implicates various radiation-related angular factors. To get more reliable results, all absorbed radiant flux densities as well as T_a, T_{mrt} and PET were averaged over the period 10-16 CET. It represents the typical time scale of outdoor heat for Central European citizens on clear-sky summer days.

The discussion of the statistical results has to consider:

- possible cross-correlations between absorbed radiant flux densities,
- different characteristic time scales of T_a, T_{mrt} and PET.

For instance, the characteristic time scale of T_{mrt} (≤ 1 h) is distinctly shorter than that of T_a (about 3 hrs within urban settings in summer).

6.2 $SVF_{90\text{-}270}$ as a human-biometeorological measure of shading

Due to the comprehensive data basis, $SVF_{90\text{-}270}$ at the different sites covers the range from 85 % (almost no shading) to 2 % (extremely pronounced shading). By use of R^2, the results of the statistical data analyses show that the absorbed short-wave radiant flux densities $K_{i,abs}$ are closer correlated with $SVF_{90\text{-}270}$ than with $SVF_{0\text{-}360}$. R^2 is the highest (0.87) for the correlation between K^*_{abs} and $SVF_{90\text{-}270}$ and the lowest (0.82) for the correlation between the absorbed short-wave radiant flux density from the upper half space ($K\downarrow_{abs}$) and $SVF_{90\text{-}270}$.

With respect to the absorbed long-wave radiant flux densities $L_{i,abs}$, the R^2 values point to weak correlations between $L\downarrow_{abs}$ as well as the absorbed long-wave radiant flux density from the lower half space ($L\uparrow_{abs}$), respectively, and $SVF_{90\text{-}270}$ (R^2 = 0.46 for $L\downarrow_{abs}$; R^2 = 0.42 for $L\uparrow_{abs}$). The remaining $L_{i,abs}$ are uncorrelated with $SVF_{90\text{-}270}$.

An increase of shading quantified by a lowering of $SFV_{90\text{-}270}$ leads to a decrease of the absorbed radiant flux densities. Only $L\downarrow_{abs}$ shows a slight increase with a decrease of $SVF_{90\text{-}270}$. The shading stronger affects the absorbed short-wave than the absorbed long-wave radiant flux densities. A shading increase expressed by a 10 % decrease of $SVF_{90\text{-}270}$ causes a lowering of

- $K\downarrow_{abs}$ by 4.3 W/m^2,
- $K_{hor,abs}$ by 20.7 W/m^2,
- $K_{vert,abs}$ by 5.1 W/m^2,
- K^*_{abs} by 25.7 W/m^2.

Taking into account of the magnitude of the R^2 values, the influence of a $SVF_{90\text{-}270}$ change on the absorbed long-wave radiant flux densities can be only estimated for $L\uparrow_{abs}$ and $L\downarrow_{abs}$. A 10 % decrease of $SVF_{90\text{-}270}$ leads to a decrease of $L\uparrow_{abs}$ by 0.1 W/m^2, but an increase of $L\downarrow_{abs}$ by 0.5 W/m^2.

As indicated by the R^2 values (each 0.87), the correlations between the relative K^*_{abs} as well as relative L^*_{abs}, respectively, and $SVF_{90\text{-}270}$ are close, whereby K^*_{abs} and L^*_{abs} are normalised by the total of K^*_{abs} and L^*_{abs}. An increased shading in terms of a 10 % decrease of $SVF_{90\text{-}270}$ leads to

- a decrease of $K^*_{abs}/(K^*_{abs} + L^*_{abs})$ by 3.6 %,
- an increase of $L^*_{abs}/(K^*_{abs} + L^*_{abs})$ by also 3.6 %.

Independent of the magnitude of $SVF_{90\text{-}270}$, the fraction of K^*_{abs} to T_{mrt} is always lower as compared to that of L^*_{abs}. In the case of an undisturbed horizon, where $SVF_{90\text{-}270}$ is near 100 %, the relative K^*_{abs} does not exceed 40 %, while the relative L^*_{abs} does not fall below 60 % (Lee et al., 2014).

T_a averaged over the period 10-16 CET is uncorrelated with both SVF_{0-360} and SVF_{90-270}. Due to the dependence of T_{mrt} on the absorbed radiant flux densities, the correlation between T_{mrt} and SVF_{90-270} is closer (R^2 = 0.77) than between PET and SVF_{90-270} (R^2= 0.33). One reason may be that PET is also influenced by T_a, VP and v, which in turn are uncorrelated with SFV_{90-270}. With respect to shading consequences, these results can be interpreted as follows: a decrease of SVF_{90-270} by 10 % leads to a lowering of

- T_{mrt} by 3.8 K,
- PET by 1.4 K.

For T_a, the tendency of a decrease by 0.2 K is indicated. The results on the correlations between different absorbed radiant flux densities as well as T_a, T_{mrt} and PET, respectively, and SVF_{90-270} have a unique character because similar investigations have not been conducted in any other studies so far.

6.3 Shading effects indicated by absorbed short-wave radiant flux densities

The cross-correlation effect explained in paper III of this thesis is distinctly expressed by the results of linear regressions between different $K_{i,abs}$ and selected human-biometeor-ological variables. For instance, T_{mrt} shows a dependence on K^*_{abs} (R^2 = 0.91), which in turn is mainly determined by the 'forcing' $K\downarrow_{abs}$ (R^2 = 0.94). Related to the correlation between T_{mrt} and SVF_{90-270} as a measure for shading (R^2 = 0.77), the correlations between T_{mrt} and $K_{i,abs}$ are closer. $K_{i,abs}$ considers the absorbed short-wave radiant flux densities in more detail than it is possible by only SVF_{90-270}, which can be regarded as a proxy variable for the radiant flux density from the upper half space related to the skyline (Lee et al., 2014). The linear regressions between T_{mrt} as dependent variable and each $K_{hor,abs}$, $K_{vert,abs}$ and $K\downarrow_{abs}$ as independent variables always reveal the same R^2 value (0.90).

As indicated by the R^2 values (≥ 0.44) presented in paper III, the correlations between PET and $K\downarrow_{abs}$, $K_{hor,abs}$, $K_{vert,abs}$ as well as K^*_{abs}, respectively, are also stronger than the correlation between PET and SVF_{90-270} (0.33). R^2 is the highest (0.51) for the linear regression between PET and $K\downarrow_{abs}$ and the lowest (0.44) for the regression between PET and $K_{hor,abs}$. As a result, it follows that the shading impact on T_{mrt} and PET can be approximately determined by SVF_{90-270} in the daytime on clear-sky summer days. However, the shading effect on both variables can be better analysed by the absorbed radiant flux densities from the three-dimensional urban environment.

The extremely low R^2 values (< 0.05) of linear regressions between T_a and $K_{i,abs}$ might be surprising at first view. But taking account of the different characteristic time scales of these variables and the averaging period over 10-16 CET, they are understandable.

The correlation results for $K_{i,abs}$ as independent variables discussed in paper III of this thesis point to the effectiveness of shading. A decrease of

- $K\downarrow_{abs}$ by 10 W/m^2 leads to a lowering of T_{mrt} by 9.1 K and PET by 4.3 K.
- $K_{hor,abs}$ by 10 W/m^2 leads to a lowering of T_{mrt} by 2.0 K and PET by 0.8 K.

- $K_{vert,abs}$ by 10 W/m^2 leads to a lowering of T_{mrt} by 7.9 K and PET by 3.6 K.
- K^*_{abs} by 10 W/m^2 leads to a lowering of T_{mrt} by 1.6 K and PET by 0.7 K.

With respect to T_a, only the tendency of a lowering by 0.6 K for a decrease of $K\downarrow_{abs}$ by 10 W/m^2 can be determined.

6.4 Shading effects indicated by absorbed long-wave radiant flux densities

As explained in paper III of this thesis, the R^2 values of linear regressions between T_{mrt} and $L_{i,abs}$ are distinctly lower than those of the regressions including $K_{i,abs}$ as independent variables. R^2 is the highest (0.76) for the regression between T_{mrt} and $L\uparrow_{abs}$. For the regressions between T_{mrt} and $L_{hor,abs}$ as well as L^*_{abs}, respectively, both R^2 values amounts to 0.40. R^2 is slightly lower (0.39) for the regression between T_{mrt} and $L_{vert,abs}$. Related to correlations between $L_{i,abs}$ and $K_{i,abs}$, the linear regression between $L\uparrow_{abs}$ and $K\downarrow_{abs}$ shows the highest R^2 (0.59). This again confirms the importance of $K\downarrow_{abs}$ as a 'forcing' variable. R^2 is lower (0.51) for the linear regression between $L\uparrow_{abs}$ and K^*_{abs}. R^2 is always below 0.20 for other regressions between $L_{i,abs}$ and $K_{i,abs}$.

In contrast to $K_{i,abs}$ as independent variables, the R^2 values of linear regressions between T_a and $L_{i,abs}$ are higher. R^2 is the highest (0.68) for $L_{hor,abs}$ and amounts to 0.66 for L^*_{abs} as well as 0.49 for $L_{vert,abs}$ as independent variables. Due to the influence of T_a on PET (Mayer et al., 2008b; Lee et al., 2013, 2014), the partly higher R^2 values of linear regressions between PET and $L_{i,abs}$ compared with those of regressions between PET and $K_{i,abs}$ are reasonable. Among the different $L_{i,abs}$, the linear regressions between PET as dependent variable and $L_{hor,abs}$ (0.73), L^*_{abs} (0.72) as well as $L\uparrow_{abs}$ (0.68) as independent variables show the highest R^2 values.

With respect to the shading potential, a decrease of

- $L\uparrow_{abs}$ by 10 W/m^2 leads to a lowering of T_a by 6.7 K, T_{mrt} by 35.3 K and PET by 20.7 K.
- $L_{hor,abs}$ by 10 W/m^2 leads to a lowering of T_a by 1.3 K, T_{mrt} by 3.2 K and PET by 2.7 K.
- $L_{vert,abs}$ by 10 W/m^2 leads to a lowering of T_a by 7.4 K, T_{mrt} by 20.9 K and PET by 16.0 K.
- L^*_{abs} by 10 W/m^2 leads to a lowering of T_a by 1.1 K, T_{mrt} by 2.8 K and PET by 2.3 K.

In order to get an impression on how realistic a decrease of 10 W/m^2 for the individual $K_{i,abs}$ and $L_{i,abs}$ could be, mean values and the respective standard deviations of the analysed variables are listed in Table 9. These results are summarised as follows:

- Mean $L_{i,abs}$ values always exceed the respective mean $K_{i,abs}$ values. However, the standard deviations of mean $L_{i,abs}$ are always lower than those of respective mean $K_{i,abs}$.
- Mean K^*_{abs} amounts to only 25 % of mean L^*_{abs}, while the standard deviation of mean L^*_{abs} is 37 % of that of mean K^*_{abs}. Taking account of the results for the dependencies of relative K^*_{abs} and relative L^*_{abs} on $SVF_{90\text{-}270}$, it can be concluded that the T_{mrt} magnitude is mainly determined by L^*_{abs}, while the T_{mrt} fluctuations are mainly governed by K^*_{abs}.

Table 9: Mean values of different human-biometeorological variables, averaged over the period 10-16 CET during all measuring days, including their standard deviations, basis: human-biometeorological investigations at different urban sites in Freiburg on clear-sky summer days from 2007 to 2010 (according to Lee et al., 2014)

variable	mean value	standard deviation
T_a	26.3 °C	3.5 K
T_{mrt}	46.5 °C	11.2 K
PET	31.6 °C	6.8 K
$K\downarrow_{abs}$	18.9 W/m^2	11.7 W/m^2
$K_{hor,abs}$	94.1 W/m^2	54.5 W/m^2
$K_{vert,abs}$	21.4 W/m^2	13.5 W/m^2
K^*_{abs}	115.5 W/m^2	67.7 W/m^2
$L\downarrow_{abs}$	24.9 W/m^2	1.7 W/m^2
$L\uparrow_{abs}$	29.9 W/m^2	2.7 W/m^2
$L_{hor,abs}$	409.2 W/m^2	22.0 W/m^2
$L_{vert,abs}$	54.8 W/m^2	3.3 W/m^2
L^*_{abs}	464.0 W/m^2	25.2 W/m^2

- Related to T_{mrt}, $L_{i,abs}$ should be measured as accurately as possible. For instance, an uncertainty of 20 % in the determination of K^*_{abs} does not change T_{mrt} as much as does a 20 % uncertainty in L^*_{abs}. This also holds true for the simulation of $L_{i,abs}$.
- As expected by the standing position of the human-biometeorological reference person and its resulting angular factors (Höppe, 1992, 1999), both mean $K_{hor,abs}$ and $L_{hor,abs}$, respectively, reach higher values than both mean $K_{vert,abs}$ and $L_{vert,abs}$, respectively. Mean $K_{vert,abs}$ amounts to 23 % of mean $K_{hor,abs}$ and mean $L_{vert,abs}$ reaches 13 % of mean $L_{hor,abs}$.
- The magnitude of the mean ratio $K_{hor,abs}$ / $L_{hor,abs}$ is mainly determined by characteristics of the measuring sites within the urban settings. Nearby buildings substantially add to the long-wave radiant flux densities, but less to the short-wave ones.
- Whereas mean $K\downarrow_{abs}$ is dominant (88 %) for mean $K_{vert,abs}$, the fractions of mean $L\downarrow_{abs}$ and mean $L\uparrow_{abs}$ to mean $L_{vert,abs}$ are distinctly lower ($L\downarrow_{abs}$: 45 %, $L\uparrow_{abs}$: 55 %).
- A decrease of 10 W/m^2 of the individual $K_{i,abs}$ and $L_{i,abs}$ by planning measures seems to be more simply realisable for $K_{hor,abs}$ and $L_{hor,abs}$. This also has implications for K^*_{abs} and L^*_{abs}.

6.5 Estimation of T_{mrt} by multiple regressions

Based on the statistical data analyses and a principal component analysis (Lee et al., 2014), T_{mrt} (in °C) averaged over the period 10-16 CET can be estimated by a multiple regression with mean K^*_{abs} and mean $L\uparrow_{abs}$ (both in W/m^2) as independent variables:

$$T_{mrt} = 0.113 \cdot K^*_{abs} + 1.535 \cdot L\uparrow_{abs} - 12.6 \quad (4)$$

Thereby, it has to be considered, that the regression (4) showing R^2 = 0.98 includes the site and weather conditions during the underlying human-biometeorological measurements in Freiburg. This basically means that the regression (4) has no general validity.

Replacing K^*_{abs} by $K{\downarrow}_{abs}$ as the easier available 'forcing' variable, the changed multiple regression

$$T_{mrt} = 0.661 \cdot K{\downarrow}_{abs} + 1.359 \cdot L{\uparrow}_{abs} - 6.7 \quad (5)$$

still has a relatively high R^2 (0.94).

Using 1-h mean values within the period 10-16 CET on clear-sky summer days instead of values averaged over the period 10-16 CET, the regressions (4) and (5) are changed into (Lee et al., 2014):

$$T_{mrt} = 0.039 \cdot K^*_{abs} + 2.535 \cdot L{\uparrow}_{abs} - 35.5 \quad (6)$$

and

$$T_{mrt} = 0.504 \cdot K{\downarrow}_{abs} + 1.977 \cdot L{\uparrow}_{abs} - 22.3 \quad (7)$$

The multiple regressions (6) and (7) have the same R^2 value of 0.93.

6.6 PET dependent on T_{mrt} and T_a

The different R^2 magnitudes of linear regressions between $K_{i,abs}$ as well as $L_{i,abs}$ as independent variables and variables characterising human thermal comfort (Lee et al., 2014) are also reflected by the R^2 values of each linear regression between PET and T_a as well as T_{mrt}, respectively. PET is linearly increasing with both T_a and T_{mrt} (Fig. 6), whereby the correlation between PET and T_{mrt} (R^2 = 0.69) is slightly closer than that between PET and T_a (R^2 = 0.62).

With respect to paper II of this thesis, the low difference between both R^2 values is surprising, as Lee et al. (2013) have obtained a higher R^2 (0.89) of the linear regression between PET and T_{mrt} as well as a lower R^2 (0.59) of the regression between PET and T_a. However, considering that

- Lee et al. (2013) used 1-h mean values within the period 10-16 CET instead of mean values over 10-16 CET in Lee et al. (2014),
- the patterns of the diurnal variations of T_a, T_{mrt} and PET are not quite similar during this period due to their different characteristic time scales,

the R^2 differences are reasonable. For instance, the correlation between T_a and T_{mrt} each averaged over the period 10-16 CET is very weak (R^2 = 0.14), while Lee et al. (2013) obtained R^2 = 0.31 from the respective linear regression based on 1-h mean values within the period 10-16 CET.

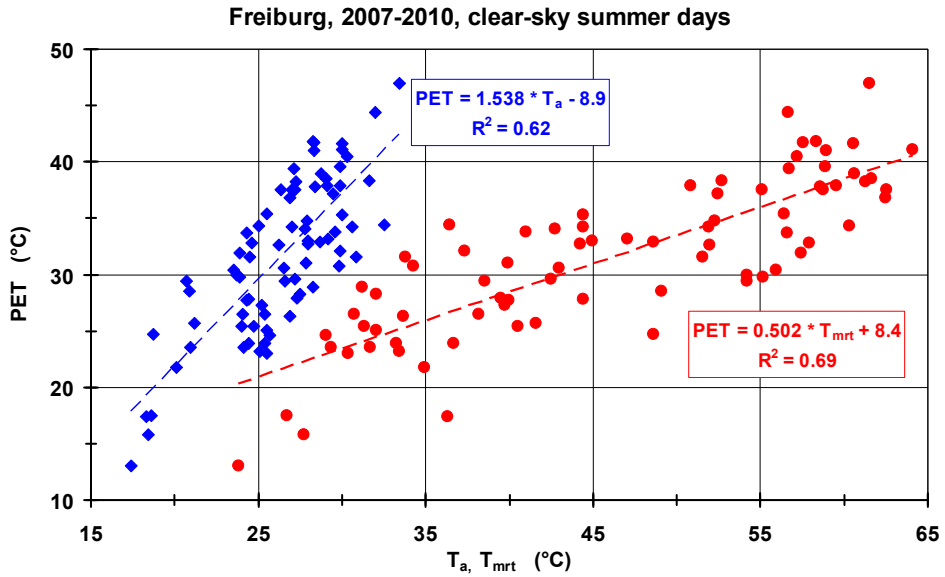

Fig. 6: Relationships between PET and T_a as well as T_{mrt} each averaged over the period 10-16 CET, basis: results of human-biometeorological measurements at different urban sites in Freiburg (according to Lee et al., 2014)

The dominant effect of T_{mrt} and T_a for daytime PET on clear-sky summer days at different urban sites in Freiburg is also indicated by the results of the short-term human-biometeorological experiments carried out by Mayer et al. (2008b) and Lee et al. (2013). It is is confirmed by the multiple regression for PET using mean values over the period 10-16 CET of all measuring campaigns considered in Lee et al. (2014):

$$PET = 0.376 \cdot T_{mrt} + 1.087 \cdot T_a - 14.5 \quad (8)$$

PET, T_{mrt} and T_a are in °C. The resulting R^2 of this regression amounts to 0.95.

If T_{mrt} is unavailable, it can be replaced by $K\downarrow_{abs}$ (in W/m^2):

$$PET = 0.340 \cdot K\downarrow_{abs} + 1.321 \cdot T_a - 9.7 \quad (9)$$

This modification leads to the same R^2 value of 0.95.

According to (2), $K\downarrow_{abs}$ (in W/m^2) can be easily calculated from $K\downarrow$ (in W/m^2):

$$K\downarrow_{abs} = 0.70 \cdot 0.06 \cdot K\downarrow \quad (10)$$

Using 1-h mean values within the period 10-16 CET on clear-sky summer days instead of values averaged over the period 10-16 CET, the regressions (9) and (10) are changed into (Lee et al., 2014):

$$PET = 0.458 \cdot T_{mrt} + 0.793 \cdot T_a - 8.2 \quad (11)$$

and

$$PET = 0.358 \cdot K\downarrow_{abs} + 1.242 \cdot T_a - 6.8 \quad (12)$$

R^2 is 0.98 for the regression (11) and 0.92 for the regression (12), respectively.

A comparison of the R^2 values between the regressions (8) and (11) as well as (9) and (12) points to the possibility to estimate daytime PET by multiple regressions in a sufficient way for complex urban settings on clear-sky summer days. They include only two independent variables characterising the exchange of radiant and sensible heat.

6.7 Impacts of changed albedo of building walls on human thermal comfort

Within urban settings such as street canyons, $K_{hor,abs}$ and $L_{hor,abs}$ as radiant flux densities influencing outdoor human thermal comfort depend on physical features of vertical building walls. In this context, urban planning is interested in information whether daytime thermal comfort can be improved on hot summer days by a change of the short-wave albedo of the building walls. The results on this issue (Fig. 7) obtained by numerical simulations with the ENVI-met model (Bruse and Fleer, 1998; Bruse, 1999), version 3.1, are related to the extreme albedo values of 0.1 and 0.9. They represent the absolutely lower and upper limitation of albedo values, which are possible for building walls.

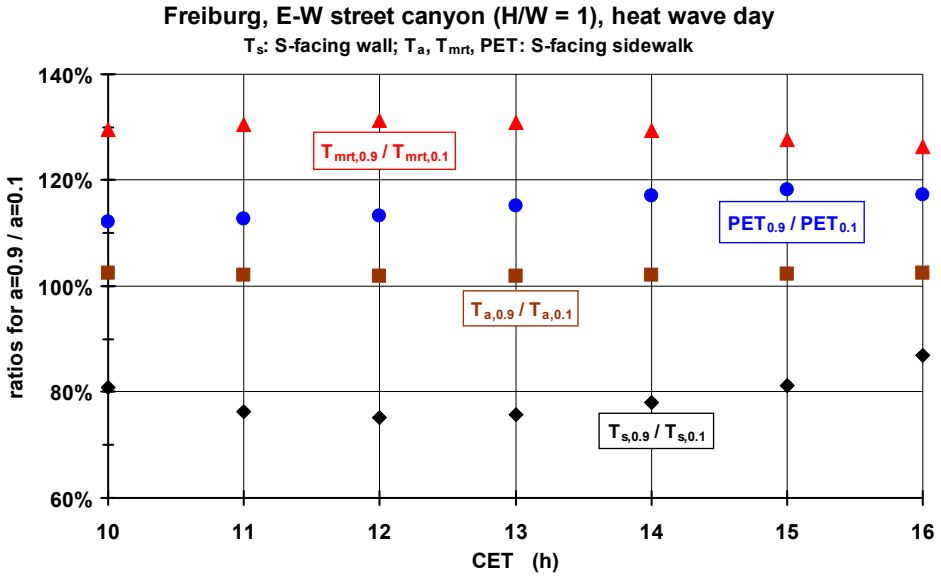

Fig. 7: Ratios of different simulated temperatures T_s of a S-facing wall as well as T_a, T_{mrt} and PET at a S-facing sidewalk for two values (0.1 and 0.9) of the short-wave albedo a of the building walls, basis: ENVI-met simulations for an E-W street canyon in Freiburg on the heat wave day of 4 August 2003 (according to Lee et al., 2014)

In the daytime, an albedo increase from 0.1 to 0.9 leads to a decrease of the surface temperature T_s of a S-facing wall as a higher albedo causes a lower absorption of the short-wave radiant flux density received by the vertical walls. Related to the S-facing wall of an E-W street canyon on a heat wave day, T_s for an albedo of 0.9 is by up to 25 % lower than T_s for an albedo of 0.1.

However, the higher wall albedo leads to an increase of the short-wave radiant flux density reflected from the vertical building walls. Therefore, slightly enhanced T_a values (up to 2 %) are simulated at the S-facing sidewalk of the E-W street canyon. Due to the standing position of the human-biometeorological reference person, the reflected short-wave radiant flux densities from the vertical walls, whose increase is higher than the decrease of the long-wave radiant flux densities from the vertical walls, are mainly responsible for the increase of T_{mrt} and PET. Related to a change of the albedo from 0.1 to 0.9, daytime T_{mrt} is increased by up to 31 % and daytime PET by up to 18 %, respectively, at the S-facing sidewalk. This means that the use of high-albedo materials of building walls resulting in lower T_s values cannot offset the increased radiant load outdoors. These findings are in line with similar results for subtropical conditions obtained by Yang et al. (2011), who also performed ENVI-met simulations.

Using the Green CTTC model, Shashua-Bar et al. (2012) simulated that the increase of the wall albedo from 0.4 to 0.7 leads to a mean T_a change of -0.5 K in the middle of a street canyon in Athens for the period 6-21 LST. The strongest T_a reduction (-0.7 K) was obtained at 15 LST. The additional simulation of PET based on the RayMan model shows a mean reduction of -0.7 K as well as a peak value of -0.9 K at 12 and 15 LST. This result is in contrary to the reported one by the ENVI-met simulation at the S-facing sidewalk of an E-W street canyon. The use of models characterised by a completely different physical basis might be the main reason for divergent results.

The investigation by Erell et al. (2014) about the impact of the wall albedo on pedestrian heat stress within street canyons (H/W = 1) located in four cities of different climate zones is based on a linkage between the CAT and the ITS model. For a hot thermal environment, the simulation results for albedo values of 0.2 (asphalt), 0.45 (concrete) and 0.7 (whitewash) point to a slight T_a reduction with increasing albedo. Using ITS (Index of Thermal Stress) as thermo-physiologically significant assessment index, the simulation study shows the same trend according to Lee et al. (2014). This means that a higher wall albedo reduces T_s, which in turn causes a lower long-wave emission. But this is offset by the increased reflected solar radiation, which leads to a higher ITS value.

Using the version 4.0 BETA of ENVI-met, Deck (2014) simulated the impacts of systematic albedo changes of vertical walls on T_a, T_{mrt} and PET at the S-facing sidewalk of a simple E-W street canyon (H/W = 1). The simulations were performed for the heat wave day of 4 August 2003. The albedo was changed from 0.2 to 0.8 in steps of 0.2. The results for an increment of the albedo by 0.2 reveal that

- T_a is linearly increased by 0.1 K,
- T_{mrt} is almost linearly increased by 4.5 K on average,
- PET is almost linearly increased by 2.7 K on average.

These detailed results confirm the findings by Lee et al. (2014), which are based on a previous version of ENVI-met and only two widely separated values of the wall albedo.

Thus, the net effect of increasing the albedo of urban surfaces may cause an increase in human thermal stress outdoors, which is particularly negative for humans during hot summer

weather like heat waves. The magnitude of the intensification of human thermal stress mainly depends on the range of the albedo modification and the atmospheric background situation.

7. Green coverage changes as a long-term preventive planning measure to mitigate human heat stress at different urban scales

7.1 Numerical simulations for human-biometeorological analyses of green coverage changes

The papers II (Lee et al., 2013) and III (Lee et al., 2014) of this thesis are based on 1-day human-biometeorological experiments conducted on clear-sky summer days from 2007 to 2010 at 87 different sites in Freiburg. Therefore, their results are spot-related and refer to the specific site conditions during the measurements. The human-biometeorological experiments, however, have the advantage that all meteorological variables necessary to calculate PET can be directly or indirectly measured with a relatively high accuracy. It cannot be obtained by numerical modelling. As the six-directional technique has been applied for the determination of T_{mrt}, results of $K_{i,abs}$ and $L_{i,abs}$ are available for all 87 sites in Freiburg (Lee et al., 2014). This relatively extensive data basis enabled a better founded analysis on their importance for T_{mrt} than that in previous studies (see chapter 6).

Besides the experimental approach, PET can be simulated by the use of suited models. Compared to experimental methods, the numerical simulation of PET has an essential advantage (see chapter 4.3), because the assessment of the human thermal comfort conditions is not limited to the current situation. The PET modification in the future caused by regional climate change and urban planning measures can be also simulated. In this context, the importance of planning measures promoting urban greening for the local mitigation of regionally predetermined heat is gradually increasing (Bowler et al., 2010; Shashua-Bar et al., 2011; Chen and Ng, 2013).

Against this background, paper IV (Lee et al., 2015) of this thesis concerns numerical simulations of green coverage changes to mitigate human heat stress. This represents the only method, which provides spatially differentiated results (Müller et al., 2014b; Lee and Mayer, 2015). The main objectives of paper IV are:

- validation of the performance of the applied version of the ENVI-met model,
- analyses of the influences of green coverage changes particularly on the mean daytime patterns of local heat in terms of T_a and human heat stress in terms of T_{mrt} and PET, respectively, related to a heat wave day.

7.2 Setup for numerical simulations using the ENVI-met model

The simulations were conducted by use of the ENVI-met model, version 4.0 BETA released in 2013, including the submodule BioMet, version 1.0 released in 2014, for the calculation of PET. Taking account of the horizontal grid width of 1 m, the simulation domain in a residential district of Freiburg (Fig. 8) had a horizontal size of 150 m · 150 m (2.25 ha). The vertical grid width also amounted to 1 m.

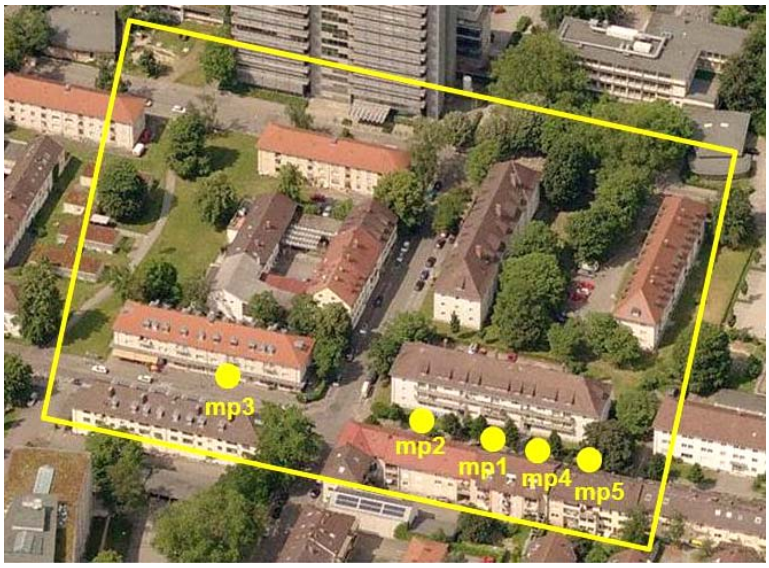

Fig. 8: Simulation domain in Freiburg (yellow outlined) and locations of human-biometeorological measuring sites (mp1 to mp5) on 27 July 2009 (according to Lee et al., 2015)

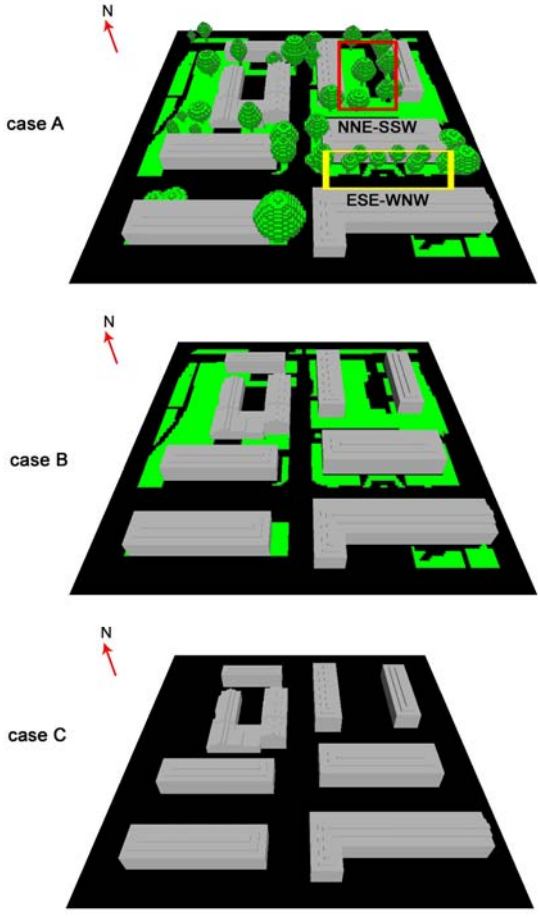

Fig. 9: Visualisation of the area input file for the ENVI-met simulations related to the case A (current land use situation), case B (current land use situation but without all trees) and case C (case B but without any green), according to Lee et al. (2015)

The current land use (case A) in the simulation domain is characterised by two- to three-storey residential houses built in the 1950s, asphalt surfaces, green areas (mostly grassland surfaces) and broad-leaved trees.

In order to investigate the human-biometeorological impacts of the green coverage changes in the simulation domain, a kind of an inverted method was applied. It started with the current land use situation in the simulation domain (case A) and subsequently reduced urban greening in a step-by-step manner by (Fig. 9)

- removing all trees (case B),
- replacing all remaining green areas by asphalt areas (case C).

The numerical simulations were conducted on two clear-sky summer days:

- 27 July 2009 only for the case A,
- 4 August 2003 for all three cases.

On 27 July 2009, T_a, T_{mrt} and PET values were available from experimental investigations at the sites mp1 to mp5 within the simulation domain (Fig. 8). They enabled the validation of the model performance.

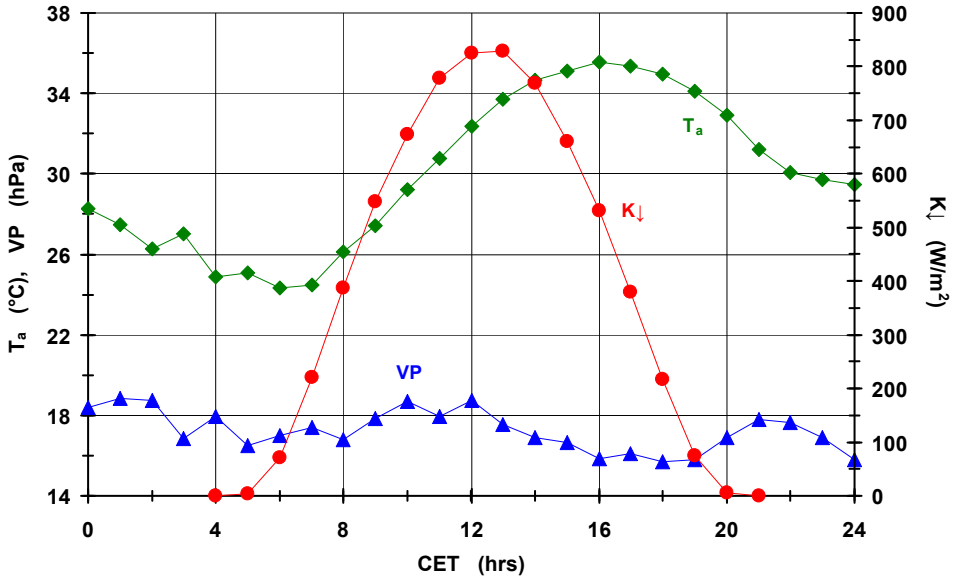

Fig. 10: 1-h mean values of short-wave radiant flux density from the upper half space K↓, air temperature T_a and water vapour pressure VP measured at the urban meteorological station in Freiburg on 4 August 2003

As the 4 August 2003 was embedded into the severe heat wave 2003 in Central and Western Europe (Rebetez et al., 2006), it represents the atmospheric conditions, which will be characteristic of the future summer weather in Central Europe as of the mid-21st century (Beniston, 2013). The local atmospheric conditions in Freiburg on this heat wave day are characterised by 1-h mean values of K↓, T_a and VP (Fig. 10) recorded at the urban meteoro-

logical station in Freiburg, which is situated at the roof of the high-rise building at the northern border in Fig. 8.

According to the cases A to C, the potential of specific green coverage changes for the spatial mitigation of human heat stress on the heat way day 4 August 2003 has been analysed in paper IV (Lee et al., 2015) of this thesis.

7.3 Validation of the performance of the ENVI-met model, version 4.0 BETA

The validation of results of ENVI-met simulations at the human-biometeorological reference height of 1.1 m a.g.l. refers to 1-h values of T_a, T_{mrt} and PET in the period 10-16 CET of 27 July 2009, i.e. it is based on 35 pairs of simulated and experimentally determined values of T_a, T_{mrt} and PET, respectively. Similar validations performed by previous versions of the ENVI-met model are based on a lower number of pairs, which ranged between 8 and 24 (Emmanuel et al., 2007; Chow and Brazel, 2012; Ng et al., 2012; Chen and Ng, 2013; Srivanit and Hokao, 2013; Yang et al., 2013; Middel et al., 2014; Müller et al., 2014b; Skelhorn et al., 2014). They mostly refer to T_a. Only one validation includes T_{mrt} (Chen and Ng, 2013), while PET has not been considered in validation studies up to now.

The results of the model validation described in detail in paper IV (Lee et al., 2015) of this thesis show that the ENVI-met simulations overestimate T_a by a nearly constant amount of about 0.2 K (Table 10). Related to the ranges of experimentally determined T_{mrt} and PET values, the overestimations of T_{mrt} and PET are increasing with their magnitude. They range from 1.8 K for $T_{mrt,experiment}$ = 30 °C to 3.3 K for $T_{mrt,experiment}$ = 60 °C and 2.8 K for $PET_{experiment}$ = 25 °C to 3.6 K for $PET_{experiment}$ = 40 °C, respectively.

Table 10: Quantitative measures of the performance of the ENVI-met and the RayMan model with simulated and experimentally determined data (sample size: each 35), coefficients a_1 and a_2 of linear regressions (form: $x_{sim} = a_1 \cdot x_{meas} + a_2$), R^2: coefficient of determination, RMSE: root mean square error, RMSEs: systematic root mean square error, RMSEu: unsystematic root mean square error, d: Willmott's index of agreement (according to Lee et al., 2015)

	ENVI-met (4.0 BETA)						
	a_1	a_2	R^2	RMSE (K)	RMSEs (K)	RMSEu (K)	d
T_a	0.996	0.3	0.85	0.66	0.19	0.62	0.95
T_{mrt}	1.050	0.3	0.86	5.49	2.39	4.94	0.95
PET	1.052	1.5	0.77	3.98	3.06	2.52	0.84
	RayMan Pro						
T_a	-	-	-	-	-	-	-
T_{mrt}	0.292	37.5	0.40	12.63	11.98	4.06	0.64
PET	0.431	22.6	0.50	6.40	6.13	1.89	0.60

The accuracy of the ENVI-met simulations is examined by different measures for model evaluation (Table 10) used in Yang et al. (2013). The R^2 values point to the strong correlation

between simulated and experimentally determined T_{mrt} values (R^2 = 0.86) and slightly lower correlations between simulated and measured T_a values (R^2 = 0.85) as well as PET values (R^2 = 0.77), respectively. Previous validations of simulated T_a values performed by use of different versions of the ENVI-met model show R^2 values in the range between 0.75 (Chen and Ng, 2013) and 0.97 (Müller et al., 2014b). Besides the used version of the ENVI-met model, it seems that the urban micro-environment at the underlying measuring sites also influence the simulation performance.

The root mean square error RMSE for T_a, T_{mrt} and PET ranges from 0.66 to 5.49 K, with higher values for T_{mrt} (5.49 K) and PET (3.98 K) as well as a lower value for T_a (0.66 K). With respect to a “good” model, the magnitude of the systematic root mean square error RMSEs should approach zero, while the value of the unsystematic root mean square error RMSEu should approach RMSE (Yang et al., 2013). RMSEs is relatively low for T_a (0.19 K), but higher for T_{mrt} (2.39 K) and PET (3.06 K). Compared to RMSE, the RMSEu values are lower by 6 % for T_a, by 10 % for T_{mrt} and by 37 % for PET. Willmott's index of agreement index d describes how error-free variables are simulated by a model. A perfect prediction for a variable is indicated by d = 1.0. In this validation process, d ranges from 0.84 (for PET) to 0.95 (for T_a and T_{mrt}). That implies that the applied version of the ENVI-met model reasonably approximates the experimentally determined results of T_a, T_{mrt} and PET.

In order to confirm the simulation capacity of the ENVI-met model, version 4.0 BETA, a comparative validation was performed by use of the spot-related model RayMan Pro, version 2.0 (Matzarakis et al., 2010), which is currently also applied worldwide for the simulation of T_{mrt} and PET (Taleghani et al., 2015). The measurements at the sites mp1 to mp5 (Fig. 8) provided the necessary T_a, v, VP values. $SVF_{0\text{-}360}$ data for these sites were calculated by the use of fish-eye photos. Related to the atmospheric conditions in the daytime of 27 July 2009 and the specific measuring sites, RayMan overestimates T_{mrt} by 16.3 K for experimentally determined T_{mrt} = 30 °C and underestimates T_{mrt} by 5.0 K for experimentally determined T_{mrt} = 60 °C (Table 10). Therefore, it is understandable that the RayMan model overestimates PET by 8.4 K for measured PET = 25 °C and underestimates PET by 0.2 K for measured PET = 40 °C. The R^2 values of the linear regressions show that the correlations between 1-h measured and experimentally determined T_{mrt} as well as PET values are distinctly closer for the ENVI-met than the RayMan model.

Taking account of the statistical measures to analyse the accuracy of the RayMan model (Table 10), the ENVI-met model, version 4.0 BETA, including the submodule BioMet, version 1.0, seems to be better suited than the RayMan model to simulate human thermal comfort by T_{mrt} and PET in complex urban settings during daytime summer heat.

7.4 Spatial human-biometeorological effects of green coverage changes in different urban sections

The investigation of the human-biometeorological mitigation potential of urban greening on a heat wave day is focused on T_a, T_{mrt} and PET. The applied inverted method takes the current land use situation (Table 11) in the simulation domain as a starting point (case A). Based on the case C, the simulation results of T_a, T_{mrt} and PET in the case B provide an estimation of the mitigation effect by introducing grassland in a completely sealed urban district. An additional implementation of trees like in the case A enables a differentiation of the impacts between trees and grassland. However, the fractions of grassland and trees, respectively, were not randomly selected. In order to obtain realistic mitigation results for an existing residential district, they were predetermined by the current land use situation (case A) in the simulation domain.

Table 11: Fractions of different land uses within the simulation domain (2.25 ha: 100 %) in Freiburg for three scenarios applied in the ENVI-met simulations on 4 August 2003 (according to Lee et al., 2015)

	scenarios		
	case A	**case B**	**case C**
land use situation	current land use	case A but without all trees	case B but without any green
building surfaces	30.5 %	30.5 %	30.5 %
asphalt surfaces	41.3 %	41.3 %	69.5 %
grassland surfaces	28.0 %	28.2 %	0.0 %
total of the cross sectional area of all trunks	0.2 %	0.0 %	0.0 %
total of the highest cross sectional area of each crown	16.6 %	0.0 %	0.0 %

The simulation results of T_a, T_{mrt} and PET are discussed in detail in paper IV (Lee et al., 2015) of this thesis. Averaged over the daytime period 10-16 CET and nocturnal period 22-05 CET, they refer not only to the whole simulation domain but also to selected sections, which are characterised in Table 12:

- ESE-WNW street canyon indicated in Fig. 9, case A,
- NNE-SSW street canyon indicated in Fig. 9, case A,
- SSW facing sidewalk of the ESE-WNW street canyon,
- NNE-facing sidewalk of the ESE-WNW street canyon.

Among both sidewalks, only the SSW-facing sidewalk is covered by street trees and grassland. The fraction of grassland at the NNE-facing sidewalk is relatively low.

Table 12: Characteristics of the ESE-WNW and NNE-SSW street canyon within the simulation domain in Freiburg in the case A

	ESE-WNW			NNE-SSW
	total	**SSW-facing sidewalk**	**NNE-facing sidewalk**	**total**
length L (m)	56	56	56	48
width W (m)	20	3	3	29
horizontal area A (m^2)	1120	168	168	1392
building height H (m)	10.3	-	-	9.6
H/W	0.5	-	-	0.3
fraction of asphalt in A (%)	71	65	93	35
fraction of grassland in A (%)	28	33	7	64
fraction of the total of the cross sectional area of all trunks in A (%)	1	2	0	1
fraction of the total of the highest cross sectional area of each crown in A (%)	26	66	0	41

The extent of the areas shaded by trees depends on (i) their canopy characteristics (e.g. dimensions) and (ii) the current sun position. With respect to the geographical location of Freiburg (47° 59' N, 7° 51' E), the solar altitude at the simulation day of 4 August 2003 varied between 46° at 10 CET (azimuth: 121°) and 38° at 16 CET (azimuth: 252°). Its peak value during this period was 59°.

The simulation results can be summarised as follows:

- The magnitude of the simulated spatial and temporal variations of T_a, T_{mrt} and PET within the whole simulation domain and its selected sections varies in dependence on the local morphology, type of green coverage and time of day. Due to energetic reasons (Souch and Grimmond, 2006), this magnitude is larger in the daytime than at night.
- Grassland instead of asphalt areas contributes to a stronger reduction of mean daytime T_a than the addition of trees to grassland. For the whole simulation domain, the fraction of asphalt surfaces is reduced from the case C (69.5 %) by 28.2 % due to the grassland coverage in the case B. This causes a lowering of mean daytime T_a by 1.1 K and mean nocturnal T_a by 0.7 K.
- The fractions of building, asphalt and grassland surfaces do not differ between the cases A and B. However, mature trees are included in case A. Their total of the highest cross sectional area of each crown amounts to 16.6 % of the area of the simulation domain (Table 11), while the total of the cross sectional area of all trunks is 0.2 %. Related to this situation, trees cause a reduction of mean daytime T_a by 0.6 K and mean nocturnal T_a by 0.2 K.
- For the whole simulation domains, a green coverage like in case A reduces mean daytime T_a by 1.7 K and mean nocturnal T_a by 0.9 K.

- With respect to the selected sections, the T_a lowering is more pronounced in the NNE-SSW street canyon due to its higher fraction of the total of the highest cross sectional area of each tree crown (Table 12). With respect to the case C, the grassland coverage (case B) leads to a reduction of mean daytime T_a by 1.4 K and mean nocturnal T_a by 0.7 K. The additional implementation of trees (case A) causes a mean T_a lowering of 0.8 K in the daytime and 0.5 K at night.
- Related to the case C, the green coverage of the case A in the NNE-SSW street canyon, where mean daytime T_a (34.5 °C) is lower than in the whole simulation domain (35.5 °C), reduces mean daytime T_a by 2.2 K. This is higher than that for the whole simulation domain (1.7 K). At night, mean T_a of the case C is lower (29.1 °C) in the whole simulation domain than in the NNE-SSW street canyon (29.7 °C). The complete green coverage of the case A in the NNE-SSW street canyon leads to a reduction of mean nocturnal T_a by 1.2 K, which is higher than that for the whole simulation domain (0.9 K).
- In contrast to the results of mean T_a, mean daytime T_{mrt} is strongly lower by tree-induced shading effects than by only grassland. Comparing the cases A and B as well as the cases B and C, the total of the highest cross sectional area of each tree crown leads to a reduction of mean daytime T_{mrt} by 6.6 K, while only grassland causes a lowering of mean daytime T_{mrt} by 2.4 K.
- Due to the relatively higher number of mature trees, the impact of the tree canopies in the NNE-SSW street canyon on the T_{mrt} reduction is stronger (11.1 K) than that in the whole simulation domain. Grassland itself in this street canyon leads to a lowering of T_{mrt} by 4.2 K.
- At night, trees cause a slight increase of mean T_{mrt} below the canopies, which is 0.4 K in the whole simulation domain and 0.8 K in the NNE-SSW street canyon. Grassland itself, however, reduces mean nocturnal T_{mrt} by 1.5 K in the whole simulation domain and by 2.1 K in the NNE-SSW street canyon, respectively.
- The pattern of the PET simulation results is similar to that of T_{mrt}. Tree canopies lower mean daytime PET by 3.0 K in the whole simulation domain and by 5.3 K in the NNE-SSW street canyon. The reduction of mean daytime PET due to only the impact of grassland amounts to 1.0 K in the whole simulation domain and 2.1 K in the NNE-SSW street canyon. At night, the tree coverage does not change mean PET in the whole simulation domain, but slightly increases mean PET by 0.2 K in the NNE-SSW street canyon. The grassland impact also leads to a lowering of mean PET by 1.1 K in the whole simulation domain and by 1.4 K in the NNE-SSW street canyon, respectively.
- In the daytime, the mean PET values for the analysed cases point to a human thermal sensation in the range "hot" according to Table 2. With respect to the heat wave day, the green coverage changes from case C to case A lead to an attenuation of the thermophysiologically significant heat within the "hot" range. Only in the NNE-facing sidewalk, the mean daytime PET values are in the thermal sensation range "warm" for each land use scenario. At night, mean PET values indicate thermally comfortable outdoor conditions for all three cases.

Related to the thermal importance of the orientation of street canyons, previous investigations (Ali-Toudert and Mayer, 2006; Holst and Mayer, 2011) have pointed to the pronounced daytime heat stress for pedestrians at the S-facing sidewalk of an E-W street canyon. In addition to this, the numerical simulations by Lee et al. (2015) also enable the analyses of the human-biometeorological effects of local green coverage changes at these sites.

With respect only to the daytime mean values, the essential simulation results of T_a, T_{mrt} and PET at both sidewalks (Table 13) are:

- In each case, the mean values of T_a, T_{mrt} and PET are higher at the SSW-facing sidewalk than those at the NNE-facing sidewalk. For T_a, this difference amounts to 1.5 K in the case A, 1.8 K in the case B and 2.3 K in the case C. The T_{mrt} difference between both sidewalks is 28.3 K in the case A, 32.9 K in the case B and 33.7 K in the case C. For PET, this difference reaches 10.3 K in the case A, 11.8 K in the case B and 11.6 K in the case C.
- The T_a mitigation at the SSW-facing sidewalk is 0.8 K for grassland (case C - case B) and 0.7 K for additional trees (case B - case A). At the NNE-facing sidewalk, the respective values are 0.3 K for grassland and 0.4 K for additional trees. In total, the T_a mitigation potential reaches 1.5 K at the SSW-facing sidewalk and 0.7 K at the NNE-facing sidewalk.

Table 13: Mean values (in °C) of the simulated T_a, T_{mrt} and PET for different land use scenarios at both sidewalks (each 168 m^2) of an ESE-WNW street canyon in the period of 10-16 CET on the heat wave day of 4 August 2003 (according to Lee et al., 2015)

	T_a		**T_{mrt}**		**PET**	
land use scenarios	SSW-facing sidewalk	NNE-facing sidewalk	SSW-facing sidewalk	NNE-facing sidewalk	SSW-facing sidewalk	NNE-facing sidewalk
case A	35.6	34.1	71.1	42.8	47.8	37.5
case B	36.3	34.5	76.0	43.1	49.8	38.0
case C	37.1	34.8	77.2	43.5	50.0	38.4

- Related to the completely sealed situation (case C), the T_{mrt} lowering at the SSW-facing sidewalk amounts to 1.2 K for grassland and 4.9 K for additional trees. At the NNE-facing sidewalk, the respective values reach 0.4 K for grassland and 0.3 K for additional trees. The total T_{mrt} mitigation potential is 6.1 K at the SSW-facing sidewalk and 0.7 K at the NNE-facing sidewalk.
- The PET mitigation at the SSW-facing sidewalk amounts to 0.2 K for grassland and 2.0 K for additional trees. At the NNE-facing sidewalk the respective values reach 0.4 K for grassland and 0.5 K for additional trees. The total T_{mrt} mitigation potential is 2.2 K at the SSW-facing sidewalk and 0.9 K at the NNE-facing sidewalk.

7.5 Human-biometeorological effects of green coverage changes at a specific site on the SSW-facing sidewalk within an ESE-WNW street canyon

The simulation results presented so far are daytime mean values (10-16 CET) for selected sections of the simulation domain. They are extended by 1-h mean T_a, T_{mrt} and PET simulation results, which are related only to the site mp5 (Fig. 8) on the SSW-facing sidewalk within the ESE-WNW street canyon (Fig. 9, case A). This site is directly situated below the crown of a maple tree with a height of 17 m. The highest diameter of its crown is 10 m. Besides this tree, comparable street trees are situated on the SSW-facing sidewalk. Therefore, this site is well-suited for the spot-related analysis of the mitigation potential by green coverage changes on a heat wave day.

The T_a, T_{mrt} and PET values simulated for the current land use (case A) are well in line with the same values determined experimentally at the site mp5. The simulation results of T_{mrt} and PET (Fig. 11) show that this site is completely shaded by the tree canopy from 11 to 14 CET. Related to the 1-h mean values at 9 CET, the reduction of T_{mrt} is 34.9 K (53 %) at 11 CET, while PET is lowered by 12.8 K (30 %). This corresponds to a change of the human thermal sensation from "hot" to "slightly warm" (Table 2). In contrast to the behaviour of T_{mrt} and PET, T_a does not reflect the shading situation.

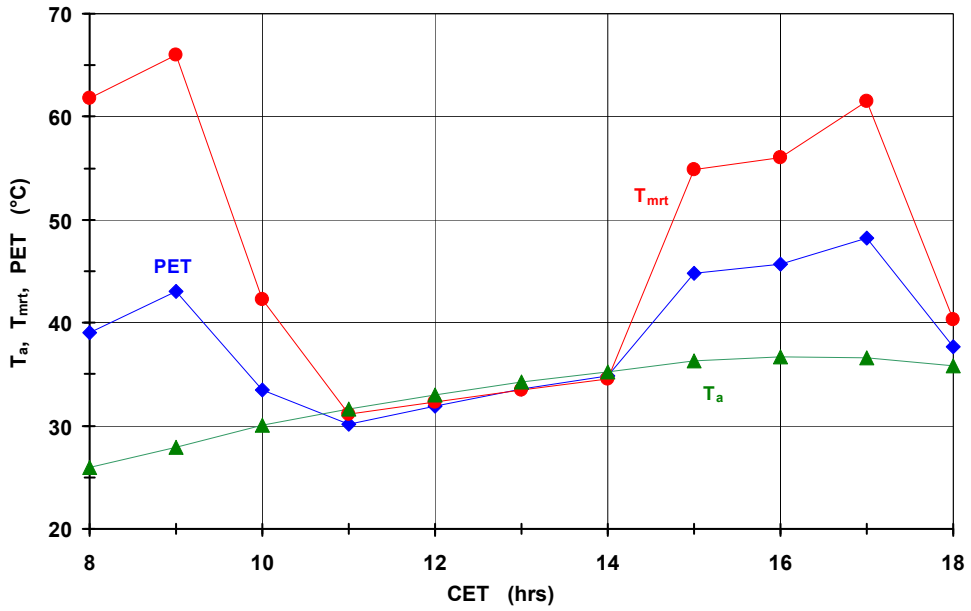

Fig. 11: Simulated 1-h T_a, T_{mrt} and PET values at the site mp5 on the SSW-facing sidewalk within the ESE-WNW street canyon in a residential district of Freiburg, heat wave day of 4 August 2003, current land use (case A)

The removal of all trees (case B) leads to an increase of T_a, which ranges between 0.8 K and 1.8 K in the period 8-18 CET (Fig. 12). An additional replacement of the remaining grassland by asphalt surfaces (case C) causes an enhancement of T_a between 1.9 K and 3.9 K. Except

for the period 14-16 CET, grassland has a higher share in the T_a reduction than the removal of the trees.

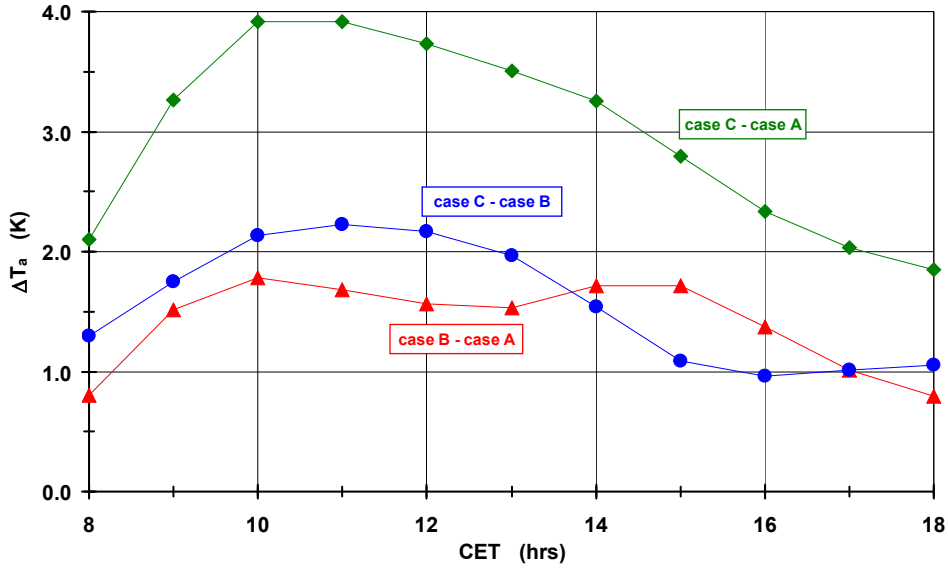

Fig. 12: Simulated 1-h T_a differences between different land use scenarios at the site mp5 on the SSW-facing sidewalk within the ESE-WNW street canyon in a residential district of Freiburg, heat wave day of 4 August 2003

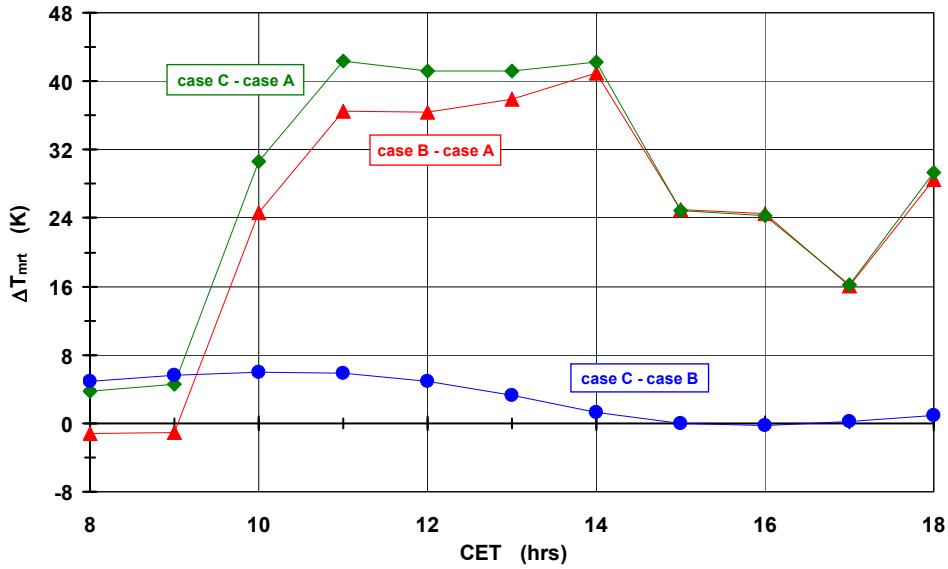

Fig. 13: Simulated 1-h T_{mrt} differences between different land use scenarios at the site mp5 on the SSW-facing sidewalk within the ESE-WNW street canyon in a residential district of Freiburg, heat wave day of 4 August 2003

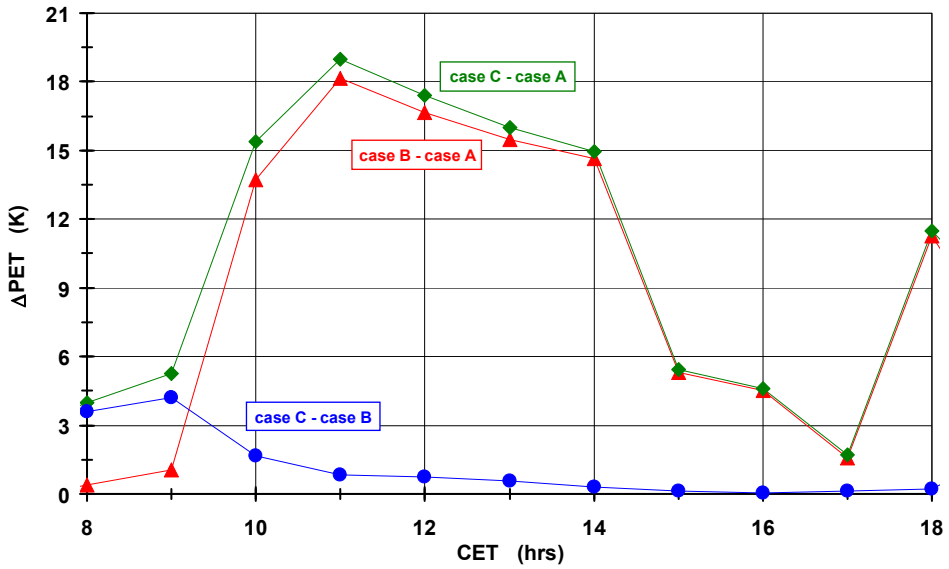

Fig. 14: Simulated 1-h PET differences between different land use scenarios at the site mp5 on the SSW-facing sidewalk within the ESE-WNW street canyon in a residential district of Freiburg, heat wave day of 4 August 2003

As expected, the response of T_{mrt} on the removal of all trees is more pronounced (Fig. 13) than that of T_a. The T_{mrt} difference (ΔT_{mrt}) between the cases B and A is suddenly increasing when the site becomes shaded. ΔT_{mrt} exceeds the threshold value of 36 K from 11-14 CET and reaches its peak value of 40.9 K at 14 CET. The additional replacement of the remaining grassland by asphalt surfaces slightly increases ΔT_{mrt}, which ranges between 1.3 K at 14 CET and 5.9 K at 11 CET. Compared to the case C, the current green coverage (case A) at the site mp5 leads to a whole reduction of T_{mrt} between 41.1 K and 42.4 K in the period 11-14 CET.

Due to the governing human-biometeorological processes on clear-sky summer days, the patterns of ΔPET (Fig. 14) are quite similar to those of ΔT_{mrt}. Related to the scenario with only buildings and asphalt surfaces (case C), the current green coverage (case A) at the investigation site causes a PET lowering, which exceeds 15 K in the period 10-14 CET. Its peak value is 19.0 K at 11 CET. The biggest fraction comes from the shading by tree canopies, which ranges between 13.7 K (10 CET) and 14.7 K (14 CET) as well as shows a peak value of 18.1 K at 11 CET. The mitigation effect by grassland is below 1.7 K in the period 10-14 CET.

Corresponding with the simulation results in different sections of the simulation domain, the simulation results for this specific site reveal that the T_a-related mitigation effect of grassland is slightly higher than that of tree canopies. In terms of T_{mrt} and PET as characteristics for human thermal comfort, tree canopies have a distinctly higher mitigation potential than it is possible for only grassland. For a heat wave day, it could be quantified by these ENVI-met simulations.

7.6 Regression analyses

For experimentally determined 1-h mean values, the results in Table 3 contain R^2 values of linear regressions between PET and further variables in order to get an impression about the correlation between PET and the selected variable on clear-sky summer days. Based on 200 pairs of values in the daytime period 10-16 CET, the R^2 values point to the closest correlation between PET and T_{mrt} (R^2 = 0.89), while the correlation between PET and T_a is distinctly lower (R^2 = 0.59).

Based on the 1-h mean simulation results of each grid within the whole simulation domain, where no buildings are situated, the correlations between PET and T_{mrt} are also closer in each case than those between PET and T_a (Table 14). For the case A, R^2 of the linear regression between PET and T_{mrt} is slightly higher (R^2 = 0.91) on the heat wave day than that on clear-sky summer days (R^2 = 0.89). R^2 of the regressions between PET and T_{mrt} is reduced in the cases B and C, whereby the R^2 difference between the cases A and B is higher than that between the cases B and C. One reason might be that the near-surface wind field is less disturbed by obstacles like trees in the case C than in the case A. This contributes to the small lowering of R^2 in the case C as the importance of v for PET is slightly increasing.

Table 14: Coefficient of determination R^2 of linear regression functions f between 1-h mean values of T_a, T_{mrt} and PET, basis: 1-h mean values in the period 10-16 CET from the numerical simulations in the whole simulation domain on the heat wave day of 4 August 2003, 109480 pairs of values in each case

scenarios	R^2		
	PET =		T_{mrt} =
	f (T_{mrt})	f (T_a)	f (T_a)
case A	0.91	0.13	0.14
case B	0.83	0.08	0.13
case C	0.80	0.08	0.12

Due to the different characteristic time scales of PET, T_{mrt} and T_a (Lee et al., 2014), the relatively low R^2 values (Table 14) of the linear regressions between PET and T_a as well as T_{mrt} and T_a are not surprising. They reflect that linear correlations between PET and T_a as well as T_{mrt} and T_a do not really exist for the extreme weather conditions on a heat wave day.

As the data volume of the simulation results is relatively extensive, the linear regression between PET and T_{mrt} enables a further quantification of the importance of T_{mrt} for PET. This meets a question, which is often put by urban planning departments. Related to

- the daytime period 10-16 CET of the heat wave day of 4 August 2003,
- the case A of the whole simulation domain and the ESE-WNW street canyon as a selected section of the whole simulation domain, respectively,

a 1-h PET change of 1.0 K corresponds a 1-h T_{mrt} change of 2.4 K and 2.6 K, respectively. These results show a slight dependence on the characteristics of the investigation area.

The multiple regression (11) to estimate PET is based on an experimental data collective obtained on clear-sky summer days (Lee et al., 2014). Using the more extensive simulation results for the case A on the heat wave day of 4 August 2003, the similar regression is:

$$PET = 0.426 \cdot T_{mrt} + 0.024 \cdot T_a + 18.1 \quad (13)$$

PET, T_{mrt} and T_a represent 1-h mean values in the period 10-16 CET, each in °C. R^2 (0.91) of the multiple regression (13) is slightly lower than R^2 (0.98) of the multiple regression (11).

Altogether, the results of these regression analyses reconfirm the elevated importance of T_{mrt} for thermo-physiological indices such as PET in the daytime of summer. It seems to be more pronounced on heat wave days than on current clear-sky summer days. This reaffirms that planning measures to mitigate local heat impacts on humans in the daytime should be primarily aimed at the reduction of T_{mrt}. The results presented in the papers of this thesis quantify the reduction potential of T_{mrt} by shading not only for current clear-sky summer days but also for heat wave days, which will represent a major challenge for urban planning in the future.

8. Discussion

Based on the results of

- retrospective analyses of climate variables,
- numerical simulations on the future regional climate,

the long-term atmospheric conditions over Central Europe point to a really occurring regional climate change (Rebetez et al., 2006, 2009; Beniston et al., 2007; Ballester et al., 2010; Barriopedro et al., 2011; Christidis et al., 2015). It can be characterised by partly different patterns of the climate variables. Among them, the results of T_a currently reveal the highest reliability (Luterbacher et al., 2004).

Independent of their definition, the intensification of heat waves in the future, which is projected by ensembles of regional climate models (Koffi and Koffi, 2008), should be seriously noticed by planning authorities in Central European cities (Grimmond et al., 2010a; Rannow et al., 2010; Masson et al., 2013; Oleson et al., 2013).

Their efforts to develop and apply measures aiming at the maintenance of local human thermal comfort even under regionally predetermined severe heat (Thorsson et al., 2011; Carter et al., 2015; Voskamp and van de Ven, 2015) have to be supported by findings of urban human-biometeorology (Ali-Toudert et al., 2006, 2007a; Chen and Ng, 2012). This includes the training of urban planners to acquaint them with the necessity to use a thermo-physiologically significant index such as PET to quantify the perception of heat by citizens (Dütemeyer et al., 2013a, 2013b).

Usually, urban planners are talking about 'temperature' as a measure for heat (Reuter and Kapp, 2012; Pascal et al., 2013). At first view, they don't understand the sense for the specification of 'temperature'. However, taking account of physical processes and resulting phenomena within the urban canopy layer, urban planners mostly realize that 'temperature' is too general. For instance, they agree to replace 'temperature' by T_a in the case of air temperature is meant.

With respect to heat, practical urban planning still feels that the impact-related heat can be described by only T_a (Reuter and Kapp, 2012), although findings in urban human-biometeorology consistently indicate that the human perception of heat can be quantified only by thermo-physiological assessment indices derived from the human heat budget. This implies that urban planners should be better informed about the progress in urban human-biometeorology (Albers et al., 2015; Groot et al., 2015).

In order to demonstrate the different importance of T_a and PET exemplarily for an urban street canyon, Fig. 15 shows a schematic overview of heat fluxes within an urban street canyon (Grimmond et al., 2010b). They are combined in the canyon heat budget, which leads to the quantification of the atmospheric heat conditions within the street canyon by T_a. The human-biometeorological concept to quantify the perception of heat includes a standing reference person, which is represented in Fig. 16 by a student within the street canyon. This reference person may be interpreted as a kind of nesting of a specific volume characterised by additional heat fluxes into the volume of the street canyon.

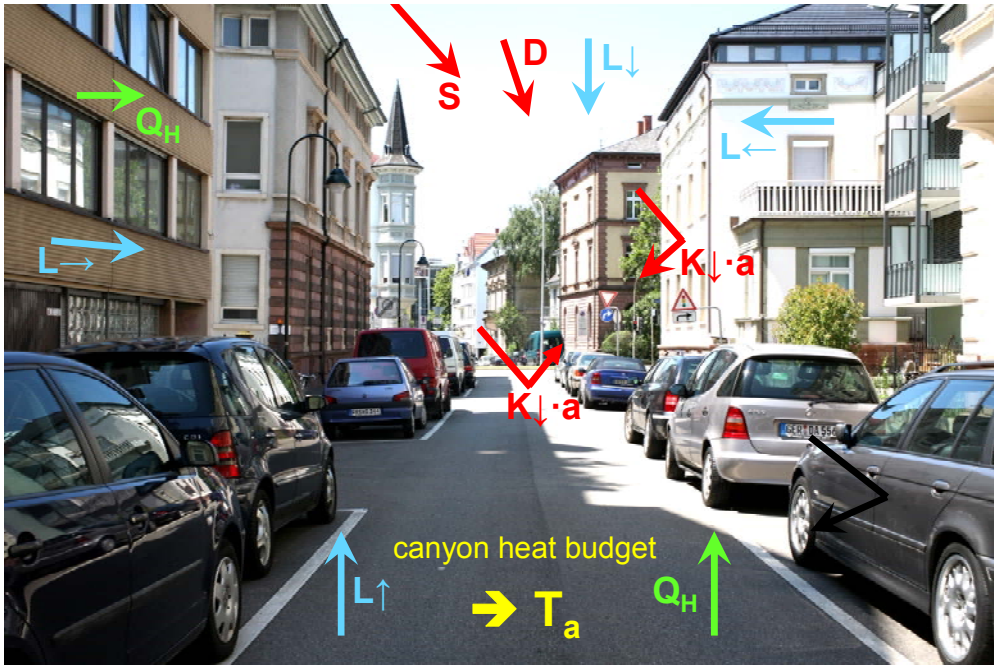

Fig. 15: Schematic overview of heat fluxes within an urban street canyon leading to the quantification of the atmospheric heat conditions by T_a (S: direct solar radiation, D: diffuse sky radiation, a: surface albedo, $K_{\downarrow} \cdot a$: reflected short-wave radiant flux density, L↓: long-wave radiant flux density from the upper half space, L↑: long-wave radiant flux density from the lower half space, L→ and L←: long-wave radiant flux densities from vertical walls, Q_H: sensible heat flux)

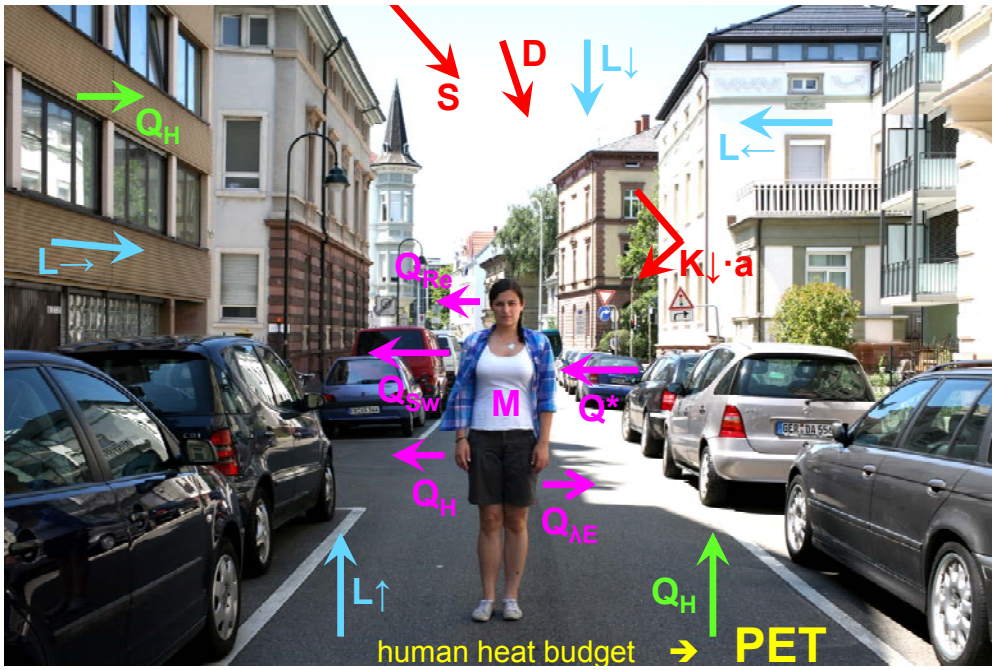

Fig. 16: Schematic overview of both heat fluxes within an urban street canyon and human heat fluxes leading to the quantification of the human perception of heat by PET (M: metabolic rate, $Q_{\lambda E}$: latent heat flux, Q*: net radiation, Q_{Sw}: heat flux due to sweat evaporation, Q_{Re}: heat flux due to respiration)

The heat fluxes of the reference person depend on both the atmospheric environmental conditions within the street canyon as well as physical and physiological features of the reference person. The human heat fluxes are combined in the human heat budget, which lead to PET as a quantitative measure for the human perception of heat within this street canyon. Thereby, it has to be considered that the human-biometeorological assessment concept for heat is aimed at the evaluation of urban spaces. This means that it is based on the stationary form of the human heat budget (Höppe, 1984, 1993; Mayer, 1993). For urban planning, this cannot be regarded as a disadvantage, as urban planning is primarily interested in the thermal assessment of urban spaces. For detailed analyses on dynamic heat aspects, e.g., how the human perception of heat is changing due to the passage from a sunny to a shaded sidewalk of a street canyon, a dynamic form of the human heat budget including specific thermo-physiological assessment indices such as the mean skin temperature has to be applied (Höppe, 1993, 1997, 2002; Vanos et al., 2010; Liu et al., 2011; Katavoutas et al., 2015).

As already mentioned, severe heat in summer will be a normal atmospheric background condition for Central European cities in the future. Related to its impacts on humans, it can be intensified or mitigated within the urban environment depending on building as well as street design and urban green coverage. Individuals have different opportunities to reduce their thermal stress level during a current heat period. In place of the vulnerable demographic group 'children' (Vanos, 2015), this is exemplarily shown for a young child, which protects its head against direct solar radiation by a peaked cap and cools down itself in a small streamlet in the city of Freiburg (Fig. 17).

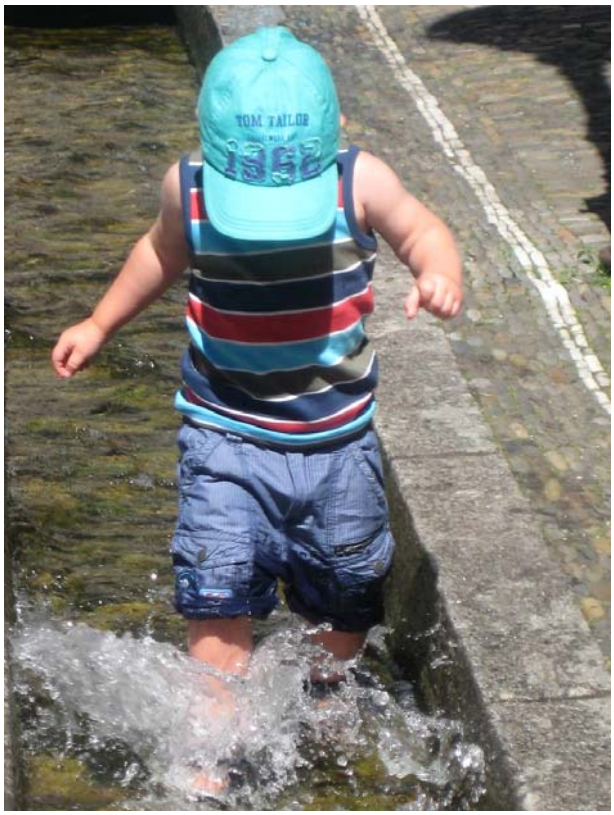

Fig. 17: Cooling of a young child by a small streamlet in the city of Freiburg

Besides wearing clothes of low heat transfer resistance, umbrellas as an individual measure against severe heat like in Hong Kong (Fig. 18) are also imaginable in Central European cities in the future.

Fig. 18: Umbrellas as an individual measure against severe heat in Hong Kong

The growing pressure on urban planning to react to severe heat in a preventive way by now arises from the following reasons.

- The design of Central European cities is not adapted to severe heat.
- Citizens in Central Europe are not adapted to severe heat.
- The fraction of the risk group 'elderly people' is increasing due to demographic change.
- The demands of the urban population for more thermal comfort are increasing.
- The development and implementation of planning measures to mitigate severe heat in the local urban scale consume time.

Discussing the effectiveness of planning measures to mitigate severe heat, it must be differentiated between

- dry heat and humid heat,
- the situation in the daytime and in the night.

The results presented in the papers II to IV of this thesis have shown for the Central European city of Freiburg that daytime mitigation measures aimed at the shading of the direct solar radiation are effective on clear-sky summer days, which are characterised by dry heat. Experiences from tropical cities, however, reveal that human stress caused by humid heat at

the pedestrian level can be most efficiently reduced by maintaining the near-surface air flow, because it is impossible to lower high moisture within the urban canopy layer by shading measures. Using the example of Hong Kong as a sea-side city in the tropics, the sea breeze considerably contributes to the mitigation of human stress in terms of humid heat (Ng, 2012; Ng and Cheng, 2012).

In the future, severe heat in Central Europe will also occur in summer. Therefore, the mentioned double strategy of planning measures to maintain local thermal comfort for citizens during regionally predetermined severe heat proves to be appropriate as the daylight hours are longer than the night hours. Measures for the daytime have the first priority due to the longer daylight hours. They should cause a reduction of the heat input into all urban spaces, i.e. outdoors and indoors. A second priority is to assign to nocturnal measures, for instance the maintenance of sufficient ventilation combined with an additional cooling of the near-surface atmosphere. This can be achieved by mountain winds or nocturnal down-slope winds.

Effective planning measures aiming at the reduction of the daytime heat input into urban spaces have been multiply investigated in terms of different issues and methodical approaches such as experiments (Ali-Toudert and Mayer, 2007b; Mayer et al., 2008b; Holst and Mayer, 2010, 2011; Oliveira et al., 2011; Lee et al., 2013, 2014) or numerical simulations (Ali-Toudert and Mayer, 2006, 2007a; Thorsson et al., 2011; Chen and Ng, 2012; Gross, 2012; Goldberg et al., 2013; Johansson et al., 2013; Müller et al., 2014b). They mostly refer to an

- optimised building and street design (Shashua-Bar and Hoffman, 2003; Ali-Toudert and Mayer, 2006, 2007a; van Hooff et al., 2014; Taleghani et al., 2015),
- optimised green infrastructure (Gill et al., 2007; Bowler et al., 2010; Oliveira et al., 2011; Maras et al., 2013; Wong and Lau, 2013; Niemelä, 2014; Perini and Magliocco, 2014; Santamouris, 2014; Klemm et al., 2015; Norton et al., 2015).

While greening of roofs and facades primarily leads to a lower heat input into interiors, front gardens, urban parks, urban forests and particularly street trees reduce the heat input into urban open spaces. As shown in the papers II to IV of this thesis, the passive cooling by street trees in the daytime, which provides local human thermal comfort at the pedestrian level on hot summer days, is caused by shading of the direct solar radiation. It results in a modification of the radiant and heat budget below the tree canopies that has to be favourably assessed from the human-biometeorological point of view.

In the meantime, the benefits of street trees for citizens have been investigated worldwide (Donovan and Butry, 2009; Loughner et al., 2012; Roy et al., 2012; Vailshery et al., 2013; Mullaney et al., 2015). This includes the shading effect of trees in different climate zones, whereby the results are mostly referred to T_a (Shashua-Bar and Hoffman, 2004; Shashua-Bar et al., 2010a, 2010b; Tsiros, 2010; Cohen et al., 2012; Ng et al., 2012) and less frequent to T_{mrt} (Lindberg and Grimmond, 2011b; Lee et al., 2013, 2014) as well as a thermo-physiological assessment index such as PET or UCTI (Lin et al., 2010, 2013; Chen and Ng,

2013; Lee et al., 2013, 2014; Coutts et al., 2015). In this context, the results of the investigations presented in the papers II to IV of this thesis have an elevated importance, as

- the statistical analyses are based on a comparatively extensive data collective from experimental human-biometeorological investigations conducted on clear-sky summer days at 87 different sites,
- the shading quantified by $SVF_{90\text{-}270}$ at these sites covers the wide range from 2 % (extremely pronounced shading) to 85 % (almost no shading),
- the shading effects are not only related to T_a, T_{mrt} and PET, but also to the three-dimensional short- and long-wave radiant flux densities, which represent the physical basis for changes of T_a, T_{mrt} and PET,
- the results of the experimental investigations, which have a spot character, are complemented by results of numerical simulations on a heat wave day,
- the numerical simulations provide results for different urban spaces within the simulation domain and compare the human-biometeorological effects of street trees with those of only grassland.

An effective shading requires vital trees, whose water and nutrient supply should be naturally ensured (Gromke et al., 2015). In addition, they should be adapted to regional climate change. Besides the shading effect, street trees have additional environmental impacts, which can be evaluated as negative at first sight:

- Street trees act as an obstacle for the near-surface air flow (Gromke and Ruck, 2007; Gromke et al., 2008; Balczó et al., 2009; Buccolieri et al., 2009).
- Street trees emit biogenic volatile organic compounds (BVOCs).

Provided that street trees are broad-leaved trees, the reduced air flow causes only slight influences on the concentration of gaseous air pollutants, as most of them show their annual maximum in the leafless period (Mayer, 1999). At this time, the reduction of the near-surface air flow is distinctly lower than that in the leaved period. In this context, it has also to be considered that tree canopies offer a mitigation potential against atmospheric particulate pollution (Litschke and Kuttler, 2008; Tallis et al., 2011; Vailshery et al., 2013).

BVOCs emitted by street tress (Kuttler 2011b; Wagner and Kuttler, 2014) represent a precursor for the formation of O_3. However, it has not been finally investigated up to now, how big is the increase of the O_3 concentration due to the BVOCs emission by one mature street tree. Thereby, the possible availability of NO within street canyons emitted by the car traffic has to be taken into account as it causes a depletion of a potentially slightly enhanced O_3 concentration. The use of trees ranked as 'low emitter plants' reduces the BVOC problem of street trees. In this context, Kuttler (2011b) has listed tree species, which are characterised by a relatively low O_3 formation potential and a high drought tolerance.

Altogether, the superficial conflicting goals of street trees do not really exist. Thus, their exceptionally positive impact on human thermal comfort remains (Goldbach and Kuttler, 2013). Related to T_a, the 'cooling effect' of well transpiring trees has been analysed by Shashua-Bar

and Hoffman (2000) as well as Kuttler (2011b). It is mainly caused by shading (about 80 %). The contribution by the evapotranspiration of the tree canopies and the resulting latent heat flux, respectively, is distinctly lower (about 20 %). The relatively low transpirational cooling by street trees in terms of T_a is confirmed in the modelling study by Gromke et al. (2015).

As reported in paper III of this thesis, the results of the experimental investigations on human thermal comfort in Freiburg point to

- the changes of the absorbed three-dimensional short- and long-wave radiant flux densities caused by shading,
- their influences on T_a, T_{mrt} and PET.

A reduction of $SVF_{90\text{-}270}$ by 10 % due to the shading of the direct solar radiation by street trees leads to a lowering of

- T_a by up to 0.2 K,
- T_{mrt} by up to 3.8 K,
- PET by up to 1.4 K.

These values are averaged over the period 10-16 CET. It represents the daily period with potential outdoor heat stress on humans in summer. The reduction of T_a lies in the range of results of other investigations, which show a mean T_a lowering up to 2-4 K for the case of complete shading by tree canopies (Shashua-Bar and Hoffman, 2004; Hamada and Ohta, 2010; Shashua-Bar et al., 2010a, 2010b; Armson et al., 2012). However, a human-biometeorologically based valuation standard for T_a changes does not exist up to now. This is also true for T_{mrt}. The magnitude of its response to changes of the shading is higher than that of T_a. However, the PET modifications by a different shading extent can be evaluated according to the PET classification in Table 2.

According to Shashua-Bar et al. (2011), the simulation results presented in paper IV show in the case of tree shading combined with a grassland surface that the contribution to an improved human thermal comfort quantified by a thermo-physiological assessment index is higher than that for only tree shading. This means that vegetation may make a substantial contribution to human thermal comfort even when its effect on T_a is relatively negligible. Previous studies (Kenny et al., 2008; Mayer et al., 2008b; Holst and Mayer, 2011; Shashua-Bar et al., 2011) have already demonstrated that the radiant exchange frequently is the dominant factor in the daytime affecting human thermal comfort in many urban environments - despite the tendency of many researchers to focus only on T_a.

9. Conclusions

The regional climate change has a lasting effect on the atmospheric background conditions for Central European cities. Increasing severe heat in summer represents a substantial challenge to urban planning as the design of the cities and their residents are not adapted to this meteorological hazard. This is aggravated by the demographic change, which leads to an increasing fraction of the vulnerable risk group 'elderly people'. Among the different options to mitigate the local human heat stress in summer, urban planning is under the pressure to develop and apply measures, which redesign urban spaces in a preventive way taking account of methods of urban human-biometeorology.

The results of the well-matched investigation approaches presented in this thesis point to the suitability of devices to shade the direct solar radiation. As a consequence, the energy flux densities from the three-dimensional surroundings are modified, which in turn mitigates human heat stress in terms of a thermo-physiological assessment index. Related to the current land use situation, the results of the experimental investigations on human thermal comfort enabled a deeper insight into the direction-specific importance of short- and long-wave radiant flux densities for T_{mrt}, which mainly governs PET on clear-sky summer days in Central Europe. Thus, urban planning can estimate how changes of physical features of building walls and streets may contribute to a local reduction of PET. The spot-related results of the experimental investigations were complemented by spatial results of numerical simulations performed on a heat wave day. In contrast to spot-related results, they better meet the requirements of urban planning, which are always related to urban spaces.

In accordance with other investigations on the local mitigation of human heat stress, the papers II to IV of this thesis point to the necessity to shade the direct solar radiation in order to maintain human thermal comfort even under severe heat as a regional meteorological hazard. Shading of the direct solar radiation as a measure against heat has been qualitatively well-known for a long time. On principle, shading can be achieved by different measures such as tree canopies, buildings, arcades, awnings, sunshades and tarpaulins stretched across streets (Fig. 19). However, shading measures in terms of awnings, sunshades and tarpaulins stretched across streets lead to a higher long-wave radiant flux density towards the pedestrian level as shading of the direct solar radiation means its absorption and warming, respectively, by these artificial shading devices. This in turn increases their surface temperature. Therefore, these shading measures are better suited at sites located near the seaside, where the daytime sea breeze causes an additional reduction of human heat stress.

For cities situated in the midland like most of the Central European cities, shading of the direct solar radiation by the three-dimensional canopies of trees represents the most effective mitigation measure against local heat stress from the human-biometeorological point of view. The importance of this kind of passive cooling has also been recognised for quite some time. But the lack of quantified results on the mitigation potential of street trees, which particularly exists for human-biometeorological variables, is reduced by recent investigations in urban human-biometeorology like the papers II to IV of this thesis.

Fig. 19: Tarpaulins stretched across a street as a local measure to mitigate human heat stress in a Mediterranean coastal city (Jaffa, Israel)

The magnitude of the mitigation of daytime heat stress by tree canopies depends on their dimensions and vitality condition. With regard to shading, their shape can be more important than their density (Kleerekoper et al., 2012). The numerical simulations included in this thesis started at the current land use situation in the simulation domain, which is characterised by mature trees, grassland and different kind of sealed surfaces. Due to a stepwise change of the green coverage, the different importance of trees and grassland for T_a, T_{mrt} and PET could be quantified. In future simulations, the obtained results should be extended by those derived for a more systematic change of the green land use. This will provide indications for the human-biometeorologically optimised green coverage oriented to the maintenance of human thermal comfort in the daytime and at night.

Focused on their planning related potential to mitigate human heat stress, different urban sites and spaces were assessed in this thesis in a thermo-physiological way. In the future, this stationary perspective should be supplemented by considering dynamic aspects. This refers to investigations aiming at the time interval that citizens must spend in a specific urban space on average that their perception of heat corresponds to the thermal assessment of this space. This information can contribute to a data basis, which is necessary for the preparation of planning-related guidelines aiming at suited measures against human heat stress. Keeping in mind the increasing severe summer heat due to regional climate change, these guidelines become increasingly important.

References

Albers, R.A.W., Bosch, P.R., Blocken, B., van den Dobbelsteen, A.A.J.F., Rovers, V., Spit, T.J.M., van de Ven, F., van Hooff, T., van Hove, L.W.A., 2015: Overview of challenges and achievements in the climate adaptation of cities and in the Climate Proof Cities program. Building and Environment 83, 1-10.

Ali-Toudert, F., Mayer, H., 2006: Numerical study on the effects of aspect ratio and orientation of an urban street canyon on outdoor thermal comfort in hot and dry climate. Building and Environment 41, 94-108.

Ali-Toudert, F., Mayer, H., 2007a: Effects of asymmetry, galleries, overhanging facades and vegetation on thermal comfort in urban street canyons. Solar Energy 81, 742-754.

Ali-Toudert, F., Mayer, H., 2007b: Thermal comfort in an east-west oriented street canyon in Freiburg (Germany) under hot summer conditions. Theoretical and Applied Climatology 87, 223-237.

An, S.M., Kim, B.S., Lee, H.Y., Kim, C.H., Yi, C.Y., Eum, J.H., Woo, J.H., 2014: Three-dimensional point cloud based sky view factor analysis in complex urban settings. International Journal of Climatology 34, 2685-2701.

Andrade, H., Alcoforado, M.-J., 2008: Microclimatic variation of thermal comfort in a district of Lisbon (Telheiras) at night. Theoretical and Applied Climatology 92, 225-237.

Andreou, E., 2013: Thermal comfort in outdoor spaces and urban canyon microclimate. Renewable Energy 55, 182-188.

Antics, A., Pascal, M., Laaidi, K., Wagner, V., Corso, M., Declercq, C., Beaudeau, P., 2013: A simple indicator to rapidly assess the short-term impact of heat waves on mortality within the French heat warning system. International Journal of Biometeorology 57, 75-81.

Armson, D., Stringer, P., Ennos, A.R., 2012: The effect of tree shade and grass on surface and globe temperatures in an urban area. Urban Forestry & Urban Greening 11, 245-255.

Arnfield, A.J., 2003: Two decades of urban climate research: A review of turbulence, exchanges of energy and water, and the urban heat island. International Journal of Climatology 23, 1-26.

Balczó, M., Gromke, C., Ruck, B., 2009: Numerical modeling of flow and pollutant dispersion in street canyons with tree planting. Meteorologische Zeitschrift 18, 197-206.

Ballester, J., Rodó, X., Giorgi, F., 2010: Future changes in Central Europe heat waves expected to mostly follow summer mean warming. Climate Dynamics 35, 1191-1205.

Barriopedro, D., Fischer, E.M., Luterbacher, J., Trigo, R.M., García-Herrera, R., 2011: The hot summer of 2010: redrawing the temperature record map of Europe. Science 332, 220-224.

Basu, R., 2009: High ambient temperature and mortality: a review of epidemiologic studies from 2001 to 2008. Environmental Health 8, 40.

Beniston, M., 2004: The 2003 heat wave in Europe: A shape of things to come? An analysis based on Swiss climatological data and model simulations. Geophysical Research Letters 31, L02202, DOI: 10.1029/2003GL0181857.

Beniston, M., 2013: Exploring the behaviour of atmospheric temperatures under dry conditions in Europe: evolution since the mid-20th century and projections for the end of the 21st century. International Journal of Climatology 33, 457-462.

Beniston, M., Stephensen, D.B., Christensen, O.B., Ferro, C.A.T., Frei, C., Goyette, S., Halsnaes, K., Holt, T., Jylhä, K., Koffi, B., Palutikof, J., Schöll, R., Semmler, T., Woth, K., 2007: Future extreme events in European climate: an exploration of regional climate model projections. Climatic Change 81, 71-95.

Blazejczyk, K., Epstein, Y., Jendritzky, G., Staiger, H., Tinz, B., 2012: Comparison of UTCI to selected thermal indices. International Journal of Biometeorology 56, 515-535.

Blazejczyk, K., Kuchcik, M., Blazejczyk, A., Milewski, P., Szmyd, J., 2014: Assessment of urban thermal stress by UTCI - experimental and modelling studies: an example from Poland. DIE ERDE 145, 16-33.

Bohnenstengel, S.I., Evans, S., Clark, P.A., Belcher, S.E., 2011: Simulations of the London urban heat island. Quarterly Journal of the Royal Meteorological Society 137, 1625-1640.

Bowler, D.E., Buyung-Ali, L., Knight, T.M., Pullin, A.S., 2010: Urban greening to cool towns and cities: A systematic review of the empirical evidence. Landscape and Urban Planning 97, 147-155.

Brandsma, T., Wolters, D., 2012: Measurement and statistical modeling of the urban heat island of the city of Utrecht (the Netherlands). Journal of Applied Meteorology and Climatology 51, 1046-1060.

Bröde, P., Krüger, E.L., Rossi, F.A., Fiala, D., 2012: Predicting urban outdoor thermal comfort by the Universal Thermal Climate Index UTCI - a case study in Southern Brazil. International Journal of Biometeorology 56, 471-480.

Bruse, M., 1999: The influences of local environment design on microclimate - development of the prognostic numerical model ENI-met for the simulation of wind, temperature and humidity distribution in urban structures. PhD thesis, University of Bochum, Germany (in German).

Bruse, M., Fleer, H., 1998: Simulating surface-plant-air interactions inside urban environments with a three-dimensional numerical model. Environmental Modelling and Software 13, 373-384.

Buccolieri, R., Gromke, C., di Sabatino, S., Ruck, B., 2009: Aerodynamic effects of trees on pollutant concentration in street canyons. Science of the Total Environment 407, 5247-5256.

Carter, J.G., Cavan, G., Connelly, A., Guy, S., Handley, J., Kazmierczak, A., 2015: Climate change and the city: Building capacity for urban adaptation. Progress in Planning 95, 1-66.

Casati, B., Yagouti, A., Chaumont, D., 2013: Regional climate projections of extreme heat events in nine pilot Canadian communities for public health planning. Journal of Applied Meteorology and Climatology 52, 2669-2698.

Charalampopoulos, I., Tsiros, I., Chronopoulou-Sereli, A., Matzarakis, A., 2013: Analysis of thermal bioclimate in various urban configurations in Athens, Greece. Urban Ecosystems 16, 217-233.

Chen, L., Ng, E., 2012: Outdoor thermal comfort and outdoor activities: A review of research in the past decade. Cities 29, 118-125.

Chen, L., Ng, E., 2013: Simulation of the effect of downtown greenery on thermal comfort in subtropical climate using PET index: a case study in Hong Kong. Architectural Science Review 56, 297-305.

Chen, L., Ng, E., An, X., Ren, C., Lee, M., Wang, U., He, Z., 2012: Sky view factor analysis of street canyons and its implications for daytime intra-urban air temperature differentials in high-rise, high-density urban areas of Hong Kong: a GIS-based simulation approach. International Journal of Climatology 32, 121-136.

Chen, Y.-C., Lin, T.-P., Matzarakis, A., 2014: Comparison of mean radiant temperature from field experiment and modelling: a case study in Freiburg, Germany. Theoretical and Applied Climatology 118, 535-551.

Chow, W.T.L., Brazel, A.J., 2012: Assessing xeriscaping as a sustainable heat island mitigation approach for a desert city. Building and Environment 47, 170-181.

Chow, W.T.L., Pope, R.L., Martin, C.A., Brazel, A.J., 2011: Observing and modeling the nocturnal park cool island of an arid city: horizontal and vertical impacts. Theoretical and Applied Climatology 103, 243-257.

Christidis, N., Jones, G.S., Stott, P.A., 2015: Dramatically increasing chance of extremely hot summers since the 2003 European heatwave. Nature Climate Change 5, 46-50.

Christidis, N., Stott, P.A., Jones, G.S., Shiogama, H., Nozawa, T., Luterbacher, J., 2012: Human activity and anomalously warm seasons in Europe. International Journal of Climatology 32, 225-239.

Cohen, P., Potchter, O., Matzarakis, A., 2012: Daily and seasonal climatic conditions of green urban open spaces in the Mediterranean climate and their impact on human comfort. Building and Environment 51, 285-295.

Cohen, P., Potchter, O., Matzarakis, A., 2013: Human thermal perception of Coastal Mediterranean outdoor urban environments. Applied Geography 37, 1-10.

Coumou, D., Rahmstorf, S., 2012: A decade of weather extremes. Nature Climate Change 2, 491-496.

Coutts, A.M., White, E.C., Tapper, N.J., Beringer, J., Livesley, S.J., 2015: Temperature and human thermal comfort effects of street trees across three contrasting street canyon environments. Theoretical and Applied Climatology, DOI: 10.1007/s00704-015-1409-y.

Deck, R., 2014: Simulations on thermal comfort for different land uses of two potential building areas in the city centre of Stuttgart. BSc thesis, Chair of Meteorology and Climatology, Faculty of Environment and Natural Resources, Albert-Ludwigs-University of Freiburg, Germany (in German).

Díaz, J., García-Herrera, R., Trigo, R.M., Linares, C., Valente, M.A., de Miguel, J.M., Hernández, E., 2006: The impact of the summer 2003 heat wave in Iberia: how should we measure it? International Journal of Biometeorology 50, 159-166.

Donovan, G.H., Butry, D.T., 2009: The value of shade: Estimating the effect of urban trees on summertime electricity use. Energy and Buildings 41, 662-668.

Dütemeyer, D., Barlag, A.-B., Kuttler, W., Axt-Kittner, U., 2013a: Urban climatic area management in local environmental planning. UVP-report 27, 173-179 (in German).

Dütemeyer, D., Barlag, A.-B., Kuttler, W., Axt-Kittner, U., 2013b: Measures against heat stress in the city of Gelsenkirchen, Germany. DIE ERDE 144, 181-201.

Égerházi, L.A., Kovács, A., Unger, J., 2013: Application of microclimate modelling and onsite survey in planning practice related to an urban micro-environment. Advances in Meteorology 2013, article ID 251586, 10 pages, http//dx.doi.org/10.1155/2013/251586.

Emmanuel, R., Rosenlund, H., Johansson, E., 2007: Urban shading - a design option for the tropics? A study in Colombo, Sri Lanka. International Journal of Climatology 27, 1995-2004.

Erell, E., Pearlmutter, D., Williamson, T., 2011: Urban microclimate - Designing the spaces between buildings. London, Earthscan.

Erell, E., Pearlmutter, D., Boneh, D., Bar Kutiel, P., 2014: Effect of high-albedo materials on pedestrian heat stress in urban street canyons. Urban Climate 10, 367-386.

Erlat, E., Türkeş, M., 2013: Observed changes and trends in numbers of simmer and tropical days, and the 2010 hot summer in Turkey. International Journal of Climatology 33, 1898-1908.

Fahmy, M., Sharples, S., 2009: On the development of an urban passive thermal comfort system in Cairo, Egypt. Building and Environment 44, 1907-1916.

Fink, A., Brücher, T., Krüger, A., Leckebusch, G., Pinto, J., Ulbrich, U., 2004: The 2003 European summer heatwaves and drought - synoptic diagnosis and impacts. Weather 59, 209–216.

Fischer, E.M., Schär, C., 2010: Consistent geographical patterns of changes in high-impact European heatwaves. Nature Geoscience 3, 398-403.

Fouillet, A., Rey, G., Wagner, V., Laaidi, K., Empereur-Bissonnet, P., Tertre, A.L., Frayssinet, P., Bessemoulin, P., Laurent, F., Crouy-Chanel, P.D., Jougla, E., Hémon, D., 2008: Has the impact of heat waves on mortality changed in France since the European heat wave of summer 2003? A study of the 2006 heat wave. International Journal of Epidemiology 37, 309-317.

Fröhlich, D., Matzarakis, A., 2013: Modeling of changes in thermal bioclimate: examples based on urban spaces in Freiburg, Germany. Theoretical and Applied Climatology 111, 547-558.

Gál, T., Unger, J., 2014: A new software tool for SVF calculations using buildings and tree-crown-databases. Urban Climate 10, 594-606.

García-Herrera, R., Díaz, J., Trigo, R.M., Luterbacher, J., Fischer, E.M., 2010: A review of the European summer heat wave of 2003. Environmental Science and Technology 40, 267-306.

Gershunov, A., Cayan, D.R., Iacobellis, S.F., 2009: The great 2006 heat wave over California and Nevada: signal of an increasing trend. Journal of Climate 22, 6181-6203.

Giannaros, T.M., Melas, D., Matzarakis, A., 2015: Evaluation of thermal bioclimate based on observational data and numerical simulations: an application to Greece. International Journal of Biometeorology 59, 151-164.

Gill, S.E., Handley, J.F., Ennos, A.R., Pauleit, S., 2007: Adapting cities for climate change: The role of the green infrastructure. Built Environment 33, 115-133.

Goldbach, A., Kuttler, W., 2013: Quantification of turbulent heat fluxes for adaptation strategies within urban planning. International Journal of Climatology 33, 143-159.

Goldberg, V., Kurbjuhn, C., Bernhofer, C., 2013: How relevant is urban planning for the thermal comfort of pedestrians? Numerical case studies in two districts of the City of Dresden (Saxony/Germany). Meteorologische Zeitschrift 22, 739-751.

Gómez, F., Cueva, A.P., Valcuende, M., Matzarakis, A., 2013: Research on ecological design to enhance comfort in open spaces of a city (Valencia, Spain). Utility of the physiological equivalent temperature (PET). Ecological Engineering 57, 27-39.

Gong, D.Y., Pan, Y.Z., Wang, J.A., 2004: Changes in extreme daily mean temperatures in summer in eastern China during 1955-2000. Theoretical and Applied Climatology 77, 25-37.

Gosling, S.N., McGregor, G.R., Páldy, A., 2007: Climate change and heat-related mortality in six cities Part 1: model construction and validation. International Journal of Biometeorology 51, 525-540.

Gosling, S.N., Lowe, J.A., McGregor, G.R., Pelling, M., Malamud, B.D., 2009: Associations between elevated atmospheric temperature and human mortality: a critical review of the literature. Climatic Change 92, 299-341.

Grimmond, C.S.B., 2007: Urbanization and global environmental change: local effects of urban warming. Geographical Journal 173, 83-88.

Grimmond, C.S.B., Roth, M., Oke, T.R., Au, Y.C., Best, M., Betts, R., Carmichael, G., Cleugh, H., Dabberdt, W., Emmanuel, R., Freitas, E., Fortuniak, K., Hanna, S., Klein, P., Kalkstein, L.S., Liu, C.H., Nickson, A., Pearlmutter, D., Sailor, D., Voogt, J., 2010a: Climate and

more sustainable cities: Climate information for improved planning and management of cities (Producers/capabilities perspective). Procedia Environmental Sciences 1, 247-274.

Grimmond, C.S.B., Blackett, M., Best, M.J., Barlow, J., Baik, J.-J., Belcher, S.E., Bohnenstengel, S.I., Calmet, I., Chen, F., Dandou, A., Fortuniak, K., Gouvea, M.L., Hamdi, R., Hendry, M., Kawai, T., Kawamoto, Y., Hondo, H., Krayenhoff, E.S., Lee, S.-H., Loridan, T., Martilli, A., Masson, V., Miao, S., Oleson, K., Pigeon, G., Porson, A., Ryu, Y.-H., Salamanca, F., Shashua-Bar, L., Steeneveld, G.-J., Tombrou, M., Voogt, J., Young, D., Zhang, N., 2010b: The international urban energy balance models comparison project: First results from phase 1. Journal of Applied Meteorology and Climatology 49, 1268-1292.

Gromke, C., Ruck, B., 2007: Influence of trees on the dispersion of pollutants in an urban street canyon - Experimental investigation of the flow and concentration field. Atmospheric Environment 41, 3287-3302.

Gromke, C., Buccolieri, R., di Sabatino, S., Ruck, B., 2008: Dispersion study in a street canyon with tree planting by means of wind tunnel and numerical investigations - Evaluation of CFD data with experimental data. Atmospheric Environment 42, 8640-8650.

Gromke, C., Blocken, B., Janssen, W., Merema, B., van Hooff, T., Timmermans, H., 2015: CFD analysis of transpirational cooling by vegetation: Case study for specific meteorological conditions during a heat wave in Arnhem, Netherlands. Building and Environment 83, 11-26.

Groot, A.M.E., Bosch, P.R., Buijs, S., Jacobs, C.M.J., Moors, E.J., 2015: Integration in urban climate adaptation: Lessons from Rotterdam on integration between scientific disciplines and integration between scientific and stakeholder knowledge. Building and Environment 83, 177-188.

Gross, G., 2012: Effects of different vegetation on temperature in an urban building environment. Micro-scale numerical experiments. Meteorologische Zeitschrift 21, 399-412.

Grumm, R.H., 2011: The Central European and Russian heat event of July - August 2010. Bulletin of the American Meteorological Society 92, 1285-1296.

Guirguis, K., Gershunov, A., Tardy, A., Basu, R., 2014: The impact of recent heat waves on human health in California. Journal of Applied Meteorology and Climatology 53, 3-19.

Gulyás, Á., Unger, J., Matzarakis, A., 2006: Assessment of the microclimatic and human comfort conditions in a complex urban environment: Modelling and measurements. Building and Environment 41, 1713-1722.

Hajat, S., Armstrong, B., Baccini, M., Biggeri, A., Bisanti, L., Russo, A., Paödy, A., Menne, B., Kosatsky, T., 2006: Impact of high temperatures on mortality - Is there an added heat wave effect? Epidemiology 17, 632-638.

Hamada, S., Ohta, T., 2010: Seasonal variations in the cooling effect of urban green areas on surrounding urban areas. Urban Forestry & Urban Greening 9, 15-24.

Hansen, J., Sato, M., Ruedy, R., 2012: Perception of climate change. Proceedings of the National Academy of Sciences USA 109, E2415-E2423.

Havenith, G., 2001: Individualized model of human thermoregulation for the simulation of heat stress response. Journal of Applied Physiology 90, 1943-1954.

He, X., Miao, S., Shen, S., Li, J., Zhang, B., Zhang, Z., Chen, X., 2014: Influence of sky view factor on outdoor thermal environment and physiological equivalent temperature. International Journal of Biometeorology, DOI 10.1007/s00484-014-0841-5.

Heudorf, U., Meyer, C., 2005: Health effects of severe heat - using the example of the heat wave and the mortality in Frankfurt/Main in August 2003. Gesundheitswesen 67, 369-374 (in German).

Höppe, P., 1984: The human heat budget. PhD thesis, Reports of the Meteorological Institute, University of Munich, No. 49 (in German).

Höppe, P., 1992: A new method to determine the mean radiant temperature outdoors. Wetter und Leben 44, 147-151 (in German).

Höppe, P., 1993: Heat balance modeling. Experientia 49, 741-746.

Höppe, P., 1997: Aspects of human biometeorology in past, present and future. International Journal of Biometeorology 40, 19-23.

Höppe, P., 1999: The physiological equivalent temperature - a universal index for the biometeorological assessment of the thermal environment. International Journal of Biometeorology 43, 71-75.

Höppe, P., 2002: Different aspects of assessing indoor and outdoor thermal comfort. Energy and Buildings 34, 661-665.

Holst, J., Mayer, H., 2010: Urban human-biometeorology: Investigations in Freiburg (Germany) on human thermal comfort. Urban Climate News 38, 5-10.

Holst, J., Mayer, H., 2011: Impacts of street design parameters on human-biometeorological variables. Meteorologische Zeitschrift 20, 541-552.

Huang, W., Kan, H., Kovats, S., 2010: The impact of the 2003 heat wave on mortality in Shanghai, China. Science of the Total Environment 408, 2418-2420.

Huth, R., Kyselý, J., Pokorná, L., 2000: A GCM simulation of heat waves, dry spells, and their relationships to circulation. Climatic Change 46, 29-60.

Huttner, S., 2012: Further development and application of the 3D microclimate simulation ENVI-met. PhD thesis, Johannes Gutenberg University Mainz, Germany.

Huynen, M.M.T.E, Martens, P., Schram, D., Weijenberg, M.P., Kunst, A.E., 2001: The impact of heat waves and cold spells on mortality rates in the Dutch population. Environmental Health Perspectives 109, 463-470.

Hwang, R.-L., Lin, T.-P., Matzarakis, A., 2011: Seasonal effect of urban street shading on long-term outdoor thermal comfort. Building and Environment 46, 863-870.

IPCC, 2007: Contribution of working group I to the fourth assessment report of the Intergovernmental Panel on Climate Change. Cambridge University Press.

Jendritzky, G., Koppe, C, 2008: Effects of thermal stress on mortality. In: Wake-up call climate. Risks to health: Dangers for plants, animals and humans (ed. by J.L. Lozán, H. Graßl, G. Jendritzky, L. Karbe and K. Reise), Hamburg, Wissenschaftliche Auswertungen, 149-153 (in German).

Jendritzky, G., de Dear, R., Havenith, G., 2012: UTCI - Why another thermal index? International Journal of Biometeorology 56, 421-428.

Johansson, E., Spangenberg, J., Gouvêa, M.L., Freitas, E.D., 2013: Scale-integrated atmospheric simulations to assess thermal comfort in different urban tissues in the warm humid summer of São Paulo, Brazil. Urban Climate 6, 24-43.

Johansson, E., Thorsson, S., Emmanuel, R., Krüger, E., 2014: Instruments and methods in outdoor thermal comfort studies - the need for standardization. Urban Climate 10, 346-366.

Kalkstein, L.S., Davis, R.E., 1989: Weather and human mortality: an evaluation of demographic and interregional responses in the United States. Annuals of the Association of American Geographers 79, 44-64.

Kántor, N., Unger, J., 2011: The most problematic variable in the course of human-biometeorological comfort assessment - the mean radiant temperature. Central European Journal of Geosciences 3, 90-100.

Kántor, N., Égerházi, L., Unger, J., 2012a: Subjective estimations of thermal environment in recreational urban spaces - Part 1: investigations in Szeged, Hungary. International Journal of Biometeorology 56, 1075-1088.

Kántor, N., Unger, J., Gulyás, Á., 2012b: Subjective estimations of thermal environment in recreational urban spaces - Part 2: international comparison. International Journal of Biometeorology 56, 1089-1101.

Kántor, N., Lin, T.-P., Matzarakis, A., 2014a: Daytime relapse of the mean radiant temperature based on the six-directional method under unobstructed solar radiation. International Journal of Biometeorology 58, 1615-1625.

Kántor, N., Kovács, A., Lin, T.-P., 2014b: Looking for simple correction functions between the mean radiant temperature from the "standard black globe" and the "six-directional" techniques in Taiwan. Theoretical and Applied Climatology, DOI 10.1007/s00704-014-1211-2.

Kastendeuch, P.P., 2013: A method to estimate sky view factors from digital elevation models. International Journal of Climatology 33, 1574-1578.

Katavoutas, G., Theoharatos, G., Flocas, H.A., Asimakopoulos, D.N., 2009: Measuring the effects of heat wave episodes on the human body's thermal balance. International Journal of Biometeorology 53, 177-187.

Katavoutas, G., Flocas, H.A., Matzarakis, A., 2015: Dynamic modeling of human thermal comfort after the transition from an indoor to an outdoor hot environment. International Journal of Biometeorology 59, 205-216.

Kenny, N.A., Warland, J.S., Brown, R.D., Gillespie, T.G., 2008: Estimating the radiation absorbed by a human. International Journal of Biometeorology 52, 491-503.

Ketterer, C., Matzarakis, A., 2014a: Human-biometeorological assessment of heat stress reduction by replanning measures in Stuttgart, Germany. Landscape and Urban Planning 122, 78-88.

Ketterer, C., Matzarakis, A., 2014b: Human-biometeorological assessment of the urban heat island in a city with complex topography - The case of Stuttgart, Germany. Urban Climate 10, 573-584.

Kleerekoper, L., van Esch, M., Salcedo, T.B., 2012: How to make a city climate-proof, addressing the urban heat island effect. Resources, Conservation and Recycling 64, 30-38.

Klein Rosenthal, J., Kinney, P.L., Metzger, K.B., 2014: Intra-urban vulnerability to heat-related mortality in New York City, 1997-2006. Health & Place 30, 45-60.

Klemm, W., Heusinkveld, B.G., Lenzholzer, S., Jacobs, M.H., van Hove, B., 2015: Psychological and physical impact of urban green spaces on outdoor thermal comfort during summertime in The Netherlands. Building and Environment 83, 120-128.

Koffi, B., Koffi, E., 2008: Heat waves across Europe by the end of the 21st century: multiregional climate simulations. Climate Research 36, 153-168.

Konstantinov, P.I., Varentsov, M.I., Malinina, E.P., 2014: Modeling of thermal comfort conditions inside the urban boundary layer during Moscow's 2010 summer heat wave (case-study). Urban Climate 10, 563-572.

Koppe, C., Jendritzky, G., 2005: Inclusion of short-term adaptation to thermal stresses in a heat load warning procedure. Meteorologische Zeitschrift 14, 271-278.

Kotthaus, S., Grimond, C.S.B., 2012: Identification of micro-scale anthropogenic CO_2, heat and moisture sources - Processing eddy covariance fluxes for a dense urban environment. Atmospheric Environment 57, 301-316.

Kovats, R.S., Ebi, K.L., 2006: Heatwaves and public health in Europe. European Journal of Public Health 16, 592-599.

Kovats, R.S., Hajat, S., 2008: Heat stress and public health: a critical review. Annual Review of Public Health 29, 41-55.

Krüger, E.L., Minella, F.O., Matzarakis, A., 2014: Comparison of different methods of estimating the mean radiant temperature in outdoor thermal comfort studies. International Journal of Biometeorology 58, 1727-1737.

Krüger, T., Held, F., Hoechstetter, S., Goldberg, V., Geyer, T., Kurbjuhn, C., 2013: A new heat sensitivity index for settlement areas. Urban Climate 6, 63-81.

Kuttler, W., 2010a: Urban climate, part I. Gefahrstoffe - Reinhaltung der Luft 70, 329-340 (in German).

Kuttler, W., 2010b: Urban climate, part II. Gefahrstoffe - Reinhaltung der Luft 70, 378-382 (in German).

Kuttler, W., 2011a: Climate change in urban areas - Part 1: Effects. Environmental Sciences Europe, 23, 11.

Kuttler, W., 2011b: Climate change in urban areas - Part 2: Measures. Environmental Sciences Europe, 23, 21.

Kyselý, J., 2002: Temporal fluctuations in heat waves at Prague-Klementinum, the Czech Republic, from 1901 - 97, and their relationships to atmospheric circulation. International Journal of Climatology 22, 33-50.

Kyselý, J., 2010: Recent severe heat waves in central Europe: how to view them in a long-term prospect? International Journal of Climatology 30, 89-109.

Kyselý, J., Kříž, B., 2008: Decreased impacts of the 2003 heat waves on mortality in the Czech Republic: an improved response? International Journal of Biometeorology 52, 733-745.

Laschewski, G., Jendritzky, G., 2002: Effects of the thermal environment on human health: an investigation of 30 years of daily mortality data from SW Germany. Climate Research 21, 91-103.

Lau, N-C., Nath, M.J., 2012: A model study of heat waves over North America: meteorological aspects and projections for the twenty-first century. Journal of Climate 25, 4761-4784.

Lau, K.K-L., Lindberg, F., Rayner, D., Thorsson, S., 2014: The effect of urban geometry on mean radiant temperature under future climate change: a study of three European cities. International Journal of Biometeorology, DOI: 10.1007/s00484-014-0898-1.

Lee, H., Mayer, H., 2013: Urban human-biometeorology supports urban planning to handle the challenge by increasing severe heat. Proc. Proc. 29th International PLEA Conference, Session I.3, 1-6.

Lee, H., Mayer, H., 2015: Green coverage changes within an ESE-WNW street canyon as a planning measure to maintain human thermal comfort on a heat wave day. Proc. 31st International PLEA Conference, PU 84, 1-8.

Lee, H., Holst, J., Mayer, H., 2013: Modification of human-biometeorologically significant radiant flux densities by shading as local method to mitigate heat stress in summer within urban street canyons. Advances in Meteorology 2013, article ID 312572, 13 pages, DOI: 10.1155/2013/312572.

Lee, H., Mayer, H., Schindler, D., 2014: Importance of 3-D radiant flux densities for outdoor human thermal comfort on clear-sky summer days in Freiburg, Southwest Germany. Meteorologische Zeitschrift 23, 315-330.

Lee, H., Mayer, H., Chen, L., 2015: Contribution of trees and grasslands to the mitigation of human heat stress in a residential district of Freiburg, Southwest Germany. Landscape and Urban Planning, DOI: 10.1016/j.landurbplan.2015.12.004.

Lehner, B., Döll, P., Alcamo, J., Henrichs, T., Kaspar, F., 2006: Estimating the impact of global change on flood and drought risks in Europe: A continental, integrated analysis. Climatic Change 75, 273-299.

Lhotka, O., Kyselý, J., 2014: Characterizing joint effects of spatial extent, temperature magnitude and duration of heat waves and cold spells over Central Europe. International Journal of Climatology, DOI: 10.1002/joc.4050.

Li, D., Bou-Zeid, E., 2013: Synergistic interactions between urban heat islands and heat waves: The impact in cities is larger than the sum of its parts. Journal of Applied Meteorology and Climatology 52, 2051-2064.

Lin, T.-P., 2009: Thermal perception, adaptation and attendance in a public park square in hot and humid regions. Building and Environment 44, 2017-2026.

Lin, T.-P., Matzarakis, A., Hwang, R.-L., 2010: Shading effect on long-term outdoor thermal comfort. Building and Environment 45, 213-221.

Lin, T.-P., Tsai, K.-T., Liao, C.-C., Huang, Y.-C., 2013: Effects of thermal comfort and adaptation on park attendance regarding different shading levels and activity types. Building and Environment 59, 599-611.

Lindberg, F., Grimmond, C.S.B., 2010: Continuous sky view factor maps from high resolution urban digital elevation models. Climate Research 42, 177-183.

Lindberg, F., Grimmond, C.S.B., 2011a: Nature of vegetation and building morphology characteristics across a city: Influence on shadow patterns and mean radiant temperatures in London. Urban Ecosystems 14, 617-634.

Lindberg, F., Grimmond, C.S.B., 2011b: The influence of vegetation and building morphology on shadow patterns and mean radiant temperatures in urban areas: model development and evaluation. Theoretical and Applied Climatology 105, 311-323.

Lindberg, F., Holmer, B., Thorsson, S., 2008: SOLWEIG 1.0 - Modelling spatial variations of 3D radiant fluxes and mean radiant temperature in complex urban settings. International Journal of Biometeorology 52, 697-713.

Lindberg, F., Holmer, B., Thorsson, S., Rayner, D., 2014: Characteristics of the mean radiant temperature in high latitude cities - implications for sensitive climate planning applications. International Journal of Biometeorology 58, 613-627.

Litschke, T., Kuttler, W., 2008: On the reduction of urban particle concentration by vegetation - a review. Meteorologische Zeitschrift 17, 229-240.

Liu, W., Lian, Z., Deng, Q., Liu, Y., 2011: Evaluation of calculation methods of mean skin temperature for use in thermal comfort study. Building and Environment 46, 478-488.

Loughner, C.P., Allen, D.J., Zhang, D.-L., Pickering, K.E., Dickerson, R.R., Landry, L., 2012: Roles of urban tree canopy and buildings in urban heat island effects: Parameterization and preliminary results. Journal of Applied Meteorology and Climatology 51, 1775-1793.

Luterbacher, J., Dietrich, D., Xoplaki, E., Grosjean, M., Wanner, H., 2004: European seasonal and annual temperature variability, trends, and extremes since 1500. Science 303, 1499-1503.

Mahmoud, A.H.A., 2011: Analysis of the microclimatic and human comfort conditions in an urban park in hot and arid regions. Building and Environment 46, 2641-2656.

Makaremi, N., Salleh, E., Jaafar, M.Z., GhaffarianHoseini, A., 2012: Thermal comfort conditions of shaded outdoor spaces in hot and humid climate of Malaysia. Building and Environment 48, 7-14.

Maras, I., Buttstädt, M., Hahmann, J., Hofmeister, H., Schneider, C., 2013: Investigating public places and impacts of heat stress in the city of Aachen, Germany. DIE ERDE 144, 290-303.

Masson, V., Lion, Y., Peter, A., Pigeon, G., Buyck, J., Brun, E., 2013: "Grand Paris": regional landscape change to adapt city to climate warming. Climatic Change 117, 769-782.

Masson, V., Marchadier, C., Adolphe, L., Aguejdad, R., Avner, P., Bonhomme, M., Bretagne, G., Briottet, X., Bueno, B., de Munck, C., Doukari, O., Hallegatte, S., Hidalgo, J., Houet, T., Le Bras, J., Lemonsu, A., Long, N., Moine, M.-P., Morel, T., Nolorgues, L., Pigeon, G., Salagnac, J.-L., Viguié, V., Zibouche, K., 2014: Adapting cities to climate change: A systematic modelling approach. Urban Climate 10, 407-429.

Matzarakis, A., Rutz, F., Mayer, H., 2010: Modelling radiation fluxes in simple and complex environments: basics of the RayMan model. International Journal of Biometeorology 54, 131-139.

Mayer, H., 1993: Urban bioclimatology. Experientia 49, 957-963.

Mayer, H., 1999: Air pollution in cities. Atmospheric Environment 33, 4029-4037.

Mayer, H., 2006: Indices for the human-biometeorological assessment of the thermal and air pollution component of climate. Gefahrstoffe - Reinhaltung der Luft 66, 165-174 (in German).

Mayer, H., Höppe, P., 1987: Thermal comfort of man in different urban environments. Theoretical and Applied Climatology 38, 43-49.

Mayer, H., Kalberlah, F., 2009: Two impact related air quality indices as tools to assess the daily and long-term air pollution. International Journal of Environment and Pollution 36, 19-29.

Mayer, H., Holst, J., Schindler, D., Ahrens, D., 2008a: Evolution of the air pollution in SW Germany evaluated by the long-term air quality index LAQx. Atmospheric Environment 42, 5071-5078.

Mayer, H., Makra, L., Kalberlah, F., Ahrens, D., Reuter, U., 2004: Air stress and air quality indices. Meteorologische Zeitschrift 13, 395-403.

Mayer, H., Holst, J., Dostal, P., Imbery, F., Schindler, D., 2008b: Human thermal comfort in summer within an urban street canyon in Central Europe. Meteorologische Zeitschrift 17, 241-250.

McGregor, G.R., 2011: Human biometeorology. Progress in Physical Geography 36, 93-109.

Meehl, G.A., Tebaldi, C., 2004: More intense, more frequent, and longer lasting heat waves in the 21st century. Science 305, 994-997.

Menberg, K., Bayer, P., Zosseder, K., Rumohr, S., Blum, P., 2013: Subsurface urban heat islands in German cities. Science of the Total Environment 442, 123-133.

Middel, A., Häb, K., Brazel, A.J., Martin, C.A., Guhathakurta, S., 2014: Impact of urban form and design on mid-afternoon microclimate in Phoenix local climate zones. Landscape and Urban Planning 122, 16-28.

Mills, G., 2014: Urban climatology: History, status and prospects. Urban Climate 10, 479-489.

Mills, G., Cleugh, H., Emmanuel, R., Endlicher, W., Erell, E., McGranahan, G., Ng, E., Nickson, A., Rosenthal, J., Steemer, K., 2010: Climate information for improved planning and management of mega cities (Needs perspective). Procedia Environmental Sciences 1, 228-246.

Monteiro, A., Carvalho, V., Oliveira, T., Sousa, C., 2013: Excess mortality and morbidity during the July 2006 heat wave in Porto, Portugal. International Journal of Biometeorology 57, 155-167.

Mullaney, J., Lucke, T., Trueman, S.J., 2015: A review of benefits and challenges in growing street trees in paved urban environments. Landscape and Urban Planning 134, 157-166.

Müller, N., Kuttler, W., Barlag, A.-B., 2014a: Analysis of the subsurface urban heat island in Oberhausen, Germany. Climate Research 58, 247-256.

Müller, N., Kuttler, W., Barlag, A.-B., 2014b: Counteracting urban climate change: adaptation measures and their effect on thermal comfort. Theoretical and Applied Climatology 115, 243-257.

Nagano, K., Horikoshi, T., 2011: Development of outdoor thermal index indicating universal and separate effects on human thermal comfort. International Journal of Biometeorology 55, 219-227.

Nastos, P.T., Matzarakis, A., 2013: Human bioclimatic conditions, trends, and variability in the Athens University Campus, Greece. Advances in Meteorology 2013, article ID 976510, 8 pages, DOI: 10.1155/2013/976510.

Ndetto, E.L., Matzarakis, A., 2013: Basic analysis of climate and urban bioclimate of Dar es Salaam, Tanzania. Theoretical and Applied Climatology 114, 213-226.

Ng, E., 2012: Towards planning and practical understanding of the need for meteorological and climatic information in the design of high-density cities: A case-based study of Hong Kong. International Journal of Climatology 32, 582-598.

Ng, E., Cheng, V., 2012: Urban human thermal comfort in hot and humid Hong Kong. Energy and Buildings 55, 51-65.

Ng, E., Chen, L., Wang, Y., Yuan, C., 2012: A study on the cooling effects of greening in a high-density city: An experience from Hong Kong. Building and Environment 47, 256-271.

Nicholls, N., Skinner, C., Loughnan, M., Tapper, N., 2008: A simple heat alert system for Melbourne, Australia. International Journal of Biometeorology 52, 375-384.

Niemelä, J., 2014: Ecology of urban green spaces: The way forward in answering major research questions. Landscape and Urban Planning 125, 298-303.

Nikolopoulou, M., Baker, N., Steemers, K., 2001: Thermal comfort in outdoor urban spaces: understanding the human parameter. Solar Energy 70, 227-235.

Nikolowski, J., Goldberg, V., Zimm, J., Naumann, T., 2013: Analysing the vulnerability of buildings to climate change: Summer heat and flooding. Meteorologische Zeitschrift 22, 145-153.

Norton, B.A., Coutts, A.M., Livesley, S.J., Harris, R.J., Hunter, A.M., Williams, N.S.G., 2015: Planning for cooler cities: A framework to prioritise green infrastructure to mitigate high temperatures in urban landscapes. Landscape and Urban Planning 134, 127-138.

Oertel, A., Emmanuel, R., Drach, P., 2015: Assessment of predicted versus measured thermal comfort and optimal comfort ranges in the outdoor environment in the temperate climate of Glasgow, UK. Journal of Building Services Engineering Research and Technology, DOI: 10.1177/0143624414564444.

Oleson, K.W., Monaghan, A., Wilhelmi, O., Barlage, M., Brunsell, N., Feddema, J., Hu, L., Steinhoff, D.F., 2013: Interactions between urbanization, heat stress, and climate change. Climatic Change, DOI: 10.1007/s10584-013-0936-8.

Oliveira, S., Andrade, H., 2007: An initial assessment of the bioclimatic comfort in an outdoor public space in Lisbon. International Journal of Biometeorology 52, 69-84.

Oliveira, S., Andrade, H., Vaz, T., 2011: The cooling effect of green spaces as a contribution to the mitigation of urban heat: A case study in Lisbon. Building and Environment 46, 2186-2194.

Onomura, S., Grimmond, C.S.B., Lindberg, F., Holmer, B., Thorsson, S., 2015: Meteorological forcing data for urban outdoor thermal comfort models from a coupled convective boundary layer and surface energy balance scheme. Urban Climate 11, 1-23.

Otto, F.E.L., Massey, N., van Oldenborgh, G.J., Jones, R.G., Allen, M.R., 2012: Reconciling two approaches to attribution of the 2010 Russian heat wave. Geophysical Research Letters 39, L04702, DOI: 10.1029/2011GL050422.

Pantavou, K., Lykoudis, S., 2014: Modeling thermal sensation in a Mediterranean climate - a comparison of linear and ordinal models. International Journal of Biometeorology 58, 1355-1368.

Pantavou, K., Theoharatos, G., Mavrakis, A., Santamouris, M., 2011: Evaluating thermal comfort conditions and health responses during an extremely hot summer in Athens. Building and Environment 46, 339-344.

Pantavou, K., Theoharatos, G., Santamouris, M., Asimakopoulos, D., 2013: Outdoor thermal sensation of pedestrians in a Mediterranean climate and a comparison with UTCI. Building and Environment 66, 82-95.

Park, S., Tuller, S.E., 2011a: Comparison of human radiation exchange models in outdoor areas. Theoretical and Applied Climatology 105, 357-370.

Park, S., Tuller, S.E., 2011b: Human body area factors for radiation exchange analysis: standing and walking postures. International Journal of Biometeorology 55, 695-709.

Park, S., Tuller, S.E., Jo, M., 2014: Application of Universal Thermal Climate Index (UTCI) for microclimatic analysis in urban thermal environments. Landscape and Urban Planning 125, 146-155.

Parlow, E., Vogt, R., Feigenwinter, C., 2014: The urban heat island of Basel - seen from different perspectives. DIE ERDE 145, 96-110.

Pascal, M., Wagner, V., Le Tertre, A., Laaidi, K., Honoré, C., Bénichou, F., Beaudeau, P., 2013: Definition of temperature thresholds: the example of the French heat wave warning system. International Journal of Biometeorology 57, 21-29.

Pascal, M., Laaidi, K., Ledrans, M., Baffert, E., Caserio-Schönemann, C., Le Tertre, A., Manach, J., Medina, S., Rudant, J., Empereur-Bissonnet, P., 2006: France's heat health watch warning system. International Journal of Biometeorology 50, 144-153.

Pearlmutter, D., Jiao, D., Garb, Y., 2014: The relationship between bioclimatic thermal stress and subjective thermal sensation in pedestrian spaces. International Journal of Biometeorology 58, 2111-2127.

Perini, K., Magliocco, A., 2014: Effects of vegetation, urban density, building height, and atmospheric conditions on local temperatures and thermal comfort. Urban Forestry & Urban Greening, http://dx.doi.org/10.1016/j.ufug.2014.03.003.

Perkins, S.E., Alexander, L.V., 2013: On the measurement of heat waves. Journal of Climate 26, 4500-4517.

Radinovíc, D., Ćurić, M., 2012: Criteria for heat and cold wave duration indexes. Theoretical and Applied Climatology 107, 505-510.

Rahmstorf, S., Coumou, D., 2011: Increase of extreme events in a warming world. Proceedings of the National Academy of Sciences of the United State of America 108, 17905-17909.

Rannow, S., Loibl, W., Greiving, S., Gruehn, D., Meyer, B.C., 2010: Potential impacts of climate change in Germany - Identifying regional priorities for adaptation activities in spatial planning. Landscape and Urban Planning 98, 160-171.

Rayner, D., Lindberg, F., Thorsson, S., Holmer, B., 2014: A statistical downscaling algorithm for thermal comfort applications. Theoretical and Applied Climatology, DOI: 10.1007/s00704-014-1329-2.

Rebetez, M., Mayer, H., Dupont, O., Schindler, D., Gartner, K., Kropp, J.P., Menzel, A., 2006: Heat and drought 2003 in Europe: a climate synthesis. Annals of Forest Science 63, 569-577.

Rebetez, M., Dupont, O., Giroud, M., 2009: An analysis of the July 2006 heat wave extent in Europe compared to the record year of 2003. Theoretical and Applied Climatology 95, 1-7.

Ren, C., Ng, E.Y., Katzschner, L., 2011: Urban climate map studies: a review. International Journal of Climatology 31, 2213-2233.

Reuter, U., Kapp, R., 2012: Climate booklet for urban development online. Ed. by the Ministry of Transport and Infrastructure of Baden-Württemberg. Stuttgart, http://www.staedtebauliche-klimafibel.de/.

Rey, G., Jougla, E., Fouillet, A., Pavillon, G., Bessemoulin, P., Frayssinet, P., Clavel, J., Hémon, D., 2007: The impact of major heat waves on all-cause and cause-specific mortality in France from 1971 to 2003. International Archives of Occupational and Environmental Health 80, 615-626.

Robine, J-M., Cheung, S.L.K., Roy, S.L., Oyen, H.V., Griffiths, C., Michel, J-P., Herrmann, F.R., 2008: Death toll exceeded 70,000 in Europe during the summer of 2003. Comptes Rendus Biologies 331, 171-178.

Robinson, P.J., 2001: On the definition of a heat wave. Journal of Applied Meteorology 40, 762-775.

Roy, S., Byrne, J., Pickering, C., 2012: A systematic quantitative review of urban tree benefits, costs, and assessment methods across cities in different climatic zones. Urban Forestry & Urban Greening 11, 351-363.

Santamouris, M., 2014: Cooling the cities - A review of reflective and green roof mitigation technologies to fight heat island and improve comfort in urban environments. Solar Energy 103, 682-703.

Schär, C., Vidale, P.L., Lüthi, D., Frei, C., Häberli, C., Liniger, M.A., Appenzeller, C., 2004: The role of increasing temperature variability in European summer heatwaves. Nature 427, 332-336.

Scherer, D., Fehrenbach, U., Lakes, T., Lauf, S., Meier, F., Schuster, C., 2013: Quantification of heat-stress related mortality hazard, vulnerability and risk in Berlin, Germany. DIE ERDE 144, 238-259.

Schuster, C., Burkart, K., Lakes, T., 2014: Heat mortality in Berlin - Spatial variability at the neighborhood scale. Urban Climate 10, 134-147.

Shashua-Bar, L., Hoffman, M.E., 2000: Vegetation as a climatic component in the design of an urban street - An empirical model for predicting the cooling effect of urban green areas with trees. Energy and Buildings 31, 221-235.

Shashua-Bar, L., Hoffman, M.E., 2003: Geometry and orientation aspects in passive cooling of canyon streets with trees. Energy and Buildings 35, 61-68.

Shashua-Bar, L., Hoffman, M.E., 2004: Quantitative evaluation of passive cooling of the UCL microclimate in hot regions in summer, case study: urban streets and courtyards with trees. Building and Environment 39, 1087-1099.

Shashua-Bar, L., Pearlmutter, D., Erell, E., 2009: The cooling efficiency of urban landscape strategies in a hot dry climate. Landscape and Urban Planning 92, 179-186.

Shashua-Bar, L., Pearlmutter, D., Erell, E., 2011: The influence of trees and grass on outdoor thermal comfort in a hot-arid environment. International Journal of Climatology 31, 1498-1506.

Shashua-Bar, L., Tsiros, I.X., Hoffman, M.E., 2010a: A modeling study for evaluating passive cooling scenarios in urban streets with trees. Case study: Athens, Greece. Building and Environment 45, 2798-2807.

Shashua-Bar, L., Tsiros, I.X., Hoffman, M.E., 2012: Passive cooling design options to ameliorate thermal comfort in urban streets of a Mediterranean climate (Athens) under hot summer conditions. Building and Environment 57, 110-119.

Shashua-Bar, L., Potchter, O., Bitan, A., Boltansky, D., Yaakov, Y., 2010b: Microclimate modelling of street tree species effects within the varied urban morphology in the Mediterranean city of Tel Avis, Israel. International Journal of Climatology 30, 44-57.

Sheridan, S.C., 2007: A survey of public perception and response to heat warnings across four North American cities: an evaluation of municipal effectiveness. International Journal of Biometeorology 52, 3-15.

Shevchenko, O., Lee, H., Snizhko, S., Mayer, H., 2014: Long-term analysis of heat waves in Ukraine. International Journal of Climatology 34, 1642-1650.

Skelhorn, C., Lindley, S., Levermore, G., 2014: The impact of vegetation types on air and surface temperatures in a temperate city: A fine scale assessment in Manchester, UK. Landscape and Urban Planning 121, 129-140.

Souch, C., Grimmond, S., 2006: Applied climatology: urban climate. Progress in Physical Geography 30, 270-279.

Srivanit, M., Hokao, K., 2013: Evaluating the cooling effects of greening for improving the outdoor thermal environment at an institutional campus in the summer. Building and Environment 66, 158-172.

Steadman, R.G., 1984: A universal scale of apparent temperature. Journal of Climate and Applied Meteorology 23, 1674-1687.

Steeneveld, G.J., Koopmans, S., Heusinkveld, B.G., Theuwes, N.E., 2014: Refreshing the role of open water surfaces on mitigating the maximum urban heat island effect. Landscape and Urban Planning 121, 92-96.

Staiger, H., Laschewski, G., Grätz, A., 2012: The perceived temperature - a versatile index for the assessment of the human thermal environment. Part A: scientific basis. International Journal of Biometeorology 56, 165-176.

Stewart, I.D., Oke, T.R., 2012: 'Local climate zones' for urban temperature studies. Bulletin of the American Meteorological Society 93, 1879-1900.

Stewart, I.D., Oke, T.R., Krayenhoff, E.S., 2014: Evaluation of the 'local climate zone' scheme using temperature observations and model simulations. International Journal of Climatology 34, 1062-1080.

Svensson, M.K., 2004: Sky view factor analysis - implications for urban air temperature differences. Meteorological Applications 11, 201-211.

Taleghani, M., Kleerekoper, L., Tenpierik, M., van den Dobbelsteen, A., 2015: Outdoor thermal comfort within five different urban forms in the Netherlands. Building and Environment 83, 65-78.

Tallis, M., Taylor, G., Sinnett, D., Freer-Smith, P., 2011: Estimating the removal of atmospheric particulate pollution by the urban tree canopy in London, under current and future environments. Landscape and Urban Planning 103, 129-138.

Tan, C.L., Wong, N.H., Jusuf, S.K., 2013: Outdoor mean radiant temperature estimation in the tropical environment. Building and Environment 64, 118-129.

Tan, J., Zheng, Y., Song, G., Kalkstein, L.S., Kalkstein, A.J., Tang, X., 2007: Heat wave impacts on mortality in Shanghai, 1998 and 2003. International Journal of Biometeorology 51, 193-200.

Tan, J., Zheng, Y., Tang, X., Guo, C., Li, L., Song, G., Zhen, X., Yuan, D., Kalkstein, A.J., Li, F., Chen, H., 2010: The urban heat island and its impact on heat waves and human health in Shanghai. International Journal of Biometeorology 54, 75-84.

Thach, T.-Q., Zheng, Q., Lai, P.-C., Wong, P.P.-Y., Chau, P.Y.-K., Jahn, H.J., Plass, D., Katzschner, L., Kraemer, A., Wong, C.-M., 2015: Assessing spatial associations between thermal stress and mortality in Hong Kong: A small-area ecological study. Science of the Total Environment 502, 666-672.

Thorsson, S., Lindberg, F., Eliasson, I., Holmer, B., 2007: Different methods for estimating the mean radiant temperature in an outdoor urban setting. International Journal of Climatology 27, 1983-1993.

Thorsson, S., Lindberg, F., Björklund, J., Holmer, B., Raynor, D., 2011: Potential changes in outdoor thermal comfort conditions in Gothenburg, Sweden due to climate change: the influence of urban geometry. International Journal of Climatology 31, 324-335.

Thorsson, S., Rocklöv, J., Konarska, J., Lindberg, F., Holmer, B., Dousset, B., Rayner, D., 2014: Mean radiant temperature - A predictor of heat related mortality. Urban Climate 10, 332-345.

Tinz, B., Freydank, E., Hupfer, P., 2008: Heat episodes in Germany in the 20th and 21st century. In: Wake-up call climate. Risks to health: Dangers for plants, animals and humans (ed. by J. L. Lozán, H. Graßl, G. Jendritzky, L. Karbe and K. Reise), Hamburg, Wissenschaftliche Auswertungen, 141-148 (in German).

Trigo, R.M., Garcia-Herrera, R., Díaz, J., Trigo, I.F., Valente, M.A., 2005: How exceptional was the early August 2003 heatwave in France? Geophysical Research Letters 32, L10701, DOI: 10.1029/2005GL022410.

Tsiros, I.X., 2010: Assessment and energy implications of street air temperature cooling by shade trees in Athens (Greece) under extremely hot weather conditions. Renewable Energy 35, 1866-1869.

Tung, C.-H., Chen, C.-P., Tsai, K.-T., Kántor, N., Hwang, R.-L., Matzarakis, A., Lin, T.-P., 2014: Outdoor thermal comfort characteristics in the hot and humid region from a gender perspective. International Journal of Biometeorology 58, 1927-1939.

UN, 2014: World urbanization prospects: The 2014 revision. New York, United Nations.

Unger, J., 2006: Modelling of the annual mean maximum urban heat island using 2D and 3D surface parameters. Climate Research 30, 215-226.

Vailshery, L.S., Jaganmohan, M., Nagendra, H., 2013: Effect of street trees on microclimate and air pollution in a tropical city. Urban Forestry & Urban Greening 12, 408-415.

van Hooff, T., Blocken, B., Hensen, J.L.M., Timmermans, H.J.P., 2014: On the predicted effectiveness of climate adaptation measures for residential buildings. Building and Environment 82, 300-316.

van Hove, L.W.A., Jacobs, C.M.J., Heusinkveld, B.G., Elbers, J.A., van Driel, B.L., Holtslag, A.A.M., 2015: Temporal and spatial variability of urban heat island and thermal comfort within the Rotterdam agglomeration. Building and Environment 83, 91-103.

Vaneckova, P., Neville, G., Tippett, V., Aitken, P., FitzGerald, G., Tong, S., 2011: Do biometeorological indices improve modelling outcomes of heat-related mortality? Journal of Applied Meteorology and Climatology 50, 1165-1176.

Vanos, J.K., 2015: Children's health and vulnerability in outdoor microclimates: A comprehensive review. Environmental International 76, 1-15.

Vanos, J.K., Warland, J.S., Gillespie, T.J., Kenny, N.A., 2010: Review of the physiology of human thermal comfort while exercising in urban landscapes and implications for bioclimatic design. International Journal of Biometeorology 54, 319-334.

Villadiego, K., Velay-Dabat, M.A., 2014: Outdoor thermal comfort in a hot and humid climate of Colombia: A field study in Barranquilla. Building and Environment 75, 142-152.

Voskamp, I.M., van de Ven, F.H.M., 2015: Planning support system for climate adaptation: Composing effective sets of blue-green measures to reduce urban vulnerability to extreme weather events. Building and Environment 83, 159-167.

Wagner, P., Kuttler, W., 2014: Biogenic and anthropogenic isoprene in the near-surface urban atmosphere - A case study in Essen, Germany. Science of the Total Environment 475, 104-115.

Walikewitz, N., Jänicke, B., Langner, M., Meier, F., Endlicher, W., 2015: The difference between the mean radiant temperature and the air temperature within indoor environments: A case study during summer conditions. Building and Environment 84, 151-161.

Wang, Y., Akbari, H., 2014: Development and application of 'thermal radiative power' for urban environmental evaluation. Sustainable Cities and Society 14, 316-322.

Watson, I.D., Johnson, G.T., 1987: Graphical estimation of sky view factors in urban environments. International Journal of Climatology 7, 193-197.

Watanabe, S., Nagano, K., Ishii, J., Horikoshi, T., 2014: Evaluation of outdoor thermal comfort in sunlight, building shade, and pergola shade during summer in a humid subtropical region. Building and Environment 82, 556-565.

Wienert, U., Kuttler, W., 2005: The dependence of the urban heat island intensity on latitude - a statistical approach. Meteorologische Zeitschrift 14, 677-686.

Wolch, J.R., Byrne, J., Newell, J.P., 2014: Urban green space, public health, and environmental justice: The challenge of making cities 'just green enough'. Landscape and Urban Planning 125, 234-244.

Wong, J.K.W., Lau, L.S.-K., 2013: From the 'urban heat island' to the 'green island'? A preliminary investigation into the potential of retrofitting green roofs in Mongkok district of Hong Kong. Habitat International 39, 25-35.

Yahia, M.W., Johansson, E., 2013: Influence of urban planning regulations on the microclimate in a hot dry climate: The example of Damascus, Syria. Journal of Housing and the Built Environment 28, 51-65.

Yahia, M.W., Johansson, E., 2014: Landscape interventions in improving thermal comfort in the hot dry city of Damascus, Syria - The example of residential spaces with detached building. Landscape and Urban Planning 125, 1-16.

Yang, F., Lau, S.S.Y., Qian, F., 2011: Thermal comfort effects of urban design strategies in high-rise urban environments in a sub-tropical climate. Architectural Science Review 54, 285-304.

Yang, X., Zhao, L., Bruse, M., Meng, Q., 2013: Evaluation of a microclimate model for predicting the thermal behavior of different ground surfaces. Building and Environment 60, 93-104.

Zeng, Y., Dong, L., 2015: Thermal human biometeorological conditions and subjective thermal sensation in pedestrian streets in Chengdu, China. International Journal of Biometeorology 59, 99-108.

Zhu, S., Guan, H., Bennett, J., Clay, R., Ewenz, C., Benger, S., Maghrabi, A., Millington, A.C., 2013: Influence of sky temperature distribution on sky view factor and its applications in urban heat island. International Journal of Climatology 33, 1837-1843.

List of figure captions

List of table captions